PERFORMANCE EVALUATION OF A SLURRIED BED GAS REACTOR

J. W. HIGHET

SUMMARY OF Ph.D. THESIS

GLASGOW UNIVERSITY, 1964.

SUMMARY.

The slurried bed reactor has been discussed in the context of exothermic gas reactions. The mathematical model has been developed with a view to providing a method for scale up in terms of Number of Reactor Units (N.R.U.), Number of Chemical Units (N.Ch.U.), a forward catalyst surface rate constant K_1 and an overall mass transfer coefficient K_g.

Experimental work was carried out in a continuous bench scale reactor to establish the value of the theoretical model. Ethylene hydrogenation on a Raney Nickel catalyst was the model reaction employed. Results were obtained using various inlet reactant flow rates and compositions. The reactor size was also varied.

Results are presented which show the performance possible with the slurried bed reactors as well as serving as data for the theoretical model. It is shown that conversion is a direct function of reactor length and an inverse function of reactor flow rate. It is also shown that the nature of the catalyst suspending liquid is of great importance to reaction rate.

A method of estimating reactor performance is presented.

For the system considered it is shown that mass transfer of the reactants from bubble to catalyst surface can be made to play a major part in controlling the reaction rate. The diffusional resistances to hydrogen are shown to be the greatest. Equation 1.2.57,

$$\frac{V_R}{F_i^M \text{ N.Ch.U.}} = \frac{1}{\eta_{gm}^2 K_1 A_{ls}} + \frac{\text{N.R.U.}}{\text{N.Ch.U.}} \frac{1}{K_g A_{glm} \eta_{gm}}$$

enables value of K_1, the forward catalyst surface reaction rate constant, and K_g, the mass transfer coefficient between bubble and catalyst surface, to be calculated from the experimental data. It is suggested that this equation has potential value in reactor design.

PERFORMANCE EVALUATION OF A SLURRIED BED GAS REACTOR.

A THESIS SUBMITTED TO THE UNIVERSITY OF GLASGOW IN FULFILMENT OF THE REQUIREMENTS FOR THE DEGREE OF DOCTOR OF PHILOSOPHY

by

JOHN W. HIGHET, B. Sc.

THURSO. APRIL, 1964.

"Double, double toil and trouble,

Fire, burn; and, cauldron, bubble"

- Shakespeare.

ACKNOWLEDGEMENTS.

The author wishes to thank Professor P. D. Ritchie for permission to undertake this research within his department. Thanks are also due to Dr. C. G. M. Slesser for his supervision and encouragement and for the many helpful discussions held with him.

The author is also indebted to the departmental workshop staff for their services, and to Mrs. W. Tait without whose kind assistance the reproduction of this work would have been extremely difficult.

INDEX.

SUMMARY.

The slurried bed reactor has been discussed in the context of exothermic gas reactions. The mathematical model has been developed with a view to providing a method for scale up in terms of Number of Reactor Units (N.R.U.), Number of Chemical Units (N.Ch.U.), a forward catalyst surface rate constant K_1 and an overall mass transfer coefficient K_g.

Experimental work was carried out in a continuous bench scale reactor to establish the value of the theoretical model. Ethylene hydrogenation on a Raney Nickel catalyst was the model reaction employed. Results were obtained using various inlet reactant flow rates and compositions. The reactor size was also varied.

Results are presented which show the performance possible with the slurried bed reactors as well as serving as data for the theoretical model. It is shown that conversion is a direct function of reactor length and an inverse function of reactor flow rate. It is also shown that the nature of the catalyst suspending liquid is of great importance to reaction rate.

A method of estimating reactor performance is presented.

For the system considered it is shown that mass transfer of the reactants from bubble to catalyst surface can be made to play a major part in controlling the reaction rate. The diffusional resistances to hydrogen are shown to be the greatest. Equation 1.2.57,

$$\frac{V_R}{F_i^M \text{ N.Ch.U.}} = \frac{1}{\eta_{gm}^2 K_1 A_{ls}} + \frac{\text{N.R.U.}}{\text{N.Ch.U.}} \cdot \frac{1}{K_g A_{glm} \eta_{gm}}$$

enables values of K_1, the forward catalyst surface reaction rate constant, and K_g, the mass transfer coefficient between bubble and catalyst surface, to be calculated from the experimental data. It is suggested that this equation has potential value in reactor design.

1. 1. INTRODUCTION.

There are three types of continuous reactor available for heterogeneous exothermic catalytic gas reactions:- fixed bed; fluidised bed; and slurried bed reactors.

In the latter reactor the bed is in the form of a slurry in which the catalyst particles are suspended in an inert liquid through which reactant gases are bubbled. Previous workers have used the name slurry phase reactor for the type but this is not meaningful.

The principle of the slurried bed reactor is well established (1)(2)(3)(4). It originated in Germany where much work has been carried out on its application to the Fischer Tropsch process (3)(4)(5). A general account of the work done in Germany before and during the war on the Fischer Tropsch synthesis, including the development of the slurried bed reactor, is given by Storch, Golumbic and Anderson (6). Today German techniques have evolved a very high level of performance, e.g. one battery of blast furnaces produces 2,250 tons of pig iron per day and the surplus blast furnace gas is converted to 140 tons per day of hydrocarbons using the Fischer Tropsch process in a slurried bed reactor (7). Work has also been done in this country (8)(9)(10) and in the U.S.A. (11) on slurried bed reactors. However, only in Germany have slurried bed reactors been used for commercial production.

A dominant problem in the design of reactors for exothermic gas reactions is the effective removal of the heat of reaction since failure to do this will cause overheating and impair reactor performance. The heat transfer characteristics of the three types of reactor are summarised.

Fixed Bed Reactors:

In these heat transfer coefficients between catalyst bed and cooling elements are relatively low [~ 5.0 Btu/hr. Ft^2 ^oF (12)(13)]. "Hot spots" arise due to different heat transfer path lengths between individual catalyst particles and cooling elements. There is no way of completely overcoming this difficulty but attempts to do so invariably lead to complex mechanical design.

Fluidised Bed Reactors:

In these, heat transfer coefficients are considerably higher [~ 50 Btu/hr Ft^2 ^oF (13)(14)] and even greater values have been reported (15).

However in the Fischer Tropsch synthesis, the catalyst may become difficult to fluidise due to carbon deposition. Scharmann (16) considers that despite overall efficient heat transfer, the "skin" temperature of the catalyst is much higher than the average bed temperature and this condition is largely responsible for carbon deposition. This theory is encouraged by

reported fractional heat transfer coefficients between gas and particles in a fluidised bed (17). Also Heminger states that the amount of carbon deposition decreases with increasing gas velocity (18). This implies that the drop in carbon formation is due to the resultant increase in heat transfer coefficients.

Slurried Bed Reactors:

The heat transfer coefficients far exceed those of the other types, values up to 1,330 Btu/ft^2 hr. ^{o}F having been reported (19)(20)(21). It has been shown by workers in this field that selectivity (i.e. production of molecules of the desired structure) is appreciably higher for slurried bed reactors due to the absence of "hot spots" which can cause cracking of product molecules (8)(11). The high heat capacity of the liquid medium and its intimate contact with catalyst and gas prevents sudden fluctuations in reactor temperature and permits of easier temperature control.

A comparison of the other features of the three types of reactor, particularly performance and cost, is more difficult. Table 1. 1. compares the performance of each for the case of the Fischer Tropsch synthesis. The table is based mainly on figures from Storch, Columbic and Anderson (6).

Table II. shows that the fluidised bed reactor operates at much higher space velocities than the other two. A disadvantage of fluidised bed reactors is that the range of flow rates is restricted by fluidisation requirements. The specific yield appears to be best for the slurried bed reactor but the space time yield is greatest in the fluidised bed reactor.

In a brief survey of the other features of the three types of reactor, it is noted that the construction of a fixed bed reactor may be very complex (6) while the fluidised bed (22)(23) and slurried bed (7) types are fairly simple although the fluidised bed reactor appears to require more auxiliaries. Catalyst life tends to be longest in the slurried bed reactor (7) while catalyst replacement is easy in fluidised and slurried bed reactors and most difficult in the fixed bed reactor. It thus appears that both capital and operating costs of the fixed bed reactor are likely to be highest. With the information available it is impossible to make a detailed comparison of the relative costs of the fluidised bed reactor and the slurried bed reactor.

It appears that, apart from its attractions in the heat transfer field, the slurried bed reactor has no serious disadvantages when compared with the other

types of reactor (8). Thus for exothermic heterogeneous gas reactions where good temperature control is essential, the slurried bed reactor is of potential value. A more quantitative knowledge than presently exists of the factors influencing reaction rate in a slurried bed reactor is desirable. Such knowledge would facilitate reactor design and perhaps enable the space time yield, the least attractive feature of the slurried bed reactor, to be improved.

In this work, a mathematical model of a bimolecular reaction occurring in a slurried bed reactor is presented as a basis for a quantitative investigation of the slurried bed system. Results from a suitable experimental model are also presented with reference to the mathematical model.

TABLE 1.1

	Fixed Bed Reactors			Fluidised Bed Reactor	Slurried Bed Reactors		
Place of Origin	Ruhrchemie Germany	Ruhrchemie Germany	U.S. Bureau of Mines	Certain American Oil Companies	I.G. Farben Germany	Rheinprussen Germany	U.S. Bureau of Mines
No. of Stages	2-3	1	1	1	1	2	1
Operating Pressure	1 or 10 ATM.	1 ATM	20 ATM	27-45 ATM	20 ATM	10 ATM	17 ATM
Operating Temperature	180-200°C	~200°C	~260°C	250-350°C	250 | 275°C	240°C	240-275°C
Type of Catalyst	Cobalt	Cobalt	Iron	Iron	Iron	Iron	Iron
Space Velocity HR^{-1}	60-100	110	300	400-500	80 | 125	101	300
Specific Yield of Feed Gas	150 gm C_3^+	104 gm C_3^+	99 gm C_3^+	150 gm C_3^+	- | 173 gm C_3^+	157 gm C_3^+	125 gm C_3^+
Space Time Yield	9-15 Kgm/M^3 CATALYST HOUR			150 Kgm/M^3 Fluidised volume hr.	10 + 15 Kg C_3/M^3 slurry hr.	14 Kg C_3^+/M^3 slurry hr.	17 Kg C_3^+/M^3 slurry hr.
Amount of Recycle	0	3:1	2:1	2:1	0	0	0
CO Conversion	~50% per stage	~40%	~70%	~90%	~70%	95%	70%
Feed Gas Composition	$2H_2$+1CO	$1.5H_2$+1CO	$1H_2$+1CO	$1.8H_2$+1CO	$1H_2$+1.3CO	$1.28H_2$+1CO	$1H_2$ + 1CO
Slurry Concentration	-	-	-	<20lbs/ft^3	150-300gm/l	12% by wt.	36.6% by wt.

1. 2. A MATHEMATICAL MODEL OF A SECOND ORDER GAS REACTION OCCURRING IN A SLURRIED BED REACTOR.

1. 2.A. This section presents basic thermodynamic and kinetic information.

1. 2.B. The various physical and chemical resistances to chemical change believed to be present in the reactor are defined. The model of the system resulting from a combination of the expressions for these resistances is shown to be extremely complex.

1. 2.C. Here an overall resistance to the reaction has been postulated. This results in a much simpler model than the previous one. A number of apparently interesting relationships are established.

1.2. A.

For the second order reaction

$$A + B \longrightarrow C$$

Forward rate $r_f = K_f(a)_a(a)_b$ - 1.2. 1.

Backward rate $r_b = K_b(a)_c$ - 1.2. 2.

and the equilibrium constant

$$K = \frac{(a)_c}{(a)_a(a)_b} = \frac{K_f}{K_b} \qquad - 1.2.\ 3.$$

At any other stage than equilibrium, the rate is

$$r = r_f - r_b = K_f \left[(a)_a(a)_b - \frac{(a)_c}{K} \right] \qquad - 1.2.\ 4.$$

In this particular case a gas reaction is being considered and it is more convenient that the effective gas pressures existing at the catalyst surface rather than the respective activities should be considered. This may be done by relating fugacities to activities.

The activity $a = f/f_o$

$$\therefore \quad K = \frac{(f)_c}{(f)_a(f)_b} \cdot \frac{(f_o)_a(f_o)_b}{(f_o)_c} \qquad - 1.2.\ 5$$

Let $\dfrac{(f_o)_a(f_o)_b}{(f_o)_c} = \phi$

For gaseous reactions, it is customary to choose as the standard state, the pure gas at 1 atmosphere fugacity

i.e. $f_o = 1$ atm.

Hence in this case $\phi = 1$ but has units of p^{+1}

Thus $$K = \frac{(f)_c}{(f)_a (f)_b} \cdot \phi \qquad - 1.2.6.$$

It is assumed that the fugacity of a gas is proportional to its mole fraction

Thus $f = f' y$

Hence $$K = \frac{(f')_c}{(f')_a (f')_b} \cdot K_y \cdot \phi \qquad - 1.2.7.$$

Where $$K_y = \frac{Y_c}{Y_a Y_b}$$

The quantity $\alpha = f'/\pi_g$

Hence $$K = \pi_g^{-1} K_\alpha . K_y . \phi \qquad - 1.2.8$$

Where $$K_\alpha = \frac{\left[f'/\pi_g\right]_c}{\left[f'/\pi_g\right]_a \left[f'/\pi_g\right]_b}$$

In a gaseous reaction a quantity K_p is frequently used. This is defined as follows :-

$$K_p = \frac{\left[Y_c \pi_g\right]}{\left[Y_a \pi_g\right]\left[Y_b \pi_g\right]} = \pi_g^{-1} K_y$$

Thus $K = K_p K_\alpha \phi$

When the gases follow the ideal gas law

$K_\alpha = 1$ and $f = p$ also $\phi = 1$

Hence $K = K_p$ numerically

For a second order heterogeneous catalytic gas reaction the forward and backward reaction rates per square centimetre of catalyst surface may be given as

$$r_{sf} = K_1' P_a P_b \qquad - 1.2.9.$$

$$r_{sb} = K_2' P_c \qquad - 1.2.10.$$

and $K_p = K_1'/K_2'$

K_p has dimensions of p^{-1}

At any stage other than equilibrium

$$r_s = K_1' \left[P_a P_b - \frac{P_c}{K_p} \right] \qquad - 1.2.11.$$

1.2. B.

The mechanism postulated and generally accepted (9) (24)(25) for a gas reaction in a slurried bed reactor supposes that reacting gases diffuse through the gas liquid interface of the bubble and into the liquid. Thereafter powerful convection currents generated by the turbulence of the system cause the reactants to pass freely to the liquid solid interface. Under certain conditions a concentration gradient of reactants may exist in the bulk liquid. The reactants then diffuse through the liquid solid interface and are adsorbed on the catalyst surface where reaction takes place. The products of the reaction then pass back to the bubble by similar processes. The progress of the gas reaction

$$A + B \longrightarrow C$$

is depicted in fig. 1.1.

In this work, the problem is approached from the basis of Whitman's two film theory which is preferred to the more sophisticated penetration theory (27) because it is not only easier to apply but it has been shown (28)(29) that the conclusions of the two theories do not differ significantly.

THE MODEL SYSTEM

A diagrammatic representation of the reaction A + B ⟶ C in a slurried bed reactor.

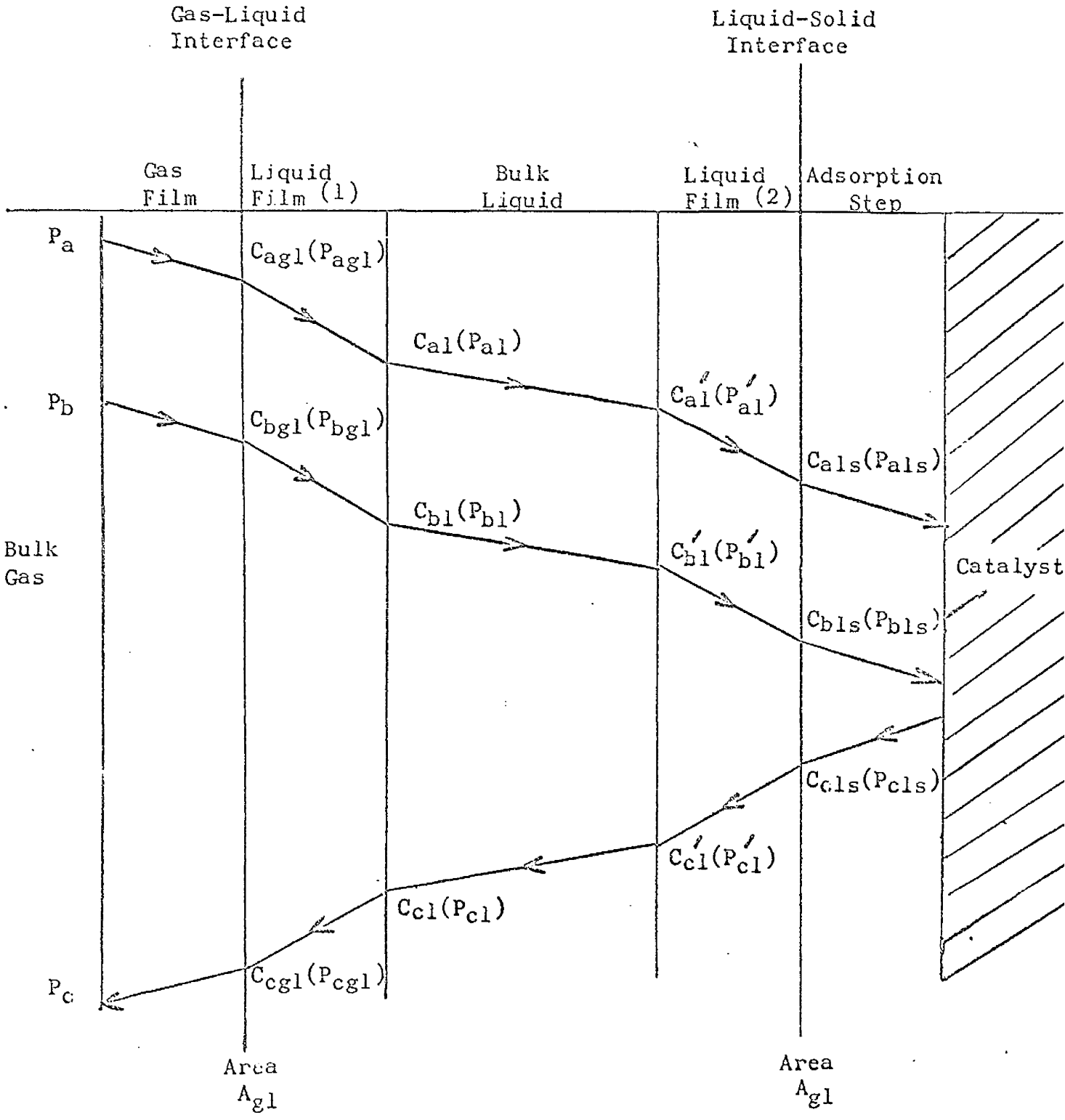

Fig. 1.1

The rates of the steps believed to occur are given below for steady state conditions in the system.

For reactant A.

From bulk gas to gas liquid interface (gas film)

$$N_a = K_{al}A_{gl}(P_a - P_{agl}) \qquad - 1.2.12.$$

From gas liquid interface to bulk liquid (liquid film 1)

$$N_a = K_{a2}A_{gl}(C_{agl} - C_{al}) \qquad - 1.2.13.$$

Down concentration gradient im bulk liquid

$$N_a = K_{a3}A_{gl}(C_{al} - C_{al}') \qquad - 1.2.14.$$

From bulk liquid to liquid solid interface (liquid film 2)

$$N_a = K_{a4}A_{ls}(C_{al}' - C_{als}) \qquad - 1.2.15.$$

Overall adsorption rate of catalyst surface

$$N_a = \psi_{fa}P_{als}A_{ls}C_v^{*} - \psi_{ra}A_{ls}C_a^{*}$$

$$= \psi_{fa}A_{ls}\left[P_{als}C_v^{*} - \frac{C_a^{*}}{S_a}\right] \qquad - 1.2.16.$$

Assuming that the gases in solution obey Henry's law

Then $C_{agl} = H_aP_{agl}$

$C_{al} = H_aP_{al}$

$C_{al}' = H_aP_{al}'$

$C_{als} = H_aP_{als}$

Thus

$$P_a - P_{agl} = \frac{N_a}{K_{al} A_{gl}}$$

$$P_{agl} - P_{al} = \frac{N_a}{H_a K_{a2} A_{gl}}$$

$$P_{al} - P_{al'} = \frac{N_a}{H_a K_{a3} A_{gl}}$$

$$P_{al'} - P_{als} = \frac{N_a}{H_a K_{a4} A_{ls}}$$

If the mechanism of the surface reaction consists of reaction between adsorbed molecules of A and B on surface active sites, here denoted by Σ, the process may be represented by the expression

$$A.\Sigma + B.\Sigma \longrightarrow C.\Sigma + \Sigma \qquad -1.2.17.$$

The rate of the forward reaction is represented by the following equation:-

$$r_f = K_{sf} A_{ls} C_a^{*} \frac{C_b^{*}}{C_t^{*}}$$

The rate of the back reaction is

$$r_b = K_{sb} A_{ls} C_c^{*} \frac{C_v^{*}}{C_t^{*}}$$

Hence $$N_a = K_{sf} A_{ls} C_a^{*} \frac{C_b^{*}}{C_t^{*}} - K_{sb} A_{ls} C_c^{*} \frac{C_v^{*}}{C_t^{*}}$$

$$= \frac{K_{sf} A_{ls}}{C_t^{*}} \left[C_a^{*} C_b^{*} - \frac{C_c^{*} C_v^{*}}{K_s} \right] \quad - 1.2.18.$$

To obtain an overall expression for the rate in terms of P_a, P_b, P_c, it is necessary to eliminate the surface potentials C_a^{*}, C_b^{*}, C_c^{*} and C_v^{*} from 1.2.18, and in consequence P_{agl}, P_{bgl}, P_{cgl}, P_{al}, P_{bl}, P_{cl}, $P_{al'}$, $P_{bl'}$, $P_{cl'}$, P_{als}, P_{bls} and P_{cls}.

This is achieved as follows

From 1.2.16

$$C_a^{*} = S_a \left[P_{als} C_v^{*} - \frac{N_a}{\psi_{fa} A_{ls}} \right]$$

Similarly $$C_b^{\ast} = S_b \left[P_{b1s} C_v^{\ast} - \frac{N_b}{\psi_{fb} L_{1s}} \right] \qquad - 1.2.20.$$

$$C_c^{\ast} = S_c \left[\frac{N_c}{\psi_{fc} L_{1s}} + P_{c1s} C_v^{\ast} \right] \qquad - 1.2.21.$$

It may be shown from 1.2.12, 1.2.13, 1.2.14, 1.2.15 that

$$P_{a1s} = P_a - N_a \left(\frac{1}{K_{a1} A_{g1}} + \frac{1}{H_a K_{a2} A_{g1}} + \frac{1}{H_a K_{a3} L_{g1}} + \frac{1}{H_a K_{a4} A_{1s}} \right) \qquad - 1.2.22.$$

and similarly

$$P_{b1s} = P_b - N_b \left(\frac{1}{K_{b1} A_{g1}} + \frac{1}{H_b K_{b2} A_{c1}} + \frac{1}{H_b K_{b3} A_{g1}} + \frac{1}{H_b K_{b4} A_{1s}} \right) \qquad - 1.2.23.$$

$$P_{c1s} = P_c + N_c \left(\frac{1}{K_{c1} A_{g1}} + \frac{1}{H_c K_{c2} A_{g1}} + \frac{1}{H_c K_{c3} A_{g1}} + \frac{1}{H_c K_{c4} L_{1s}} \right) \qquad - 1.2.24.$$

The surface concentrations of A, B, C and vacant active sites may be related by the following equation

$$C_t^{*} = C_v^{*} + C_a^{*} + C_b^{*} + C_c^{*} \qquad - 1.2.25.$$

Hence $$C_t^{*} = C_v^{*} + S_a\left[P_{als}\, C_v^{*} - \frac{N_a}{\psi_{fa}\Lambda_{ls}}\right] + S_b\left[P_{bls}C_v^{*} - \frac{N_b}{\psi_{fb}\Lambda_{ls}}\right] + S_c\left[\frac{N_c}{\psi_{fc}\Lambda_{ls}} + P_{cls}C_v^{*}\right]$$

$$= C_v^{*}\left[1 + S_aP_{als} + S_bP_{bls} + S_cP_{cls}\right] - \frac{S_aN_a}{\psi_{fa}\Lambda_{ls}} - \frac{S_bN_b}{\psi_{fb}\Lambda_{ls}} + \frac{S_cN_c}{\psi_{fc}\Lambda_{ls}}$$

Hence $$C_v^{*} = \frac{C_t^{*} + \frac{S_aN_a}{\psi_{fa}\Lambda_{ls}} + \frac{S_bN_b}{\psi_{fb}\Lambda_{ls}} - \frac{S_cN_c}{\psi_{fc}\Lambda_{ls}}}{1 + S_aP_{als} + S_bP_{bls} + S_cP_{cls}}$$

- 1.2.26.

It is now possible to substitute in the original rate equation 1.2.17 expressions which contain only C_t^* P_a, P_b, P_c, $N_a (= N_b = N_c)$, A_{gl}, A_{ls} and the rate coefficients for the various steps. All of these quantities are capable of measurement if practical difficulties can be overcome. An extremely large and unwieldy equation is obtained which has little practical importance.

There are several different mechanisms at the catalyst surface for this type of reaction (31). Only one has been considered as this approach is considered to end in an impasse irrespective of mechanism. Since a theoretical model of practical value is desired, a different approach must be employed.

1.2. C.

In the specification of any rate process it is useful to have an overall coefficient such as is common in heat and mass transfer. It is convenient to express rate as being equal to (overall coefficient) x (area) x (driving force).

When in gas absorption, the driving force is given by $(P_a - P_{ao})$ the instantaneous rate may be written as

$$N_a = KA(P_a - P_{ae})$$

where K is the overall coefficient, A the area, P_{ae} the pressure of gas in equilibrium with the concentration of gas in liquid.

The group $\int \frac{dP_a}{(P_a - P_{ae})}$ has been defined (62) as the number of overall gas transfer units N.T.U. The height of a transfer unit is defined as $\frac{Z}{N.T.U.}$

This concept has been extended to gas catalytic reactors by Lamplichler (32) and elaborated by Hurt (33) for a first order gas reaction. Both defined a new quantity - the height of a reactor unit (H.R.U.). Narsimhan and Doraiswamy (34) have attempted to apply it to a second order reaction.

In the case of combined mass transfer and chemical reaction as encountered in the slurried bed reactor, the driving force is difficult to define. It is reasonable to hold the upper limit as the partial pressure of the reacting gas in the gas bubble and the lower limit as

that pressure of the reacting gas which would be in equilibrium with the product partial pressure at that point in the reactor.

If in the case under consideration

$$\frac{P_c}{P_a^* P_b^*} = K_p \qquad - 1.2.27.$$

Then, the driving force is given by $(P_a - P_a^*)$

It is now possible to postulate overall instantaneous rate equations for the process for both reactants

$$N_a = \bar{K}_{ga} A_{gl} (P_a - P_a^*) \qquad - 1.2.28.$$

$$N_b = \bar{K}_{gb} A_{gl} (P_b - P_b^*) \qquad - 1.2.29.$$

A_{gl} has been chosen in preference to A_{ls} because in the slurried bed reactor the solid liquid interfacial area may be made very large if desired, whereas, for a given gas flow rate, the gas liquid area can only be changed slightly (24). It therefore seems logical to base this work on the gas-liquid interfacial area assuming that the liquid-solid interface can be altered to have no influence on the reaction rate.

The reaction is mole for mole

$$\therefore N_a = N_b = N_c$$

$$\text{Hence } P_a - P_a^* = \frac{\bar{K}_{gb}}{\bar{K}_{ga}} (P_b - P_b^*) \qquad - 1.2.30.$$

At any point in the reactor, the relationship between P_b and P_a is given by $P_b = \alpha' P_a$

Similarly at the reactor inlet

$$P_{bi} = \alpha P_{ai}$$

The relationship between α and α' is given in note 1.

Equation 1.2. 30 may be written

$$\frac{\overline{K}_{ga}}{P_b - P_b^*} = K' = \frac{\overline{K}_{gb}}{P_a - P_a^*}$$

$$\therefore \quad \overline{K}_{ga} = K' P_b - K' P_b^*$$

$$\therefore \quad P_b^* = P_b - \frac{\overline{K}_{ga}}{K'}$$

$$= P_b - \frac{\overline{K}_{ga}}{\overline{K}_{gb}} (P_a - P_a^*) \qquad - 1.2.31.$$

But $P_b = \alpha' P_a$

$$\therefore \quad P_b^* = \alpha' P_a - \frac{\overline{K}_{ga}}{\overline{K}_{gb}} P_a + \frac{\overline{K}_{ga}}{\overline{K}_{gb}} P_a^*$$

$$= P_a(\alpha' - \frac{\overline{K}_{ga}}{\overline{K}_{gb}}) + \frac{\overline{K}_{ga}}{\overline{K}_{gb}} P_a^*$$

or $P_b^* = \alpha' P_a - \frac{\overline{K}_{ga}}{K'}$

Now $K_p = \frac{P_c}{P_a^* P_b^*} = \frac{P_c}{P_a^* \left[\alpha' P_a - \frac{\overline{K}_{ga}}{\overline{K}_{gb}} (P_a - P_a^*)\right]}$

$$= \frac{P_c}{P_a^{*}\left[P_a(\alpha' - \frac{\bar{K}_{ga}}{\bar{K}_{gb}}) + \frac{\bar{K}_{ga}}{\bar{K}_{gb}} P_a^{*}\right]}$$

$$= \frac{P_c}{P_a^{*} P_a (\alpha' - \frac{\bar{K}_{ga}}{\bar{K}_{gb}}) + P_a^{*2} \frac{\bar{K}_{ga}}{\bar{K}_{gb}}} \qquad - 1.2.32.$$

This is of the form

$$d = \frac{a}{bx + cx^2}$$

where $a = P_c$

$$b = P_a\left[\alpha' - \frac{\bar{K}_{ga}}{\bar{K}_{gb}}\right] = P_a(\alpha' - c)$$

where $c = \frac{\bar{K}_{ga}}{\bar{K}_{gb}}$

$d = K_p$

$x = P_a^{*}$

P_a^{*} is the variable which is of interest.

The original equation may be written as

$$x^2 + \frac{bx}{c} - \frac{a}{cd} = 0$$

The solutions of these equations are as follows:-

$$x = \frac{-b}{2c} + \sqrt{\frac{a}{cd} + \frac{b^2}{4c^2}} \qquad \text{root A}$$

$$x = \frac{-b}{2c} - \sqrt{\frac{a}{cd} + \frac{b^2}{4c^2}} \qquad \text{root B}$$

Writing these out fully

$$P_a^{\ast} = \frac{-P_a(\alpha' - \frac{\bar{K}_{ga}}{\bar{K}_{gb}})}{2\frac{\bar{K}_{ga}}{\bar{K}_{gb}}} + \sqrt{\frac{P_c}{K_p\frac{\bar{K}_{ga}}{\bar{K}_{gb}}} + \left[\frac{P_a(\alpha' - \bar{K}_{ga})}{2\frac{\bar{K}_{ga}}{\bar{K}_{gb}}}\right]^2}$$

Now $\dfrac{P_c}{K_p\frac{\bar{K}_{ga}}{\bar{K}_{gb}}}$ is always positive as is $\left[\dfrac{P_a(\alpha' - \bar{K}_{ga})}{2\frac{\bar{K}_{ga}}{\bar{K}_{gb}}}\right]^2$

$$\left|\sqrt{\frac{P_c}{K_p\frac{\bar{K}_{ga}}{\bar{K}_{ga}}} + \left[\frac{P_a(\alpha' - \bar{K}_{ga})}{2\frac{\bar{K}_{ga}}{\bar{K}_{gb}}}\right]^2}\right| \text{ is always } > \left|\frac{-P_a(\alpha' - \frac{\bar{K}_{ga}}{\bar{K}_{gb}})}{2\frac{\bar{K}_{ga}}{\bar{K}_{gb}}}\right|$$

Hence root B always has a negative value and may be disregarded.

From a consideration of root A, it can be shown that when K_p is large $P_a^{\ast}$ will be small

ie. as $K_p \longrightarrow \infty$ $\quad P_a^{\ast} \longrightarrow 0$

For large values of K_p, greater than 10^6 say, P_a^* may reasonably be assumed to be 0.

Equation 1.2.28 then becomes

$$N_a = \overline{K}_{ga} A_{gl} P_a \qquad - 1.2.33.$$

Such a reaction might be said to follow pseudo first order kinetics.

Through the reactor, the flow varies with conversion. It can be shown that, at that point in the reactor where the conversion is x, the flow F_x is given by (note 2)

$$F_x = \frac{\pi_g F_i^M \alpha}{(1+\alpha)(\pi_g - P_a)} \qquad - 1.2.34.$$

Similarly $$F_x = \frac{\pi_g F_i^M \beta}{(1+\beta)(\pi_g - P_b)} \qquad - 1.2.35.$$

Consider now an element of reactor dZ at the point where conversion is x

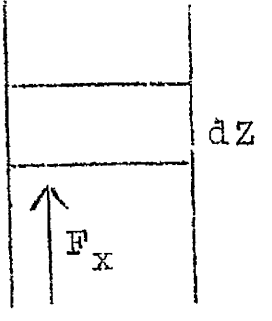

Moles of A converted in element dZ are given by

$$N_a' = \overline{K}_{ga} A_{gl} (P_a - P_a^{*}) \gamma \, dZ$$

Under the conditions existing (K_p large)

$$P_a^{*} \longrightarrow 0$$

$$\therefore \quad N_a' = \overline{K}_{ga} A_{gl} P_a \gamma \, dZ \qquad - 1.2.36.$$

$$\text{Also moles of } N_a' = \frac{d P_a . F_x}{\pi_g} \qquad - 1.2.37.$$

$$\text{or} \quad N_a = \frac{d P_a}{\pi_g} \cdot \frac{F_x}{\gamma \, dZ}$$

Note:- F_x refers to the molal flow rate of gases A, B and C only in reactor and does not include the molal flow rate of the vapour from the liquid medium.

Hence equating 1.2.36 and 1.2.37

$$\frac{d P_a}{\pi_g} F_x = \overline{K}_{ga} A_{gl} P_a \gamma \, dZ$$

$$\therefore \quad \frac{d P_a}{\pi_g} \cdot \frac{F_i^{M} \alpha \pi_g}{(1 + \alpha)(\pi_g - P_a)} = \overline{K}_{ga} A_{gl} P_a \gamma \, dZ$$

If this expression is integrated over the reactor

$$\frac{\alpha}{\pi_{gm}(1+\alpha)} \int_{P_{ao}}^{P_{ai}} \frac{\pi_g \, d P_a}{P_a(\pi_g - P_a)} = \frac{\bar{K}_{ga} A_{glm} \gamma}{F_i^M} \int_0^Z dZ \qquad - 1.2.38.$$

In the integration, it is assumed that $\bar{K}_{ga}$ and A_{glm} are constant.

$$\therefore \quad \frac{\alpha}{(1+\alpha)} \left[\ln \frac{P_{ai}}{P_{ao}} + \ln \frac{\pi_{go} - P_{ao}}{\pi_{gi} - P_{ai}} \right] = \frac{\bar{K}_{ga} A_{glm} \gamma Z \pi_{gm}}{F_i^M} \qquad - 1.2.39.$$

$$\text{or} \quad \frac{V_R}{F_i^M} = \frac{\alpha}{\pi_{gm}(1+\alpha) \bar{K}_{ga} A_{glm}} \left[\ln \frac{P_{ai}}{P_{ao}} + \ln \frac{\pi_{go} - P_{ao}}{\pi_{gi} - P_{ai}} \right] \qquad - 1.2.40$$

$$\text{Also} \quad \frac{V_R}{F_i^M} = \frac{\beta}{\pi_{gm}(1+\beta) \bar{K}_{gb} A_{glm}} \left[\ln \frac{P_{bi}}{P_{bo}} + \ln \frac{\pi_{go} - P_{bo}}{\pi_{gi} - P_{bi}} \right]$$

It is of interest to compare the above equations with a conventional reactor design equation:-

$$\text{eg.} \quad \frac{V_R}{F_i^M} = \int_0^x \frac{dx}{r}$$

where r is the apparent reaction rate in terms of x, the conversion.

Equation 1.2.38 may be written thus

$$\frac{\alpha}{(1+\alpha)} \int_{P_{ao}}^{P_{ai}} \frac{\pi_g \, dP_a}{P_a (\pi_g - P_a)} = \frac{\overline{K}_{ga} A_{glm} \delta \pi_{gm}}{F_i^M} \int_0^Z dZ$$

$$\frac{\alpha}{(1+\alpha)} \int_{P_{ao}}^{P_{ai}} \frac{\pi_g \, dP_a}{P_a (\pi_g - P_a)} = \frac{\overline{K}_{ga} A_{glm} \pi_{gm} Z}{F_i^M}$$

The number of reactor units is here defined as

$$\text{N.R.U.} = \frac{\alpha}{1+\alpha} \int_{P_{ao}}^{P_{ai}} \frac{\pi_g \, dP_a}{P_a (\pi_g - P_a)}$$

$$= \frac{\alpha}{1+\alpha} \left[\ln \frac{P_{ai}}{P_{ao}} - \ln \frac{\pi_{go} - P_{ao}}{\pi_{gi} - P_{ai}} \right] \quad - 1.2.41.$$

If $\text{N.R.U.} = \dfrac{Z}{\text{H.R.U.}}$, it follows that

$$\text{H.R.U.} = \frac{F_i^M}{\overline{K}_{ga} A_{glm} \delta \pi_{gm}} \quad - 1.2.42.$$

It should be possible to assemble the height of a reactor unit from components dealing with mass transfer (H.T.U.), and chemical reaction (H.Ch.U.).

This is next attempted.

The Overall Mass Transfer Coefficient.

Equation 1.2.11 states that the rate of a catalytic gas reaction on a defined area of catalyst surface is given by

$$r = K_1'(P_a P_b - \frac{P_c}{K_p})$$

In the case of the slurried bed reactor, the effective partial pressures which correspond most nearly to P_a.P_b and P_c are P_{als}.P_{bls} and P_{cls}. It is desirable to relate P_{als}.P_{bls} and P_{cls} to P_a,P_b and P_c the bulk gas pressures.

From 1.2.12, 1.2.13, 1.2.14 and 1.2.15 it may be shown that

$$N_a \left(\frac{1}{K_{a1} A_{gl}} + \frac{1}{K_{a2} H_a A_{gl}} + \frac{1}{K_{a3} H_a A_{gl}} + \frac{1}{K_{a4} H_a A_{ls}} \right) = (P_a - P_{als}) \qquad - 1.2.43.$$

The overall mass transfer coefficient may be defined as

$$\frac{1}{K_{ga}} = \frac{1}{K_{a1}} + \frac{1}{K_{a2} H_a} + \frac{1}{K_{a3} H_a} + \frac{A_{gl}}{K_{a4} H_a A_{ls}} \qquad - 1.2.44.$$

$$\text{and} \quad N_a = K_{ga} A_{gl} (P_a - P_{als}) \qquad - 1.2.45.$$

Similar expressions may be obtained for B and C.

The Chemical Rate Coefficient.

A chemical rate coefficient K_r may be defined in the following terms

$$N_a = K_{ra} A_{ls} (P_{als} - P_a^{*}) \qquad - 1.2.46.$$

In terms of equation 1.2.11, the rate per unit

reactor volume is given by

$$N_a = K_1 A_{ls}\left(P_{als}P_{bls} - \frac{P_{cls}}{K_p}\right)$$

When K_p is large

$$K_{ra}P_{als} = K_1 P_{als}P_{bls}$$

$$\therefore \quad K_{ra} = K_1 P_{bls} \qquad - 1.2.47.$$

When $P_{bls} = \delta' P_{als}$

Then $\delta' = \frac{\pi_g}{P_{als}}\left(1 - \frac{1}{\delta}\right) + \frac{1}{\delta}$ (Note 1)

where $\delta = \frac{P_{blsi}}{P_{alsi}}$

$$\therefore \quad K_{ra} = K_1\left[\pi_g\left(1 - \frac{1}{\delta}\right) + \frac{P_{als}}{\delta}\right] \qquad - 1.2.48.$$

Since K_{ra} is a function of P_{als} it cannot be a true coefficient. However it can be used to relate other coefficients. In equation 1.2.28

$$N_a = \bar{K}_{ga}A_{gl}(P_a - P_a^{*})$$

$$= \bar{K}_{ga}A_{gl}\left[(P_a - P_{als}) + (P_{als} - P_a^{*})\right]$$

$$= \bar{K}_{ga}A_{gl}\left[\frac{N_a}{K_{ga}A_{gl}} + \frac{N_a}{K_r A_{ls}}\right]$$

whence $$\frac{1}{\bar{K}_{ga}} = \frac{1}{K_{ga}} + \frac{1}{K_{ra}}\cdot\frac{A_{gl}}{A_{ls}} \qquad - 1.2.49.$$

A similar expression may be obtained for reactant B.

The inference of this equation is that in a slurried bed reactor when $\frac{1}{K_{ra}} \frac{A_{gl}}{A_{ls}}$ becomes $\gg \frac{1}{K_{ga}}$, the overall process coefficient $\frac{1}{K_{ga}}$ becomes effectively $\frac{1}{K_{ga}}$.

Under other conditions $\frac{1}{K_{ga}}$ is not a true coefficient.

The rate at the catalyst surface is given by equation 1.2.11

$$N_a = K_1 A_{ls}(P_{als}P_{bls} - \frac{P_{als}}{K_p})$$

If K_p is large:-

$$N_a = K_1 A_{ls} P_{als} P_{bls} \qquad - 1.2.50$$

If the chemical reaction is not the rate controlling step, then N_a is a function of mass transfer alone, and P_{als} and P_{bls} will be small.

Irrespective of what regime is controlling, equation 1.2.50 is true.

Substituting for P_{als} and P_{bls} from equation 1.2.45 etc., and equating with 1.2.37

$$\frac{F_x}{\gamma dz} \frac{dP_a}{\pi_g} = N_a = K_1 A_{ls}\left(P_a - \frac{N_a}{K_{ga}A_{gl}}\right)\left(P_b - \frac{N_b}{K_{gb}A_{gl}}\right)$$

$$- 1.2.51.$$

This equation is easily solvable for limiting cases only.

There are 2 possibilities -

1. One mass transfer term dominant and the forward rate constant influential. Suppose $K_{ga} < K_{gb}$

From equation 1.2.51

$$\frac{F_x}{\gamma\, dZ} \cdot \frac{dP_a}{\pi_g} = K_1 A_{1s}\left(P_a - \frac{N_a}{K_{ga}A_{gl}}\right) P_b$$

$$= K_1 A_{1s}\left(P_a - \frac{F_x\, dP_a}{\gamma\, dZ\, \pi_g} \cdot \frac{1}{K_{ga}A_{gl}}\right) P_b$$

$$\therefore \frac{F_x}{\gamma\, dZ} \frac{dP_a}{\pi_g}\left(1 + \frac{K_1 A_{1s}\alpha' P_a}{K_{ga}A_{gl}}\right) = K_1 A_{1s} P_a P_b$$

$$\therefore \frac{F_x dP_a}{\gamma\, dZ\, \pi_g} = \frac{K_1 A_{1s}\alpha' P_a}{1 + \frac{K_1 A_{1s}\alpha' P_a}{K_{ga}A_{gl}}}$$

Substituting for F_x and rationalising

$$\frac{V_R}{F_i^M} = \frac{\alpha}{1+\alpha} \int_{P_{ao}}^{P_{ai}} \frac{\frac{dP_a}{K_1 A_{1s}\alpha' P_a^2(\pi_g - P_a)}}{1 + \frac{K_1 A_{1s}\alpha' P_a}{A_{gl} K_{ga}}}$$

$$= \frac{\alpha^2}{K_1 A_{1s}(1+\alpha)} \int_{P_{ao}}^{P_{ai}} \frac{dP_a}{\{\pi_g(\alpha - 1) + P_a\} P_a \{\pi_g - P_a\}}$$

$$+ \frac{\alpha}{(1+\alpha) K_{ga} A_{glm}} \int_{P_{ao}}^{P_{ai}} \frac{dP_a}{P_a(\pi_g - P_a)}$$

$$= \frac{\alpha^2}{(1+\alpha)K_1 A_{1s} \pi_{gm}^2}\left[\frac{-1}{\alpha(\alpha-1)} \ln\frac{\pi_{gi}(\alpha-1)+P_{ai}}{\pi_{go}(\alpha-1)+P_{ao}} + \frac{1}{\alpha-1}\ln\frac{P_{ai}}{P_{ao}} + \frac{1}{\alpha}\ln\frac{(\pi_{go}-P_{ao})}{(\pi_{gi}-P_{ai})}\right] + \frac{\alpha}{(1+\alpha)K_{ga}A_{g1}\pi_{gm}} \ln\frac{(\pi_{go}-P_{ao})}{(\pi_{gi}-P_{ai})}\frac{P_{ai}}{P_{ao}}$$

- 1.2.52.

(For integration see Note 3.)

When $\alpha = 1$ (Note 4)

$$\frac{V_R}{F_i^M} = \frac{\alpha}{(1+\alpha)K_1 A_{1s}\pi_{gm}^2}\left[\ln\frac{P_{ai}}{P_{ao}} + \ln\frac{\pi_{go}-P_{ao}}{\pi_{gi}-P_{ai}} + \left(\frac{\pi_{go}}{P_{ao}} - \frac{\pi_{gi}}{P_{ai}}\right)\right]$$

$$+ \frac{\alpha}{(1+\alpha)K_{ga}A_{g1m}\pi_{gm}} \ln\frac{(\pi_{go}-P_{ao})}{(\pi_{gi}-P_{ai})}\frac{P_{ai}}{P_{ao}} \qquad - 1.2.53.$$

The number of chemical units is defined as

$$N.Ch.U_a = \left[\frac{-1}{\alpha(\alpha-1)} \ln\frac{\pi_{gi}(\alpha-1)+P_{ai}}{\pi_{go}(\alpha-1)+P_{ao}} + \frac{1}{(\alpha-1)}\ln\frac{P_{ai}}{P_{ao}} - \frac{1}{\alpha}\ln\frac{\pi_{go}-P_{ao}}{\pi_{gi}-P_{ai}}\right] \qquad - 1.2.54.$$

$$\text{or } N.Ch.U_a = \frac{\alpha}{1+\alpha}\left[\ln\frac{P_{ai}}{P_{ao}} + \ln\frac{\pi_{go}-P_{ao}}{\pi_{gi}-P_{ai}} + \left(\frac{\pi_{go}}{P_{ao}} - \frac{\pi_{gi}}{P_{ai}}\right)\right] \qquad - 1.2.55.$$

The number of chemical units is a measure of the driving force overcoming the chemical resistance as opposed to the diffusional resistance.

From 1.2.53

$$\frac{V_R}{F_i^M} = \frac{N.Ch.U_a}{\pi_{gm}^2 K_1 A_{1s}} + \frac{N.R.U_a}{K_{ga}A_{g1m}\pi_{gm}} \qquad - 1.2.56.$$

$$\therefore \frac{V_R}{F_i^M \, N.Ch.U_a} = \frac{1}{\pi_{gm}^2 K_l A_{ls}} + \frac{N.R.U_a}{N.Ch.U_a} \cdot \frac{1}{K_{ga} A_{glm} \pi_{gm}} \quad - 1.2.57.$$

This equation is of conceivable importance in reactor design.

The height of a transfer unit $H.T.U = \frac{Z}{H.T.U_a}$

N.T.U. is here defined as $= \frac{K_{ga} A_{glm} \gamma Z \pi_{gm}}{F_i^M}$

(N.T.U. is less easy to define precisely than in the case of simple gas absorption).

Hence $Z = \frac{N.Ch.U_a}{K_l A_{ls} \gamma \pi_{gm}^2} + N.R.U_a \, H.T.U_a$ From 1.2.57

$$\therefore 1 = \frac{F_i^M}{K_l \gamma \pi_{gm}^2 H.Ch.U_a} + \frac{H.T.U_a}{H.R.U_a}$$

$$\therefore H.Ch.U_a = \frac{1}{\left(1 - \frac{H.T.U_a}{H.R.U_a}\right)} \cdot \frac{F_i^M}{K_l A_{ls} \gamma \pi_{gm}^2} \quad - 1.2.58.$$

---

2. In this case the forward rate constant is dominant and K_{ga} is large

Equation 1.2.53 becomes $\frac{V_R}{F_i^M \, N.Ch.U_a} = \frac{1}{\pi_{gm}^2 K_l A_{ls}}$ - 1.2.59.

and $H.Ch.U. = \frac{F_i^M}{K_l A_{ls} \gamma \pi_{gm}^2}$ - 1.2.60

Note 1. $\frac{P_{bi}}{P_{ai}} = \alpha = \frac{Y_{bi}}{Y_{ai}}$; $\frac{P_b}{P_a} = \alpha' = \frac{Y_b}{Y_a}$

α' may be related to α

$$F_x = \frac{F_i^M \alpha}{(1+\alpha)(1-Y_a)} \qquad \text{(see note 2)}$$

Now $F_x Y_a + F_x Y_b + F_x Y_c = F_x$

Also, from a mass balance $F_x Y_a = F_i^M Y_{ai} - F_x Y_c$

$$\therefore F_x Y_a = F_i^M Y_{ai} - F_x + F_x Y_a + F_x Y_b$$

$$\therefore F_x = F_i^M Y_{ai} + F_x Y_b$$

$$\therefore \frac{F_i^M \alpha}{(1+\alpha)(1-Y_a)} = F_i^M Y_{ai} + \frac{F_i^M \alpha Y_b}{(1+\alpha)(1-Y_a)}$$

$$\therefore \frac{\alpha}{(1+\alpha)(1-Y_a)} = Y_{ai} + \frac{\alpha Y_b}{(1+\alpha)(1-Y_a)}$$

$$\therefore Y_b = 1 - \frac{Y_{ai}(1+\alpha)(1-Y_a)}{\alpha} = 1 - \frac{(1-Y_a)}{\alpha}$$

Now $\alpha' Y_a = Y_b$

$$\therefore \alpha' Y_a = 1 - \frac{(1-Y_a)}{\alpha} = \frac{1}{\alpha}(\alpha - 1) + \frac{Y_a}{\alpha}$$

$$\therefore \alpha' = \frac{1}{\alpha Y_a}(\alpha - 1) + \frac{1}{\alpha}$$

$$\therefore \alpha' = \frac{1}{Y_a}\left(1 - \frac{1}{\alpha}\right) + \frac{1}{\alpha}$$

$$\text{or } \alpha' = \frac{\pi_g}{P_a}\left(1 - \frac{1}{\alpha}\right) + \frac{1}{\alpha}$$

Note 2. In the slurried bed reactor, certain complications arise in defining the mole fractions of the components. Normally the mole fraction of a gas in a mixture equals the partial pressure of the gas divided by total pressure. However, in the slurried bed reactor, the liquid medium present exerts a partial pressure. The total pressure of gas in the reactor is hence equal to the total pressure less the partial pressure of the liquid. The total pressure used to define mole fractions in this work is therefore the total reactor pressure less the liquid partial pressure

$$\pi_g = \pi_r - \pi_l$$

According to this, mole fraction of A $= \frac{p_a}{\pi_g}$

" " " B $= \frac{p_b}{\pi_g}$

" " " C $= \frac{p_c}{\pi_g}$

These mole fractions are thus equal to the mole fractions of gas in any mixture free of liquid vapour and prevent confusion in practice when inlet and outlet vapour free streams are being analysed and the results used to compute the partial pressures existing within the reactor.

Through the reactor, the flow of gas varies with conversion. The flow at any point in the reactor where the conversion is x may be deduced thus:-

Suppose the inlet partial pressures of A and B are related thus

$$P_{bi} = \alpha P_{ai}$$

Inlet molar flow rate = F_i^M

Moles A entering reactor = $F_i^M \frac{P_{ai}}{\pi_{gi}}$

Moles B entering reactor = $F_i^M \frac{P_{bi}}{\pi_{gi}}$

At point where conversion is x, flow of reactants is F_x.

In the type of reaction being discussed

Moles C formed = Moles A used = Moles B used

Moles A used = $F_i^M \frac{P_{ai}}{\pi_{gi}} - F_x \frac{P_a}{\pi_g}$ — (A)

= Moles B used = $F_i^M \frac{P_{bi}}{\pi_{gi}} - F_x \frac{P_b}{\pi_g}$

$= F_i^M \alpha \frac{P_{ai}}{\pi_{gi}} - F_x \frac{P_b}{\pi_g}$ — (B)

= Moles C produced = $F_x \frac{P_c}{\pi_g}$ — (C)

$$\therefore F_i^M \frac{P_{ai}}{\Pi_{gi}} - F_x \frac{P_a}{\Pi_g} = F_i^M \propto \frac{P_{ai}}{\Pi_{gi}} - F_x \frac{P_b}{\Pi_g}$$

$$\therefore F_x \frac{P_b}{\Pi_g} = F_i^M \propto \frac{P_{ai}}{\Pi_{gi}} - F_i^M \frac{P_{ai}}{\Pi_{gi}} + F_x \frac{P_a}{\Pi_g} \quad \text{— (D)}$$

$$\therefore \frac{P_b}{\Pi_g} = \frac{F_i^M}{F_x} \propto \frac{P_{ai}}{\Pi_{gi}} - \frac{F_i^M}{F_x} \frac{P_{ai}}{\Pi_{gi}} + \frac{P_a}{\Pi_g} \quad \text{— (E)}$$

Since $P_a + P_b + P_c = \Pi_g$

$$\frac{P_a F_x}{\Pi_g} + \frac{P_b F_x}{\Pi_g} + \frac{P_c F_x}{\Pi_g} = \frac{\Pi_g F_x}{\Pi_g}$$

$$\therefore \frac{P_c F_x}{\Pi_g} = F_x \left[1 - \frac{P_b}{\Pi_g} - \frac{P_a}{\Pi_g} \right] \quad \text{— (F)}$$

Substitution of E into F gives

$$\frac{P_c F_x}{\Pi_g} = F_x - \frac{P_a F_x}{\Pi_g} - \frac{F_i^M \propto P_{ai}}{\Pi_{gi}} + \frac{F_i P_{ai}}{\Pi_{gi}} - \frac{F_x P_a}{\Pi_g}$$

$$= F_x \left[1 - \frac{2P_a}{\Pi_g} \right] + F_i^M \left[\frac{P_{ai}}{\Pi_{gi}} - \frac{\propto P_{ai}}{\Pi_{gi}} \right] \quad \text{— (G)}$$

Since moles A used = Moles C formed

Substitution of (G) into (C) gives:-

$$F_i^M \frac{P_{ai}}{\pi_{gi}} - F_x \frac{P_a}{\pi_g} = F_x \left[1 - \frac{2P_a}{\pi_g}\right] + F_i^M \left[\frac{P_{ai}}{\pi_{gi}} - \frac{\alpha P_{ai}}{\pi_{gi}}\right]$$

$$\therefore \quad F_x \left[1 - \frac{P_a}{\pi_g}\right] = \frac{F_i^M}{\pi_{gi}} \left[P_{ai} - P_{ai} + \alpha P_{ai}\right]$$

$$= \frac{F_i^M \alpha P_{ai}}{\pi_{gi}}$$

$$\therefore \quad F_x = \frac{F_i^M \alpha \frac{P_{ai}}{\pi_{gi}}}{1 - \frac{P_a}{\pi_g}}$$

Now $P_{ai} + P_{bi} = \pi_{gi}$

$$\therefore \quad P_{ai} + \alpha P_{ai} = \pi_{gi}$$

$$\therefore \quad P_{ai} = \frac{\pi_{gi}}{1 + \alpha}$$

$$\therefore \quad F_x = \frac{F_i^M \alpha \frac{\pi_{gi}}{\pi_{gi}(1 + \alpha)}}{1 - \frac{P_a}{\pi_g}} \qquad \text{— (H)}$$

$$\therefore \quad F_x = \frac{\pi_g F_i^M \alpha}{(1+\alpha)(\pi_g - P_a)}$$

$$\text{or} \quad F_x = \frac{F_i^M \alpha}{(1+\alpha)(1 - Y_a)}$$

$$\text{Similarly} \quad F_x = \frac{\pi_g F_i^M \beta}{(1+\beta)(\pi_g - P_b)}$$

$$\text{where } \beta = \frac{1}{\alpha}$$

Note 3.

The integration of $\dfrac{dP_a}{\left[\pi(\alpha - 1) + P_a\right] P \left[\pi_g - P_a\right]}$

Let $\pi_g(\alpha - 1) = A$

and $\pi_g = B$

As it is desired to integrate the expression between the limits P_{ai} and P_{ao}, the expression becomes

$$\int_{P_{ao}}^{P_{ai}} \frac{dP_a}{(A + P_a) P_a (B - P_a)}$$

Before this can be integrated it must be split into partial fractions thus:-

$$\int_{P_{ao}}^{P_{ai}} \left[\frac{-1}{A(A + B)(A + B)} + \frac{1}{ABP_a} + \frac{1}{B(A + B)(B - P_a)} \right] dP_a$$

$$= \int_{P_{ao}}^{P_{ai}} \frac{-dP_a}{A(A + B)(A + P_a)} + \int_{P_{ao}}^{P_{ai}} \frac{dP_a}{ABP_a} + \int_{P_{ao}}^{P_{ai}} \frac{dP_a}{B(A + B)(B - P_a)}$$

$$= \left[\frac{-1}{A(A+B)} \ln(A + P_a) + \frac{1}{AB} \ln P_a - \frac{1}{B(A+B)} \ln(B - P_a) \right]_{P_{ao}}^{P_{ai}}$$

$$= \frac{1}{\alpha(\alpha-1)\pi_g^2} \left[\ln \pi_g(\alpha - 1) + P_a \right]_{P_{ao}}^{P_{ai}} + \frac{1}{(\alpha-1)\pi_g^2} \left[\ln P_a \right]_{P_{ao}}^{P_{ai}}$$

$$- \frac{1}{\pi_g^2} \left[\ln(\pi - P_a) \right]_{P_{ao}}^{P_{ai}}$$

$$= \frac{1}{\pi_g^2} \left[\frac{-1}{\alpha(\alpha-1)} \ln \frac{\pi_{gi}(\alpha-1) + P_{ai}}{\pi_{go}(\alpha-1) + P_{ao}} \right] + \frac{1}{\alpha - 1} \ln \frac{P_{ai}}{P_{ao}}$$

$$+ \frac{1}{\alpha} \ln \frac{\pi_{go} - P_{ao}}{\pi_{gi} - P_{ai}}$$

Note 4.

Consider the expression

$$\left[\frac{-1}{\alpha(\alpha-1)}\ln\frac{\pi_{gi}(\alpha-1)+P_{ao}}{\pi_{go}(\alpha-1)+P_{ai}}+\frac{1}{(\alpha-1)}\ln\frac{P_{ai}}{P_{ao}}\right]$$

$$=\left[\frac{-1}{\alpha(\alpha-1)}\ln\frac{P_{ai}\left[\frac{1+(\alpha-1)\pi_{gi}}{P_{ai}}\right]}{P_{ao}\left[1+\frac{(\alpha-1)\pi_{go}}{P_{ao}}\right]}+\frac{1}{(\alpha-1)}\ln\frac{P_{ai}}{P_{ao}}\right]$$

$$=\frac{-1}{\alpha(\alpha-1)}\ln\frac{P_{ai}}{P_{ao}}+\frac{1}{\alpha-1}\ln\frac{P_{ai}}{P_{ao}}$$

$$-\frac{1}{\alpha(\alpha-1)}\left\{\ln\left[1+\frac{(\alpha-1)\pi_{gi}}{P_{ai}}\right]-\ln\left[1+\frac{(\alpha-1)\pi_{go}}{P_{go}}\right]\right\}$$

The expansion of the log terms in $\{\ \}$ gives

$$\frac{-1}{\alpha(\alpha-1)}\ln\frac{P_{ai}}{P_{ao}}+\frac{1}{\alpha-1}\ln\frac{P_{ai}}{P_{ao}}$$

$$-\frac{1}{\alpha(\alpha-1)}\left[\frac{(\alpha-1)\pi_{gi}}{P_{ai}}-\frac{(\alpha-1)^2\pi_{gi}^2}{2P_{ai}^2}+\frac{(\alpha-1)^3\pi_{gi}}{3P_{ai}^3}\cdots\right]$$

$$+\frac{1}{\alpha(\alpha-1)}\left[\frac{(\alpha-1)\pi_{go}}{P_{ao}}-\frac{(\alpha-1)^2\pi_{go}^2}{2P_{ao}^2}+\frac{(\alpha-1)^3\pi_{go}^3}{3P_{ao}^3}\cdots\right]$$

When $\alpha \simeq 1$ this series need not be taken further than the first term. Hence the expression becomes

$$\ln \frac{P_{ai}}{P_{ao}} \left[\frac{1}{\alpha - 1} - \frac{1}{\alpha(\alpha - 1)} \right] - \frac{1}{\alpha} \left[\frac{\pi_{gi}}{P_{ai}} - \frac{\pi_{go}}{P_{gi}} \right]$$

$$= \frac{1}{\alpha} \left[\ln \frac{P_{ai}}{P_{ao}} + \left(\frac{\pi_{go}}{P_{ao}} - \frac{\pi_{gi}}{P_{ai}} \right) \right]$$

Hence N.Ch.U. may be written as

$$\text{N.Ch.U.} = \frac{\alpha^2}{(1+\alpha)} \left[\frac{1}{\alpha} \left\{ \ln \frac{P_{ai}}{P_{ao}} + \left(\frac{\pi_{go}}{P_{ao}} - \frac{\pi_{gi}}{P_{ai}} \right) \right\} + \frac{1}{\alpha} \ln \frac{\pi_{go} - P_{ao}}{\pi_{gi} - P_{ai}} \right]$$

$$= \frac{\alpha}{(1+\alpha)} \left[\ln \frac{P_{ai}}{P_{ao}} + \ln \frac{\pi_{go} - P_{ao}}{\pi_{gi} - P_{ai}} + \left(\frac{\pi_{go}}{P_{ao}} - \frac{\pi_{gi}}{P_{ai}} \right) \right]$$

1. 3. THE EXPERIMENTAL MODEL.

An experimental model is required to test the mathemetical model. The hydrogenation of ethylene in a slurried bed reactor is considered to provide a suitable model.

$$C_2H_4 + H_2 \longrightarrow C_2H_6$$

At 18°C, ΔH_F = -32,732 cals/gm mol., and the reaction is highly exothermic. This reaction has a large equilibrium constant at normal temperatures (Appendix I). While it has been claimed to be a first order reaction under certain conditions (35), it is a bimolecular reaction and it is here considered to be a second order reaction (36). Calderbank has also used the hydrogenation of ethylene in the study of slurried bed reactors (10).

Undergraduate research has claimed the reaction to be almost free of side reactions at temperatures below 100°C although methane formation can occur at higher temperatures. It was decided to carry out the reaction at 75°C for most of the work and ignore the possibility of methane formation. While the reaction is exothermic, previous work on small scale slurried bed reactors with exothermic reactions has shown that, at elevated temperatures, heat must be added, rather than removed, to maintain the temperature (24). This is presumably due to heat losses exceeding heat

production. Any small scale reactor must include provision for heat addition and temperature control. Previous work (9)(24) indicated Raney nickel as a suitable hydrogeneration catalyst in a slurried bed. Also in the light of previous work (9)(24) the use of a cyclic hydrocarbon such as xylene is envisaged as the catalyst suspending medium.

The experimental reactor had to be designed to allow variation of the parameters of reactor length and volume, gas flow rate, inlet gas composition and operating temperature. Operating data of a fundamental nature must also be easily measurable. This includes:

(a) Flow rate of inlet gas stream.

(b) Composition of inlet gas stream.

(c) Composition of outlet gas stream.

(d) Flow rate of outlet gas stream.

(e) Operating temperature.

(f) Gas liquid interfacial area.

(g) Liquid solid interfacial area.

Thus the experimental model may be specified as a slurried bed reactor for hydrogenating ethylene at 75°C with Raney nickel suspended in xylene as the slurried bed. The detail design was determined by the experimental requirements listed above.

The work is subject to certain limitations. For financial reasons, the apparatus has been restricted to bench scale. The glass apparatus eventually used can only be operated at atmospheric pressure.

APPARATUS AND EXPERIMENTAL PROCEDURE.

2. 1. THE EXPERIMENTAL LAYOUT is shown in Fig. 2. 1. Gas is pumped from the gas holder C through the flowmeter D, the gas purification system E and the wet gas meter F by the gas pump G. The gas then flows to the reactor H. The reaction products pass through the cooler I to the gas analysis unit J and finally are vented from the system after passing through the wet gas meter K.

2. 2. REACTANT GAS SUPPLY SYSTEM.

Hydrogen and ethylene from the high pressure cylinders A are metered through a system of valves, at pressures only slightly above atmospheric, into the gas holder C, via the wet gas meter B. The gas holder consists of the inner tube of a large lorry tyre. It has a capacity of approximately 100 litres. The reactant gases from the holder pass through the flow meter D. This is a capillary flow meter with a manometer containing a coloured liquid. Its purpose is to indicate the steadiness of the flow. As the reactant gas may contain traces of O_2 and CO_2, which are catalyst poisons, an absorption train, E, of a 12½% pyrogallol + 17½% KOH solution, an ammoniacal cuprous chloride solution (11.5g. $CuCl_2$/ 50 cc distilled water + 43cc. NH_4OH) and dilute HCL is necessary. These solutions remove O_2, CO, and NH_3 respectively. The gas then passes through a cumulative Parkinson & Cowan wet gas

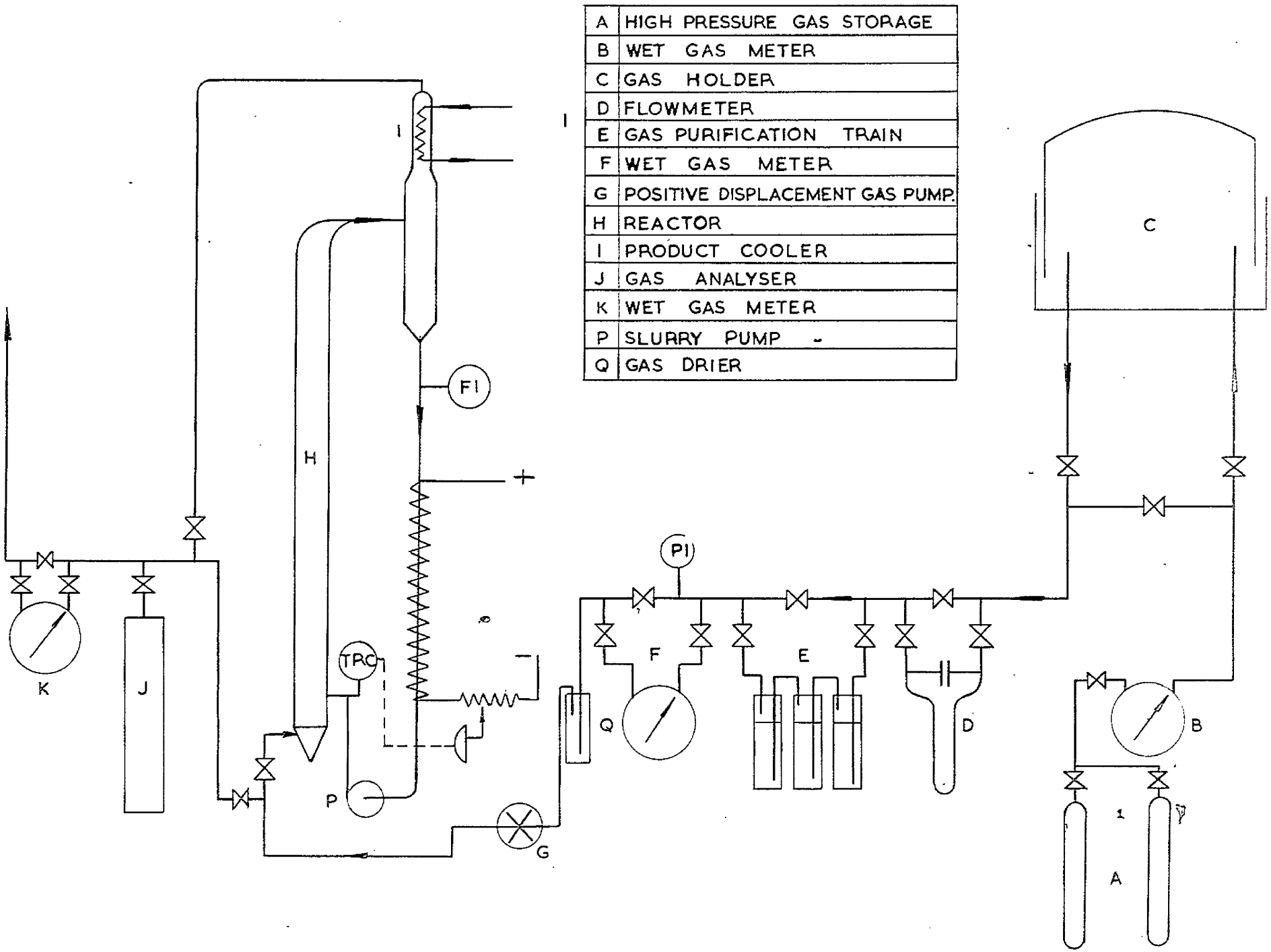

FIG. 2.1. REACTION SYSTEM LAYOUT.

meter. This is an accurate flow meter but only operates in the pressure range ± 10 ins. water gauge.

The gas then passes through a needle adjustment valve and a wash bottle containing granular calcium chloride for gas drying to the gas injection pump G. This is a variable speed Watson Marlowe H.R. flow inducer. The gas is then pumped to the reactor. The rubber tubing used in this pump required constant attention and is lubricated by French chalk.

2. 3. THE REACTOR SYSTEM. This is shown in Fig. 2. 2. Reactor columns of different lengths may be inserted. Standard reactors were made from 3.3cms. ID glass tubing and were fitted into the system by means of B.40 Q.F.V. cone and socket joints. The reactor diameter is restricted due to the position of the downcomer from the separator. The separator and much of the piping is made of glass.

Section A consists of teflon tubing the length of which was changed according to reactor length. The type of joint mainly used in the circuit is shown in Fig. 2. 3. Q.F.V. B.10 cone and socket joints were also used. Section B, between the separator and the pump incorporating the heater and the flowmeter, is erected in a semi-permanent

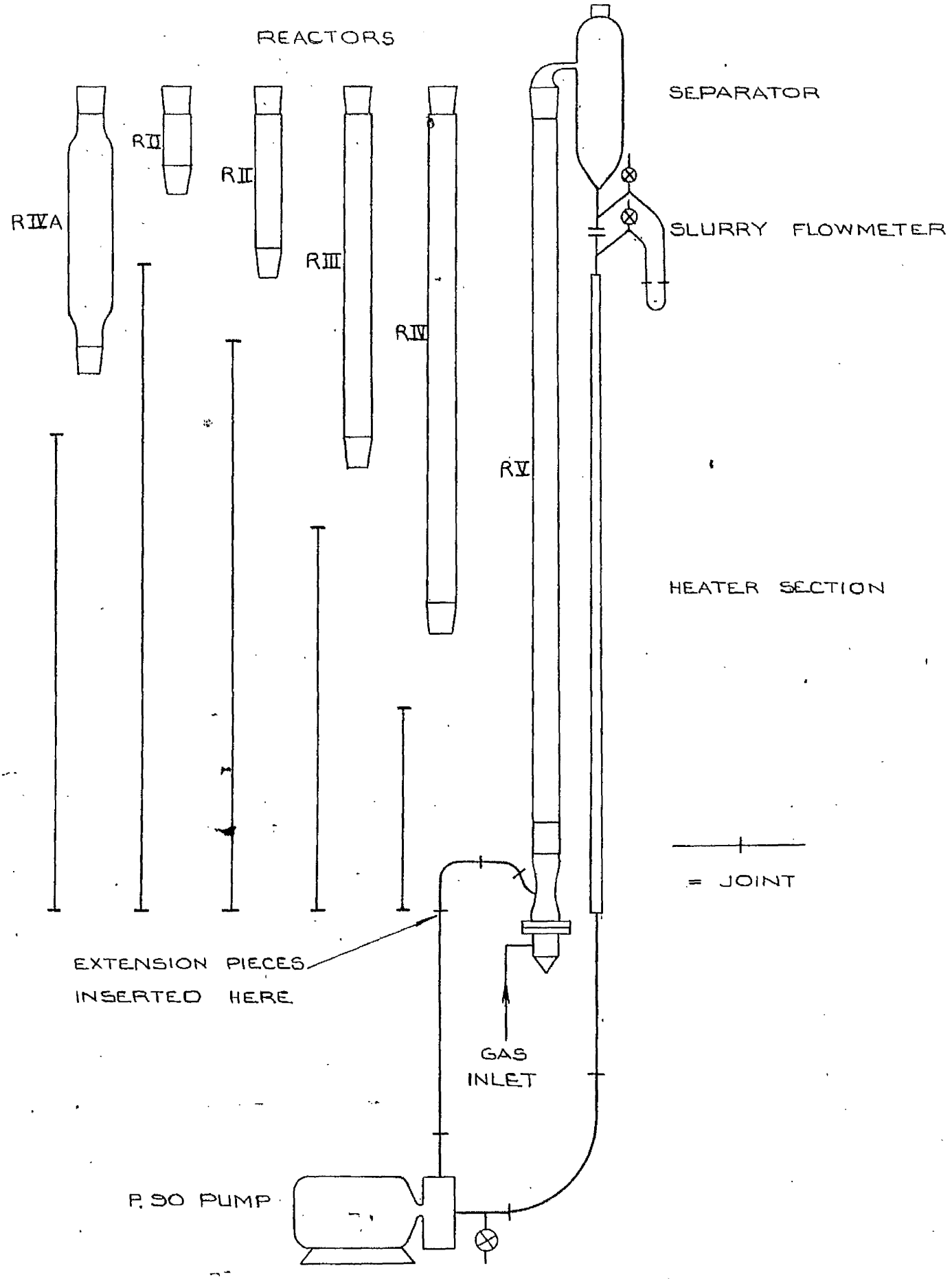

SCALE:- 1/10 FULL SCALE

FIG. 2.2 REACTOR LAYOUT.

manner while Section A may be altered at will.

The flow meter consists of a constriction in the downcomer with upstream and downstream tappings. These are connected to a manometer by the teflon type joint illustrated in Fig. 2. 3. Mercury is used as the manometer liquid. The slurry heater consists of 48 ft. of 26 S.W.G. nichrome wire wound round asbestos paper on a $\frac{3}{8}$" O.D. glass tube. The windings are lagged by asbestos rope. At 250 volts, this heater has a rating of 650 watts. The heater output is controlled by a variac connected to a Honeywell Brown temperature recorder controller via a pneumatic diaphram valve. The T.R.C. input signal is obtained from a copper constantan thermocouple located down-:stream from the pump. A P90 teflon contrifugal pump, supplied by Glen Creston, and with a rated output of 12 litres water/minute against 1 metre head of water is used for slurry circulation.

The gas distribution system is shown in Fig. 2. 4. The gas distributor is a spinarette with 1800 0.105 m,m holes. The base piece is made of brass and is coupled to the reaction system via a KBM/1 Q.V.F. joint.

As a liquid condenser and product cooler, a small condenser is fitted on top of the separator.

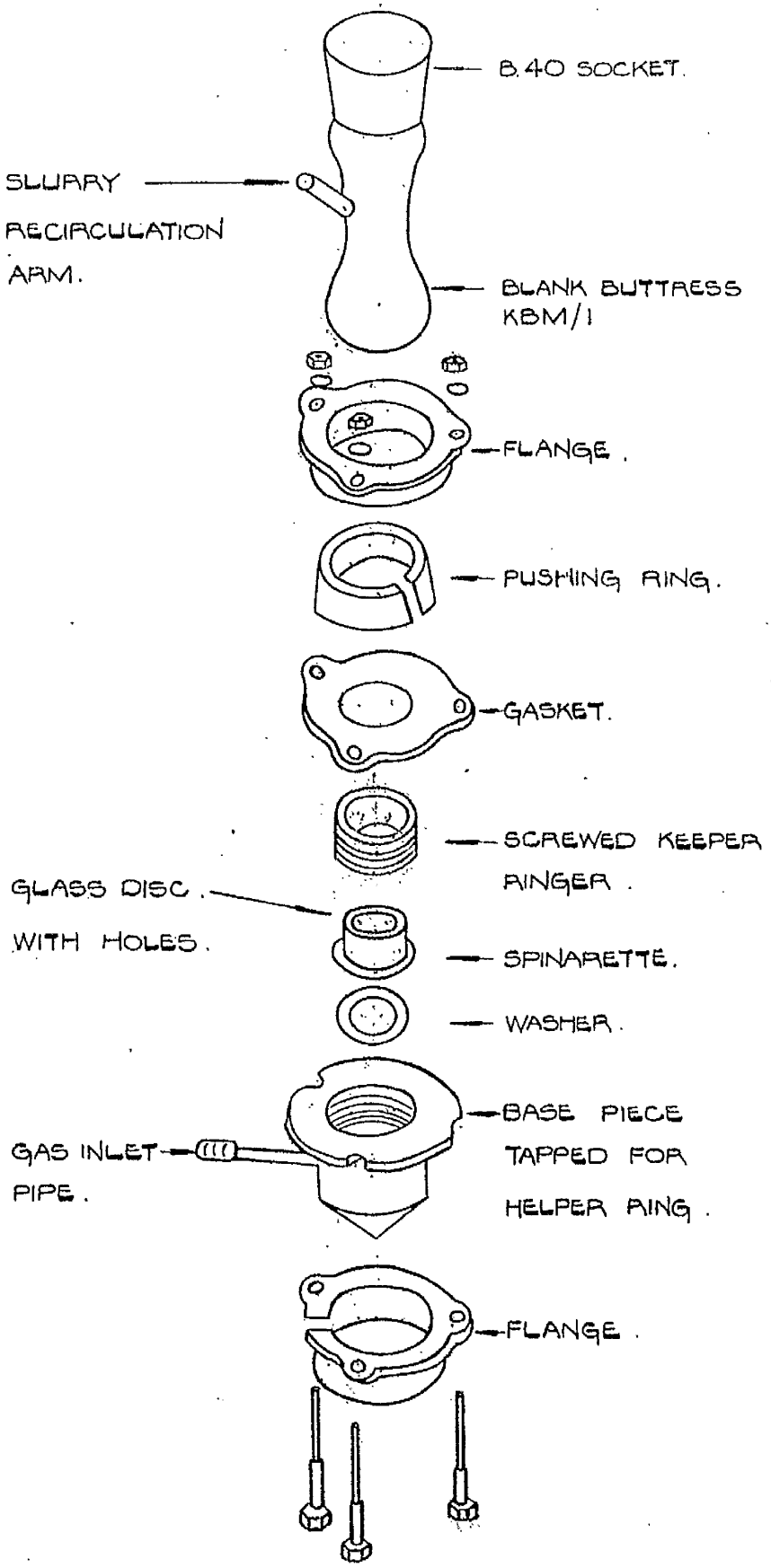

FIG. 2.4. GAS DISTRIBUTION SYSTEM.

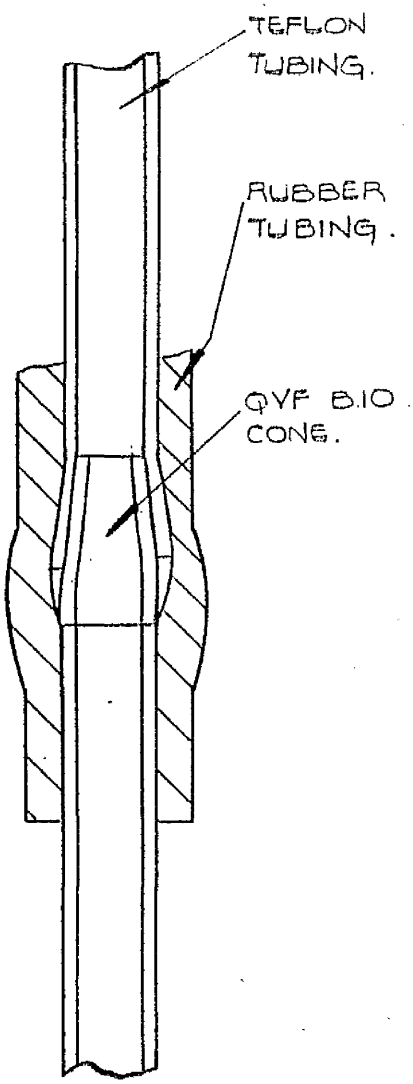

FIG. 2.3. XYLENE PROOF JOINT.

2. 4. THE GAS ANALYSIS SYSTEM. (Fig. 2. 5.)

The gas analyser operates on the constant volume principle and is an integral part of the system. Samples of inlet or outlet gas may be drawn in conveniently from the narrow bore main gas line. The apparatus is capable of analysing % ethylene content only. Results may be repeated to ± 0.1%. The volume % (mole fraction) of ethylene present in a sample is calculated from $\frac{H_1 - H_2}{H_1} \times 100$ where H_1 and H_2 are the initial and final height differences in the mercury levels in the two limbs.

The ethylene absorption solution used consists of 200 gms. of mercuric nitrate dissolved in 1000 c.c. of 2N nitric acid and the solution is saturated with sodium nitrate (37). About 12 c.c. of this solution absorbs 40 c.c. ethylene quantitatively after 2 minutes.

2. 5. DEVELOPMENT OF THE APPARATUS.

Previous work in the R.C.S.T.(38) on ethylene hydrogenation in a bench scale slurried bed reactor has shown that heat addition to the system was necessary due to heat losses exceeding heat generated. Direct heat supply presented a number of problems especially if various reactor sizes were to be used. Undesirable radial temperature effects are also obtained in such a

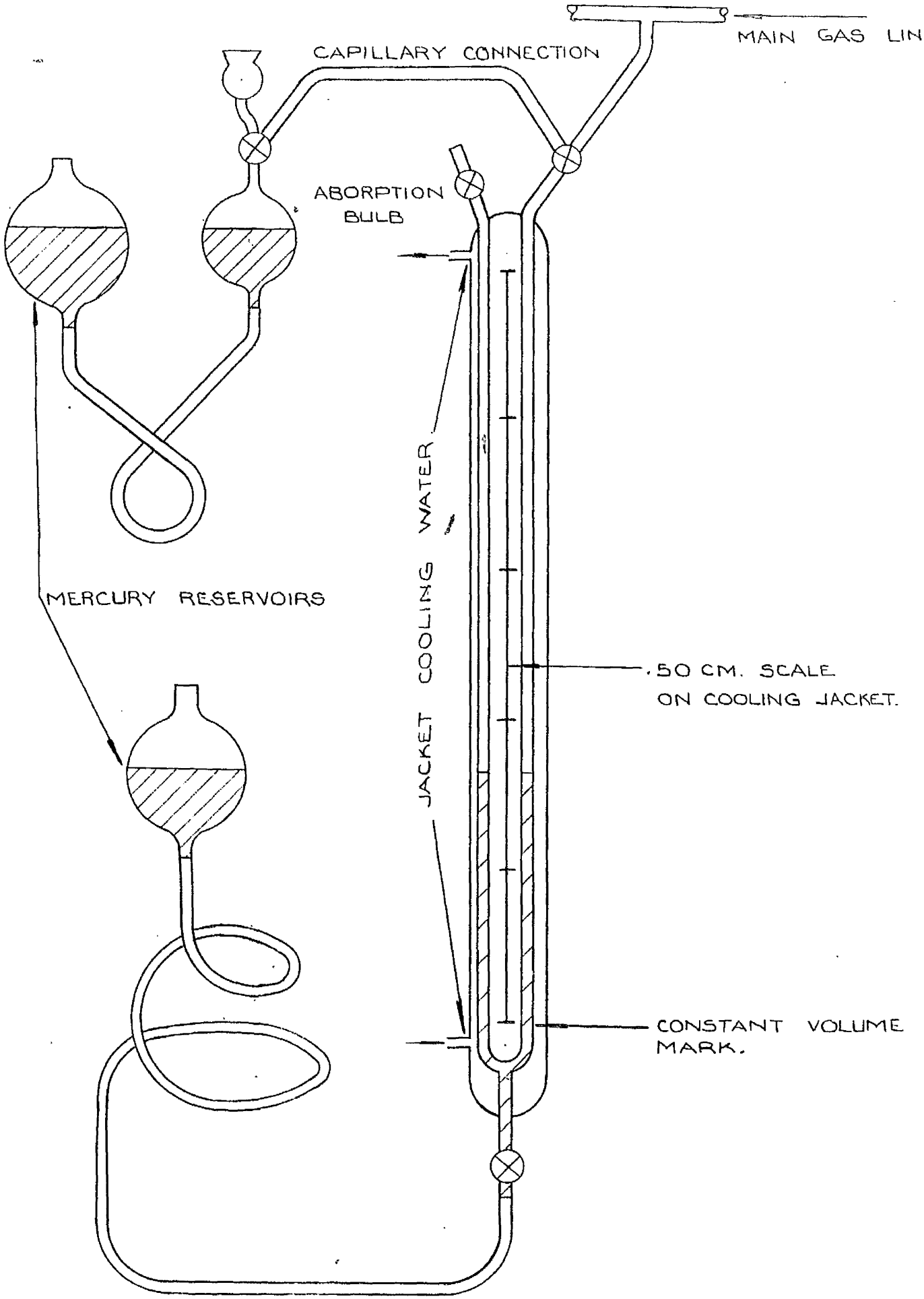

FIG. 25. GAS ANALYSIS APPARATUS.

system. It was therefore decided to supply heat externally to the reactor. The slurry thus had to be pumped from the reactor through some form of heat exchanger and back into the reactor. Xylene, the proposed suspending medium, was found to attack rubber and polymers generally with the exception of P.T.F.E. Difficulty was encountered in obtaining a suitable pump. Finally the P.T.F.E. centrifugal pump described elsewhere was obtained and this performed satisfactorily. The joints in the external slurry circuit also gave considerable trouble. It was found, with the glass apparatus initially used, these had to be flexible and reasonably easy to break open and remake. Eventually the type of joint shown in Fig. 2. 3. was developed. This joint was found to be exceptionally resistant to any liquids which do not attack P.T.F.E. Its success depends on the airseal formed by the rubber tubing. Without this leakage occurs due to the poor adhesion of P.T.F.E. to glass.

A metal apparatus was designed concurrently with the preliminary work. For various unfortunate reasons the apparatus was built in copper. It had a designed working limit of 50 p.s.i.g. Various reactor sizes were available and the problems of fragility obtained with the glass apparatus were

absent. Unfortunately it was discovered that copper poisons Raney nickel and the apparatus was useless. This poisoning effect is in fact indicated by Berkmann, Morell and Egloff (39). Thus this part of the work was wasted and work was resumed on the glass apparatus whose flexibility in using different reactor sizes had to be increased to the present level. High pressure operation was also impossible.

The development of the reactant gas supply system also presented certain problems. Previous practice (24), (38), (40) involves mixing reactant gases direct from the high pressure storage. This system appears to be subject to frequent fluctuations in flow rate and composition and requires constant supervision. After some investigation, a system where gas of a constant composition could be pumped from a reservoir at a constant rate to the reactor was envisaged. A large tyre inner tube was found to be a suitable reservoir. Gas may be stored at atmospheric pressure irrespective of the amount of gas present. No problems of gas solution are involved as is the case with wet gasometers.

Gas pumping constituted another obstacle. Most gas pumps were found to leak slightly through diaphrams or piston rings, either expelling reaction gas or

inducing air. Both phenomena are highly undesirable as accurate flow measurement and gas analysis become impossible. However, the flow inducer eventually used overcame these difficulties.

Methods of gas analysis were also considered. Bone and Wheeler type analysis apparatus (24) and the thermal conductivity cell method (40) have been used previously. The first was felt to be too slow and the second to be too sensitive to gas impurities. Accordingly, considerable work on the analysis of H_2, C_2H_4, C_2H_6 and CH_4 mixtures in a Janek (41) type gas chromatograph apparatus was carried out. Sufficiently accurate results were never obtained and the work was eventually abandoned.

Recourse was made to the apparatus described earlier. This enabled the composition of the outlet gas to be calculated in terms of H_2, C_2H_4, and C_2H_6, provided the inlet compositions were known in terms of H_2 and C_2H_4. The method assumed no other gases to be present. Quick results of inlet and outlet gas compositions were obtainable but the apparatus is limited and is considered to be the least satisfactory aspect of the experimental work.

2. 6. EXPERIMENTAL OPERATING PROCEDURE.

The line connecting the reactor to the gasometer was shut off. One of the gas cylinders was brought into line and meter B and associated lines were purged thoroughly. The required amount of gas was then metered into the gas holder. This procedure was repeated for the other gas and a gas mixture of the desired composition obtained. The gas holder was then isolated and left for a time to allow diffusional mixing to take place. Meanwhile the various clips and valves were set in such a manner that the surge associated with start up would not blow any absorbent or manometer liquid into the system.

The gas pump G was set in motion and the whole system purged with gas. The reactor was then filled with the liquid and the requisite amount of catalyst. The reactor by pass was brought into line and reactant gas pumped through and analysed until constant values of the inlet composition were obtained.

Gas pumping was stopped and the reactor outlet line opened. Condenser water was turned on. The slurry recycle pump P was started gently to prevent any mercury from the manometer being forced into the

system. Mercury causes immediate poisoning of the Raney nickel catalyst and can clog the gas distributor by amalgam formation. The required temperature was set on the controller and the control system activated. When operating temperature was reached and the reactor has settled down to constant temperature operation, gaswas injected at the required flow rate. When steady state conditions obtained the various instrument readings required were noted at suitable intervals of time for the duration of the run. After the passage of a reasonable volume of product gas, outlet gas analyses were commenced. These were continued periodically until the end of the run. Runs with very low inlet gas flow rates lasted up to 3 hours, while for runs at very high flow rates 20 minutes was generally sufficient. The difference in operating time was due to a longer time being required at low flow rates before a reasonable sample of product gas could be drawn from the system. The run was generally terminated when outlet gas analyses attained an approximately constant value.

2. 7. CATALYST PREPARATION.

Raney Nickel catalyst (42) was prepared according to the method of Covert and Adkins (43). This is believed to produce catalyst of fairly uniform activity.

To a solution of 500 gms. of sodium hydroxide in 2000 cc. of distilled water in a 5 litre beaker, 500 gms. of finely ground Aluminium-Nickel alloy (50 - 50 w/w) were added slowly over a period of 5 hours. During this addition, the temperature is kept below 20°C. otherwise hydrogen evolution is excessive. Cooling is effected by immersing the beaker in a bath containing a freezing mixture of salt and ice. When the addition of the alloy was complete, the mixture was heated to a temperature of 95-100°C. and kept at this temperature for four hours with occasional stirring.

Next 700 cc. of 19% sodium hydroxide were added and the mixture kept at 95-100°C. for a period of three hours or until the evolution of hydrogen had ceased. The mixture was then diluted to 5 litres with distilled water. The clear solution of sodium aluminate resulting is decanted. The nickel thus left is washed several times by decantation with distilled water till the supernatant liquid is

neutral to litmus. Small amounts of carbonate in the caustic used led to the formation of fairly insoluble aluminium compounds and much washing was required to remove these. When washing was completed, the catalyst was washed with 95% ethanol several times and maintained under that medium.

Before use with xylene or decalin, the catalyst in ethanol was transferred to a flask and an equal volume of the required solvent was added. The ethanol was then distilled off. When all was removed, the catalyst particles no longer agglomerated but dispersed easily throughout the liquid and remained suspended for longer periods before settling. When an aqueous suspension of the catalyst was required, the alcohol was merely washed away.

3. RESULTS AND DISCUSSION.

3. 1. EXPERIMENTAL RESULTS.

From the results tabulated later it will be seen that the results obtained from the reactors are repeatable. Two methods are available for calculating the reactor performance as % of reactant converted to product. One depends on the inlet and outlet gas analysis figures, while the other depends on the measured inlet and outlet gas flow rates. If only the reaction $C_2H_4 + H_2 \rightarrow C_2H_6$ takes place, the ratio of inlet to outlet volume for any inlet C_2H_4:H_2 ratio at a given conversion (defining % conversion as the % of reactant entering converted to the product) may be calculated and it is possible to construct the following table:-

TABLE 3. 1.

	C_2H_4:H_2 = 1:1	C_2H_4:H_2 = 2:1	C_2H_4:H_2 = 1:2
%C_2H_4 Conversion	Inlet:Outlet Volume	Inlet:Outlet Volume	Inlet:Outlet Volume
0	1:1	1:1	1:1
10	1.05:1	1.07:1	1.035:1
20	1.11:1	1.155:1	1.07:1
30	1.18:1	1.25:1	1.111:1
40	1.25:1	1.365:1	1.155:1
50	1.33:1	1.50:1	1.20:1
60	1.43:1		1.25:1
70	1.54:1		1.305:1
80	1.67:1		1.365:1
90	1.82:1		1.43:1
100	2.00:1		1.50:1

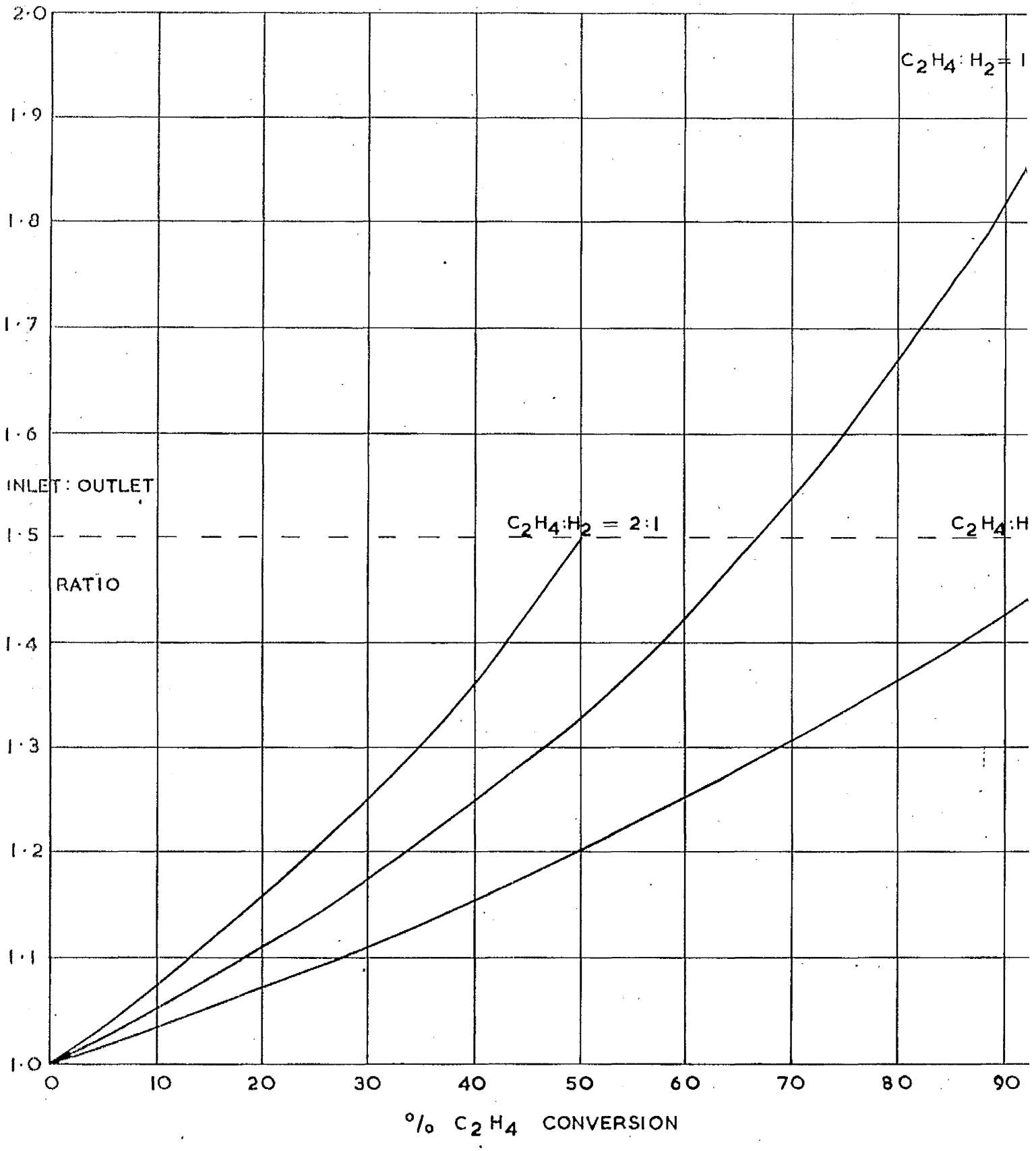
2·0
1·9
1·8
1·7
1·6
INLET : OUTLET
1·5
RATIO
1·4
1·3
1·2
1·1
1·0
C2H4 : H2 = 1
C2H4:H2 = 2:1
C2H4:H
0
10
20
30
40
50
60
70
80
90
% C2H4 CONVERSION

FIG. 3.1.

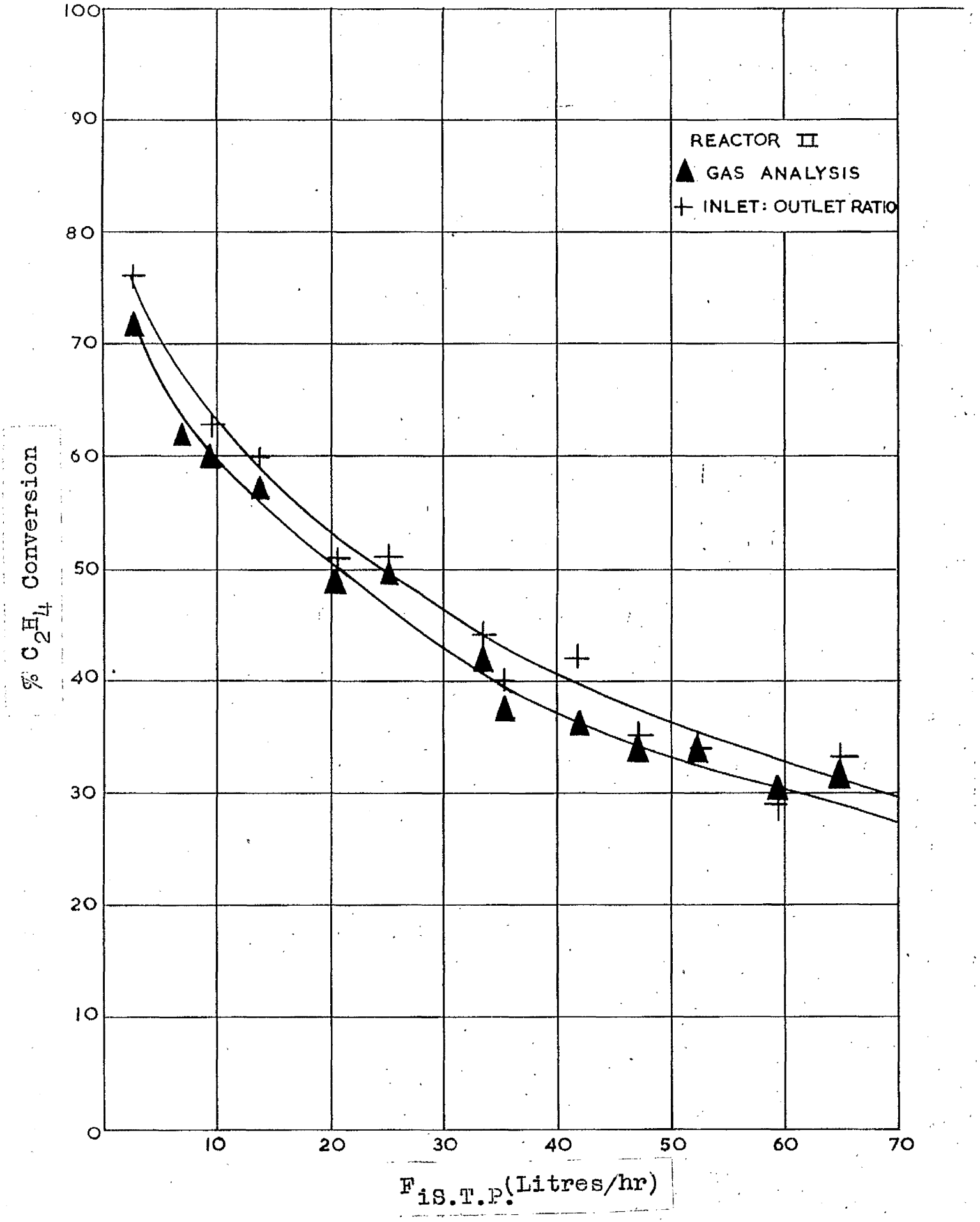
REACTOR II
GAS ANALYSIS
INLET: OUTLET RATIO
% C_2H_4 Conversion
F_{i} S.T.P. (Litres/hr)
0
10
20
30
40
50
60
70
80
90
100

FIG. 3.2

Using fig. 3.1. the % Conversion may be read off the appropriate chart. This method is very sensitive to system changes and is rather inflexible. It provides a useful check however om the worth of results calculated from gas analyses, e.g. fig. 3.2. Normally, conversion figures obtained from the volume reduction method are somewhat higher. This is attributed to experimental error arising from leaks and meter inaccuracies.

The following tables show the results obtained from the various reactors.

The reactors are designated thus:

TABLE 3. 1.

REACTOR	System Volume cc.	Reactor Volume cc.	Reactor Height cm.	Cross Sectional Area cm^2	Slurry Recycle
R V	1200	990	112	8.6	Yes
R IV	1000	790	86	8.6	Yes
R III	800	560	62	8.6	Yes
R II	575	335	37.5	8.6	Yes
R I	480	230	26.5	8.6	Yes
R O	420	140	16.5	8.6	Yes
R IVA	1000	790	49.5	13.8	Yes
R IVB	800	800	86	8.6	No

Discrepancies between actual reactor volumes and the volumes indicated by length and mean diameter are due to slight irregularities in shape.

STANDARD CONDITIONS.

Xylene was the catalyst suspending medium in all cases unless otherwise stated. Likewise the reactor operating temperature was 75°C; the catalyst concentra-:tion in the slurry was 2.5gms/100 c.c. and the slurry recirculation rate was 90 litres/hour.

TABLE 3. 2. REACTOR V. Series A.

A	θ	F_i	Y_{ai}	Y_{ao}	G	π	T_R °C	F_o
1	40	29.4	51.2	37.9	0.25	76.7	14.5	23.0
2	40	28.9	51.2	31.0	0.5	"	"	19.9
3	35	28.9	51.2	29.8	1	"	"	19.7
4	30	30.2	51.0	24.4	2	"	"	19.65
5	30	29.9	51.0	26.5	3	"	"	18.4
6	30	29.5	51.0	24.8	4	76.6	16	19.3
7	35	28.9	51.0	23.0	5	"	"	18.2

TABLE 3. 3. REACTOR V. Series B.

B	θ	F_i	Y_{ai}	Y_{ao}	π	T_R °C	F_o
1	15	78.5	0.512	0.310	76.35	16	54.9
2	32	67.2	"	0.301	"	"	46.4
3	24	57.9	"	0.289	75.71	16.5	40.0
4	24	44.25	"	0.286	"	"	30.1
5	40	33.65	"	0.254	"	"	22.2
6	36	24.6	0.475	0.207	"	"	15.4
7	48	18.3	"	0.190	"	"	11.4
8	60	6.35	"	0.101	"	"	-
9	120	3.35	0.50	0.085	75.65	14	-
10	12	82.2	"	0.306	"	"	-
11	24	50	"	0.287	"	"	-
12	28	46	0.512	0.288	"	"	-
13	28	30.4	"	0.255	73.5	"	-
14	60	7.97	"	0.130	"	"	-

TABLE 3. 4. REACTOR IV. Series C.

C	θ	F_i	Y_{ai}	Y_{ao}	π	T_R °C	F_o
1	16	77.6	0.51	0.352	74.54	16.5	58.4
2	24	56	"	0.341	"	"	41.5
3	28	45.2	"	0.316	"	"	33.1
4	28	33.6	0.512	0.285	"	"	23.7
5	44	18.1	"	0.237	73.6	16	11.95
6	60	10.3	"	0.195	"	"	6.56
7	150	3.26	0.48	0.094	"	"	1.79
8	16	71	"	0.306	"	"	51.1
9	20	42.2	0.481	0.282	74.1	17.5	29.6
10	40	29.8	"	0.238	"	"	19.1
11	32	21.4	0.47	0.221	"	"	13.9
12	60	14.7	"	0.187	"	"	9.8
13	120	7.82	"	0.148	"	"	4.63

TABLE 3. 5. REACTOR III. Series D.

D	θ	F_i	Y_{ai}	Y_{ao}	π	T_R °C	F_o
1	16	70	0.512	0.386	76.1	13	55.2
2	20	64.6	0.515	0.388	"	"	51
3	24	53.4	0.500	0.363	"	"	-
4	24	46.6	0.507	0.350	75.8	"	-
5	24	37.8	"	0.325	"	"	-
6	24	30.3	"	0.314	"	"	-
7	36	19.1	"	0.276	"	"	-
8	66	12.3	0.505	0.244	"	13.5	-
9	180	3.65	"	0.136	"	"	-
10	16	71.6	"	0.384	"	"	-
11	20	45.2	"	0.356	75.4	13	-
12	28	33.9	"	0.314	"	"	-
13	60	18.5	"	0.283	"	"	-
14	120	4.35	"	0.184	"	"	-

TABLE 3. 6. REACTOR II. Series E.

E	θ	F_i	Y_{ai}	Y_{ao}	π	T_R °C	F_o
1	20	93.7	0.520	0.455	74.75	15	82.1
2	20	63.6	"	0.431	"	"	54.5
3	28	50.5	"	0.419	"	"	41.4
4	40	45	"	0.409	"	"	35.8
5	40	27	0.510	0.348	75.1	"	20.3
6	40	15	0.525	0.322	"	"	10.5
7	60	10.4	"	0.307	"	"	7.11
8	180	3.12	"	0.240	"	"	1.93
9	28	69.3	"	0.430	74.8	14	57.6
10	28	56	"	0.423	"	"	46.4
11	32	37.6	0.500	0.387	"	"	30.2
12	32	35.8	"	0.369	"	"	28.0
13	40	22	"	0.337	"	"	16.4
14	90	7.75	"	0.275	"	"	5.32

TABLE 3. 7. REACTOR I. Series F.

F	θ	F_i	Y_{ai}	Y_{ao}	π	T_R °C	F_o
1	24	65.9	0.520	0.454	74.6	16.5	57.3
2	28	53.9	"	0.441	"	"	46.0
3	28	35.1	"	0.416	"	"	28.6
4	40	25.3	"	0.401	"	"	20.4
5	40	19.8	0.500	0.356	75.6	18	15.0
6	60	8.79	"	0.302	"	"	61.0
7	152	3.56	0.488	0.213	"	"	2.24
8	24	77.4	"	0.425	"	"	67.9
9	24	61.4	0.520	0.453	76	"	53.3
10	24	52.9	"	0.450	"	"	46.0
11	28	43.5	"	0.436	"	"	36.7
12	32	31.3	"	0.420	"	"	25.6
13	92	6.75	"	0.311	"	"	4.66

TABLE 3. 8. REACTOR O. Series G.

G	θ	F_i	Y_{ai}	Y_{ao}	π	T_R °C	F_o
1	20	78	0.490	0.454	76.8	20	71.4
2	24	57.1	"	0.445	"	"	50.0
3	28	46.3	"	0.439	"	"	40.7
4	36	26.9	"	0.414	"	"	22.5
5	40	18.2	"	0.380	76.5	"	15.05
6	96	7.95	"	0.317	"	"	5.98
7	140	4.08	"	0.262	"	"	2.74
8	24	67.75	"	0.445	"	"	61.0
9	32	53.2	"	0.439	"	"	46.3
10	32	39.9	0.512	0.451	76.1	"	34.1
11	36	22.1	"	0.410	"	"	17.1
12	36	14.7	"	0.365	"	"	11.15
13	76	6.4	"	0.315	"	"	4.48

TABLE 3. 9. REACTOR IVA. Series H.

H	θ	F_i	Y_{ai}	Y_{ao}	π	T_R °C	F_o
1	24	77.3	0.491	0.370	76.9	17	61.5
2	28	65.9	"	0.365	"	"	52.5
3	32	52.6	"	0.351	"	"	41.4
4	36	25.7	"	0.309	"	"	19.35
5	48	15.3	"	0.260	76.4	19	10.6
6	92	6.84	"	0.214	"	"	4.57
7	160	4.7	"	0.195	"	"	3.02
8	24	56.1	0.490	0.354	77.2	18	45.0
9	32	39.4	"	0.346	"	"	31.1
10	32	30.5	"	0.326	"	"	23.4
11	48	18.8	"	0.297	"	"	13.8
12	60	10.2	"	0.263	"	"	7.20

TABLE 3. 10. REACTOR IVB. Series C.'

C	θ	F_i	Y_{ai}	Y_{ao}	π	T_R °C	F_o
1	24	78.0	0.513	0.358	75.7	19	-
2	28	57.3	"	0.324	"	"	-
3	28	41.5	"	0.294	"	"	-
4	36	35.2	0.505	0.273	"	"	-
5	36	27.4	"	0.239	"	"	-
6	36	20.9	0.491	0.222	76.1	"	-
7	60	12.9	"	0.174	"	"	-
8	148	3.3	"	0.222	"	"	-
9	24	66.0	0.487	0.331	76.2	"	-
10	24	46.1	"	0.302	"	"	-
11	32	30.1	"	0.257	"	"	-
12	40	16.8	"	0.191	"	"	-
13	60	8.18	"	0.214	76.7	"	-
14	120	4.77	"	0.223	"	"	-

TABLE 3. 11. REACTOR V. Series I, $C_2H_4:H_2$ = 2:1

I	θ	F_i	Y_{ai}	Y_{ao}	π	T_R °C	F_o
1	24	73.6	0.674	0.62	75.1	15	58.9
2	36	55.6	0.676	0.615	"	"	43.8
3	32	46.9	0.677	0.609	"	"	38.2
4	32	27.8	0.680	0.582	"	"	21.3
5	52	13.5	0.680	0.552	"	"	9.6
6	120	4.4	0.680	0.544	74.1	"	4.4

TABLE 3. 12. REACTOR V. Series J, $C_2H_4:H_2$ = 1:2

J	θ	F_i	Y_{ai}	Y_{ao}	π	T_R °C	F_o
1	24	80	0.315	0.0575	73.6	16	56.5
2	32	63.5	0.314	0.0446	"	"	43.5
3	32	50.7	0.331	0.044	"	"	34.3
4	36	31.4	0.331	0.010	"	"	33.6
5	40	19	0.329	0.000	"	"	12.35

TABLE 3. 13. REACTOR II. Series M, $C_2H_4:H_2$ = 2:1

M	θ	F_i	Y_{ai}	Y_{ao}	π	T_R °C	F_o
1	16	73.4	0.676	0.653	76.0	17	69.2
2	32	54.9	"	0.645	"	"	49.9
3	32	45.7	"	0.646	"	"	28.7
4	36	31.3	"	0.625	"	"	26.5
5	36	17.8	0.661	0.602	75.1	"	15.0
6	52	10.1	"	0.585	"	"	7.85
7	88	5.60	"	0.574	"	"	4.21

TABLE 3. 14. REACTOR II Series N, $C_2H_4:H_2$ = 1:2

N	θ	F_i	Y_{ai}	Y_{ao}	Π	T_R °C	F_o
1	20	73.9	0.313	0.173	74.9	17	62.1
2	24	64.0	0.293	0.168	"	"	51.8
3	28	48.4	0.299	0.157	"	"	38.6
4	32	41.0	"	0.134	"	"	31.7
5	28	37.6	"	0.124	75.1	"	28.75
6	36	21.75	"	0.086	"	"	15.8
7	64	9.25	"	0.033	"	"	6.37
8	84	5.1	"	0.025	"	"	3.46

Before these results could be analysed it was necessary to derive a number of functions. The calculation of these is now discussed.

The total gas pressures at inlet and outlet are required. $76.\Pi_{gi} = \Pi + \Pi_1 - \Pi_s$

$$= \Pi + \frac{Z\rho_s}{13.6} - \Pi_s$$

Π_s may be obtained by reference to fig. 3.36

e.g. For run B 3, $\Pi = \frac{76.35}{76}$ atm.

$$\Pi_s = \frac{8.2}{76} \text{ atm.}$$

$$\Pi_1 = \frac{112 \times 0.816}{13.6 \times 76} \qquad \rho_s = 0.816 \text{ gms/cc at } 75^\circ C \text{ (49)}$$

$$= \frac{6.72}{76} \text{ atm.}$$

Hence $\Pi_{gi} = \frac{76.35 + 6.72 - 8.2}{76} = \frac{74.87}{76} = 0.986$ atm.

$$\Pi_{go} = \Pi - \Pi_s$$

$$= \frac{76.35 - 8.2}{76} = 0.893 \text{ atm.}$$

The mean column pressure is calculated from

$$\pi_{gm} = \frac{\pi_{gi} + \pi_{go}}{2} = \frac{0.986 + 0.893}{2} = 0.940 \text{ atm}$$

The % conversion of a reactant, C, is required.

Consider reactant A. (C_2H_4)

It has been shown in 2. 4. that

$$\frac{H_1 - H_2}{H_1} = Y_a$$

F_i^M = total feed moles

Y_{ai} = mole fraction C_2H_4 in inlet

Moles $C_2H_4 = F_i^M Y_{ai}$. Moles $H_2 = F_i^M(1-Y_{ai})$.

Conversion = x, moles C_2H_4 converted to C_2H_6/mole C_2H_4 in $C_2H_4 + H_2 \rightarrow C_2H_6$

At Outlet moles $C_2H_6 = F_i^M Y_{ai}\ x$

moles $C_2H_4 = F_i^M Y_{ai}(1 - x)$

moles $H_2 = F_i^M(1 - Y_{ai}) - F_i^M Y_{ai}\ x$

Let Y_{ao} = C_2H_4 mole fraction in outlet stream

$$Y_{ao} = \frac{F_i^M Y_{ai}(1 - x)}{F_i^M Y_{ai}\ x + F_i^M Y_{ai}(1 - x) + F_i^M(1 - Y_{ai}) - F_i^M Y_{ai}\ x}$$

$$= \frac{Y_{ai} - Y_{ai}\ x}{1 - Y_{ai}\ x}$$

Hence $$x = \frac{Y_{ai} - Y_{ao}}{Y_{ai}(1 - Y_{ao})}$$

$$C = \frac{Y_{ai} - Y_{ao}}{Y_{ai}(1 - Y_{ao})} \cdot 100$$

e.g. run C2

$Y_{ai} = 0.512$ $Y_{ao} = 0.341$

$$C = \frac{0.512 - 0.341}{0.512(1 - 0.341)} \cdot 100$$

When the reactants are present in equal quantities only the % conversion of component A has been calculated.

The % conversion C′ based on volume reduction is calculated thus:-

F_i = 56 litres/hr.

F_o = 41.5 litres/hr.

$\frac{F_i}{F_o} = \frac{56}{41.5} = 1.35$

From fig. 3. 1., C′ is read off as 56%

The inlet flow rate at S.T.P., F_{iSTP}, is obtained in the normal way from F_i, e.g. D 10

Π = 75.8 F_i = 71.6

T_R = 13.5°C

$F_{iSTP} = 71.6 \cdot \frac{75.8}{76} \cdot \frac{273}{286.5} = 68.2$ litres/hr.

F_i^M the molar flow rate is derived directly from F_{iSTP}. $F_i^M = \frac{F_{iSTP}}{22.4}$

The space time yield, N_C^* is obtained thus

$$N_C^* = \frac{F_i^M Y_{ai} x}{V_R}$$

e.g. E 7 F_i^M = 0.435

Y_{ai} = 0.525

x = 0.60

V_R = 0.335

$$N_C^* = \frac{0.435 \times 0.525 \times 0.60}{0.335} = 0.41 \text{ moles/litre hr.}$$

The partial pressure terms used, P_{ai} say, may be calculated as follows:-

$$P_{ai} = Y_{ai} \Pi_{gi}$$

e.g. F 12 $Yai = 0.52$

$\Pi_{gi} = 0.911$

$P_{ai} = 0.52 \cdot 0.911 = 0.471$

P_{bi}, P_{ao}, P_{bo} may be calculated in similar fashion.

α is defined by $P_{bi} = \alpha P_{ai}$

$$\therefore \alpha = \frac{P_{bi}}{P_{ai}} = \frac{Y_{bi}\Pi_{gi}}{Y_{ai}\Pi_{go}} = \frac{Y_{bi}}{Y_{ai}}$$

The group $\frac{\alpha}{1+\alpha}$ has greater practical use

$$\frac{\alpha}{1+\alpha} = \frac{\frac{Y_{bi}}{Yai}}{1 + \frac{Y_{bi}}{Y_{ai}}} = Y_{bi}$$

e.g. for G 9 $\frac{\alpha}{1+\alpha} = 0.51$

Similarly for $\frac{\beta}{1+\beta}$

From a knowledge of Y_{ai} and Y_{ao}, Y_{bo} may be calculated.

From 1. 2. Note 3

$$F_o^M = \frac{\Pi_{go} F_i^M \alpha}{(1+\alpha)(\Pi_{go} - P_{ao})}$$

Now $F_i^M = F_i^M Y_{ai} + F_i^M Y_{bi}$

$F_o^M = F_o^M Y_{ao} + F_o^M Y_{bo} + F_o^M Y_{Co}$

$$F_o^M Y_{Co} = F_i^M Y_{ai} - F_o^M Y_{ao} = F_i^M Y_{ai} - \frac{\Pi_{go} F_i \alpha Y_{ao}}{(1+\alpha)(\Pi_{go} - P_{ao})}$$

It may then be shown by substitution that

$$Y_{bo} = 1 - Y_{ai} \frac{(1+\alpha)(1 - Y_{ao})}{\alpha}$$

e.g. B 12

$$Y_{bo} = 1 - \frac{0.512}{0.488} \cdot \frac{0.712}{1}$$

$$= 1 - 0.746$$

$$= 0.254$$

$\overline{K}_{ga}$ and $\overline{K}_{gb}$ may be calculated from equation 1.2.40

e.g. $$\overline{K}_{ga} = \frac{F_i^M \alpha}{V_R \cdot \Pi_{gm} (1+\alpha) A_{glm}} \cdot \left[\ln \frac{P_{ai}}{P_{ao}} + \ln \frac{\Pi_{go} - P_{ao}}{\Pi_{gi} - P_{ai}} \right]$$

Consider C 10

$$\overline{K}_{ga} = \frac{1.215 \cdot 0.519}{0.79 \cdot 0.90 \cdot 0.92} \cdot \left[0.785 + 0.300 \right]$$

$$= 1.05$$

In like manner, $NRU_{a,b}$ and $NChU_{a,b}$ may be calculated from equations 1.2.41 and 1.2.55.

$$N.R.U_a = \frac{\alpha}{1+\alpha} \cdot \left[\ln \frac{P_{ai}}{P_{ao}} + \ln \frac{\Pi_{gi} - P_{ao}}{\Pi_{gi} - P_{ai}} \right]$$

$$N.Ch.U_a = \frac{\alpha}{1+\alpha} \cdot \left[\ln \frac{P_{ai}}{P_{ao}} + \ln \frac{\Pi_{go} - P_{ao}}{\Pi_{gi} - P_{ai}} + \left(\frac{\Pi_{go}}{P_{ao}} - \frac{\Pi_{gi}}{P_{ai}} \right) \right]$$

Note:- The values of A_{glm} quoted are discussed fully in Appendix 2, and those of A_{ls} in Appendix 3.

TABLE 3 15. Series A.

C	C′	A_{gl}	A_{ls}	$\frac{A_{ls}}{A_{gl}}$
25.4	43	0.97	0.617	0.636
57.3	62	0.97	1.25	1.275
59.5	64	0.97	2.47	2.54
68.9	70	0.97	4.95	5.11
65.4	69	0.97	7.40	7.63
68.5	69	0.97	9.85	10.15
71.4	74	0.97	12.35	12.75

TABLE 3. 16. Series B.

Π_{gi}	Π_{go}	Π_{gm}	F_{iSTP}	F_i^M	A_{glm}	N_C*	$\frac{Z}{F_{iSTP}}$	$\frac{V_R}{F_i^M}$
0.986	0.893	0.940	74.5	3.33	1.575	0.985	1.51	0.298
"	"	"	63.7	2.84	1.355	0.865	1.765	0.349
0.978	0.885	0.932	54.5	2.44	1.265	0.769	2.05	0.407
"	"	"	41.5	1.85	1.118	0.591	2.72	0.535
"	"	"	31.6	1.41	0.922	0.492	3.56	0.703
"	"	"	23.1	1.03	0.692	0.351	4.87	0.961
"	"	"	17.2	0.77	0.520	0.274	6.55	1.380
"	"	"	5.97	0.267	0.227	0.116	18.8	3.720
0.977	0.884	0.931	3.18	0.142	0.134	0.065	35.4	6.990
"	"	"	78.0	3.62	1.695	1.02	1.44	0.284
"	"	"	47.4	2.24	1.20	0.676	2.38	0.467
"	"	"	43.6	2.06	1.12	0.655	2.58	0.507
0.949	0.855	0.902	28.0	1.36	0.880	0.475	4.02	0.792
"	"	"	7.33	0.328	0.254	0.146	15.35	3.03

TABLE 3. 17. Series C.

Π_{gi}	Π_{go}	Π_{gm}	F_{iSTP}	F_i^M	A_{glm}	N_C^*	$\frac{Z}{F_{iSTP}}$	$\frac{V_R}{F_i^M}$
0.940	0.869	0.905	71.9	3.21	1.83	0.995	1.20	0.246
"	"	"	51.8	2.32	1.46	0.755	1.66	0.341
"	"	"	41.9	1.87	1.17	0.671	2.06	0.423
"	"	"	31.1	1.39	0.98	0.558	2.79	0.569
0.928	0.857	0.893	16.55	0.739	0.54	0.348	5.20	1.07
"	"	"	9.42	0.421	0.33	0.210	9.13	1.88
"	"	"	2.98	0.133	0.15	0.0716	28.9	5.95
"	"	"	65.0	2.91	1.69	0.925	1.325	0.272
0.937	0.864	0.900	38.6	1.725	1.10	0.605	2.23	0.459
"	"	"	27.2	1.215	0.92	0.488	3.17	0.650
"	"	"	19.6	0.875	0.63	0.354	4.40	0.905
"	"	"	13.45	0.601	0.45	0.265	6.40	1.315
"	"	"	7.15	0.349	0.26	0.167	12.00	2.27

TABLE 3. 18 Series D.

Π_{gi}	Π_{go}	Π_{gm}	F_{iSTP}	F_i^M	A_{glm}	N_C^*	$\frac{Z}{F_{iSTP}}$	$\frac{V_R}{F_i^M}$
0.940	0.889	0.915	66.9	2.98	1.59	1.09	0.928	0.188
"	"	"	61.7	2.76	1.46	1.025	1.005	0.203
"	"	"	51.0	2.28	1.35	0.875	1.22	0.246
0.937	0.886	0.912	44.5	1.99	1.26	0.856	1.395	0.282
"	"	"	36.1	1.61	1.12	0.776	1.72	0.348
"	"	"	28.9	1.29	0.985	0.647	2.14	0.435
"	"	"	18.2	0.812	0.600	0.464	3.41	0.690
"	"	"	11.75	0.525	0.368	0.324	5.28	1.070
"	"	"	3.48	0.156	0.153	0.118	17.8	3.580
"	"	"	68.2	3.04	1.60	1.07	0.91	0.184
0.931	0.880	0.906	43.0	1.92	1.23	0.795	1.44	0.292
"	"	"	32.2	1.44	0.935	0.715	1.93	0.389
"	"	"	17.55	0.784	0.576	0.434	3.54	0.715
"	"	"	4.12	0.184	0.154	0.129	15.05	3.04

TABLE 3. 19 Series E.

η_{gi}	η_{go}	η_{gm}	F_{iSTP}	F_i^M	A_{glm}	N_C^*	$\frac{Z}{F_{iSTP}}$	$\frac{V_R}{F_i^M}$
0.904	0.873	0.888	87.5	3.91	1.92	1.395	0.429	0.0856
"	"	"	59.5	2.66	1.475	1.240	0.630	0.126
"	"	"	47.1	2.11	1.22	1.105	0.795	0.159
"	"	"	42.0	1.88	1.14	1.06	0.894	0.178
0.908	0.877	0.892	25.3	1.13	0.82	0.855	1.48	0.297
"	"	"	14.1	0.63	0.465	0.561	2.66	0.532
"	"	"	9.75	0.435	0.32	0.410	3.85	0.771
"	"	"	2.92	0.13	0.087	0.146	12.85	2.58
0.904	0.873	0.888	65.0	2.94	1.61	1.47	0.577	0.114
"	"	"	52.5	2.34	1.35	1.24	0.715	0.143
"	"	"	35.2	1.57	1.045	0.87	1.065	0.213
"	"	"	33.5	1.50	1.02	0.93	1.12	0.223
"	"	"	20.6	0.92	0.655	0.676	1.62	0.364
"	"	"	7.25	0.345	0.25	0.320	5.17	0.971

TABLE 3. 20. Series F.

η_{gi}	η_{go}	η_{gm}	F_{iSTP}	F_i^M	A_{glm}	N_C^*	$\frac{Z}{F_{iSTP}}$	$\frac{V_R}{F_i^M}$
0.893	0.870	0.882	60.9	2.72	1.62	1.44	0.436	0.085
"	"	"	49.8	2.22	1.35	1.365	0.532	0.104
"	"	"	32.5	1.45	1.05	1.12	0.815	0.169
"	"	"	23.4	1.035	0.837	0.89	1.135	0.222
0.906	0.883	0.895	18.5	0.825	0.62	0.865	1.435	0.279
"	"	"	8.20	0.366	0.251	0.451	3.24	0.629
"	"	"	3.32	0.149	0.122	0.227	7.99	0.155
"	"	"	72.2	3.22	1.77	0.089	0.366	0.0715
0.911	0.888	0.900	57.5	2.59	1.51	1.38	0.461	0.0887
"	"	"	49.6	2.22	1.34	1.23	0.535	0.1035
"	"	"	40.8	1.83	1.17	1.19	0.650	0.126
"	"	"	29.4	1.315	0.96	0.985	0.900	0.175
"	"	"	6.34	0.283	0.197	0.373	4.18	0.813

TABLE 3. 21. Series G.

π_{gi}	π_{go}	π_{gm}	F_{iSTP}	F_i^M	A_{glm}	N_C^*	$\frac{Z}{F_{iSTP}}$	$\frac{V_R}{F_i^M}$
0.913	0.898	0.906	73.2	3.27	1.795	1.55	0.232	0.043
"	"	"	53.9	2.405	1.45	1.64	0.307	0.058
"	"	"	43.6	1.95	1.26	1.27	0.378	0.072
"	"	"	25.3	1.13	0.845	1.045	0.652	0.124
0.909	0.894	0.902	17.1	0.765	0.625	0.967	0.965	0.183
"	"	"	7.45	0.333	0.29	0.602	2.22	0.420
"	"	"	3.83	0.171	0.159	0.378	4.3	0.817
"	"	"	63.2	2.82	1.63	1.635	0.265	0.049
"	"	"	50.0	2.23	1.39	1.500	0.330	0.0626
0.903	0.889	0.897	37.2	1.665	1.14	1.32	0.444	0.084
"	"	"	20.6	0.92	0.74	1.135	0.800	0.152
"	"	"	13.7	0.611	0.503	1.01	1.205	0.228
"	"	"	5.96	0.266	0.244	0.545	2.77	0.525

TABLE 3. 22. Series H.

π_{gi}	π_{go}	π_{gm}	F_{iSTP}	F_i^M	A_{glm}	N_C^*	$\frac{Z}{F_{iSTP}}$	$\frac{V_R}{F_i^M}$
0.955	0.899	0.927	73.6	3.29	0.945	0.802	0.672	0.240
"	"	"	62.7	2.80	0.840	0.703	0.79	0.283
"	"	"	50.1	2.24	0.718	0.613	0.990	0.353
"	"	"	24.4	1.09	0.444	0.359	2.03	0.725
0.948	0.892	0.920	14.4	0.644	0.292	0.255	3.44	1.23
"	"	"	6.43	0.288	0.139	0.129	7.70	2.75
"	"	"	4.42	0.198	0.104	0.920	11.2	4.00
0.962	0.906	0.934	54.8	2.45	0.755	0.650	0.905	0.322
"	"	"	37.5	1.67	0.605	0.465	1.32	0.474
"	"	"	29.8	1.33	0.510	0.410	1.66	0.595
"	"	"	17.9	0.80	0.342	0.278	2.77	0.988
"	"	"	9.71	0.434	0.204	0.169	5.10	1.825

TABLE 3. 23. Series C'.

Π_{gi}	Π_{go}	Π_{gm}	F_{iSTP}	F_i^M	A_{glm}	N_C^*	$\frac{Z}{F_{iSTP}}$	$\frac{V_R}{F_i^M}$
0.958	0.884	0.921	73.4	3.28	1.68	0.991	1.17	0.244
"	"	"	53.3	2.38	1.46	0.795	1.64	0.336
"	"	"	38.6	1.73	1.09	0.668	2.23	0.467
"	"	"	32.8	1.46	0.98	0.581	2.62	0.548
"	"	"	25.5	1.14	0.795	0.500	3.37	0.700
0.965	0.891	0.928	19.6	0.876	0.645	0.380	4.40	0.912
"	"	"	12.1	0.54	0.411	0.259	7.1	1.48
"	"	"	3.1	0.138	0.139	0.059	27.8	5.80
0.967	0.892	0.929	61.9	2.76	1.52	0.804	1.39	0.290
"	"	"	43.3	1.94	1.18	0.645	1.99	0.413
"	"	"	28.2	1.26	0.865	0.486	3.05	0.635
"	"	"	15.8	0.705	0.525	0.322	5.45	1.135
0.971	0.897	0.934	7.7	0.344	0.288	0.150	11.2	2.32
"	"	"	4.5	0.201	0.175	0.085	19.1	3.98

TABLE 3. 24. Series I.

Π_{gi}	Π_{go}	Π_{gm}	F_{iSTP}	F_i^M	A_{glm}	N_C^*	$\frac{Z}{F_{iSTP}}$	$\frac{V_R}{F_i^M}$
0.971	0.877	0.924	69.5	3.1	1.66	0.447	1.62	0.32
"	"	"	52.4	2.34	1.38	0.374	2.15	0.425
"	"	"	43.8	1.96	1.22	0.341	2.57	0.505
"	"	"	26.2	1.17	0.83	0.277	4.30	0.846
"	"	"	12.4	0.555	0.445	0.161	9.06	1.79
"	"	"	4.26	0.191	0.176	0.0575	26.4	5.19

TABLE 3. 25. Series J.

Π_{gi}	Π_{go}	Π_{gm}	F_{iSTP}	F_i^M	A_{glm}	N_C^*	$\frac{Z}{F_{iSTP}}$	$\frac{V_R}{F_i^M}$
0.952	0.858	0.905	73.0	3.26	1.7	0.899	1.54	0.304
"	"	"	58.2	2.60	1.45	0.740	1.93	0.381
"	"	"	46.5	2.08	1.25	0.625	2.42	0.476
"	"	"	28.8	1.29	0.885	0.421	3.90	0.768
"	"	"	17.4	0.775	0.619	0.258	6.46	1.28

TABLE 3. 26 Series M.

Π_{gi}	Π_{go}	Π_{gm}	F_{iSTP}	F_i^M	A_{glm}	N_C^*	$\frac{Z}{F_{iSTP}}$	$\frac{V_R}{F_i^M}$
0.918	0.888	0.903	69.1	3.09	1.72	0.621	0.544	0.109
"	"	"	51.6	2.31	1.42	0.640	0.727	0.145
"	"	"	43.0	1.92	1.25	0.487	0.873	0.175
"	"	"	27.4	1.22	1.12	0.538	1.37	0.274
0.908	0.877	0.892	16.6	0.74	0.596	0.327	2.26	0.452
"	"	"	9.41	0.42	0.362	0.231	3.99	0.795
"	"	"	5.21	0.233	0.198	0.142	7.2	1.500

TABLE 3. 27 Series N.

Π_{gi}	Π_{go}	Π_{gm}	F_{iSTP}	F_i^M	A_{glm}	N_C^*	$\frac{Z}{F_{iSTP}}$	$\frac{V_R}{F_i^M}$
0.906	0.874	0.890	68.5	3.06	1.64	1.54	0.548	0.110
"	"	"	59.2	2.65	1.51	1.28	0.635	0.127
"	"	"	44.9	2.00	1.27	1.005	0.835	0.168
"	"	"	38.0	1.70	1.13	0.970	0.985	0.197
0.908	0.877	0.893	34.7	1.55	1.24	0.925	1.08	0.216
"	"	"	20.2	0.904	0.691	0.629	1.86	0.370
"	"	"	8.60	0.384	0.322	0.316	4.36	0.871
"	"	"	4.75	0.212	0.196	0.178	7.90	1.58

TABLE 3. 28. Series B. Component A.

C	C'	$\frac{\alpha}{1+\alpha}$	P_{ai}	P_{ao}	$\overline{K}_{ga}$	NRU_a	$NChU_a$
57.2	60	0.488	0.505	0.277	0.926	0.411	1.03
59.0	62	"	"	0.269	0.975	0.434	1.1
61.0	62	"	0.500	0.256	0.961	0.461	1.2
61.9	64	"	"	0.253	0.795	0.468	1.225
67.6	69	"	"	0.225	0.906	0.547	1.515
71.1	75	0.525	0.465	0.183	1.07	0.659	2.09
74.2	75	"	"	0.168	1.13	0.759	2.41
87.8	-	"	"	0.089	1.38	1.097	5.51
91.0	-	0.50	0.488	0.075	1.36	1.185	6.06
55.9	-	"	"	0.270	0.915	0.408	1.045
59.8	-	"	"	0.253	0.87	0.452	1.195
61.5	-	0.488	0.500	0.254	1.12	0.466	1.205
67.5	-	"	0.486	0.218	0.891	0.56	1.52
86.0	-	"	0.486	0.111	1.39	0.963	4.26

TABLE 3. 29. Series B. Component B.

$\frac{\beta}{1+\beta}$	Y_{bo}	P_{bi}	P_{bo}	$\overline{K}_{gb}$	NRU_b	$NChU_b$
0.512	0.276	0.482	0.246	1.07	0.472	1.275
"	0.267	"	0.239	1.11	0.492	1.365
"	0.252	0.478	0.223	1.145	0.529	1.515
"	0.250	"	0.221	1.155	0.539	1.54
"	0.216	"	0.191	0.908	0.647	1.96
0.475	0.281	0.513	0.249	0.952	0.489	1.28
"	0.267	"	0.236	0.794	0.527	1.405
"	0.186	"	0.165	0.940	0.744	2.40
0.50	0.085	0.488	0.075	1.36	1.185	6.06
"	0.306	"	0.270	0.915	0.408	1.045
"	0.287	"	0.254	0.868	0.452	1.195
0.512	0.254	0.477	0.224	0.995	0.530	1.50
"	0.218	0.463	0.186	1.00	0.629	1.93
"	0.087	"	0.074	0.961	0.667	5.50

TABLE 3. 30 Series C. Component A.

C	C′	$\frac{\alpha}{1+\alpha}$	P_{ai}	P_{ao}	$\overline{K}_{ga}$	NRU_a	$NChU_a$
47.9	54	0.49	0.479	0.306	0.771	0.314	0.746
50.4	56	"	"	0.296	0.756	0.341	0.817
55.7	54	"	"	0.274	0.891	0.398	0.840
62	59.5	0.488	0.481	0.248	0.905	0.473	1.235
70.5	69	"	0.475	0.202	1.16	0.599	1.71
77	72.5	"	"	0.167	1.28	0.713	2.26
89	90	0.52	0.445	0.080	1.43	1.135	5.67
52.3	56	"	"	0.262	0.935	0.383	1.00
57.6	60	0.519	0.450	0.243	0.975	0.444	1.205
66	72	"	"	0.205	1.05	0.563	1.66
68	70	0.53	0.440	0.191	1.17	0.588	1.865
74	75	"	"	0.161	1.34	0.699	2.42
80.5	81.5	"	"	0.128	1.62	0.840	3.30

TABLE 3. 31. Series C. Component B.

$\frac{\beta}{1+\beta}$	Y_{bo}	P_{bi}	P_{bo}	$\overline{K}_{gb}$	NRU_b	$NChU_b$
0.51	0.326	0.461	0.283	0.862	0.351	0.875
"	0.315	"	0.274	0.835	0.377	0.960
"	0.289	"	0.250	0.99	0.432	1.170
0.512	0.249	0.459	0.217	1.07	0.540	1.545
"	0.199	0.453	0.171	1.335	0.689	1.705
"	0.156	"	0.138	1.51	0.840	3.06
0.48	0.164	0.483	0.141	1.03	0.820	2.82
"	0.359	"	0.308	0.775	0.318	0.73
0.481	0.345	0.487	0.289	0.818	0.370	0.839
"	0.294	"	0.254	0.855	0.459	1.170
0.47	0.309	0.497	0.267	0.852	0.436	1.07
"	0.279	"	0.241	0.948	0.504	1.295
"	0.245	"	0.211	1.12	0.590	1.62

TABLE 3. 32. Series D. Component A.

C	C'	$\frac{\alpha}{1+\alpha}$	P_{ai}	P_{ao}	$\overline{K}_{ga}$	NRU_a	$NChU_a$
40.1	42	0.488	0.482	0.343	0.92	0.25	0.563
40.3	42.5	0.485	0.485	0.345	0.932	0.252	0.563
43	-	0.50	0.470	0.323	0.930	0.280	0.655
47.6	-	0.493	0.475	0.310	0.986	0.319	0.756
53.2	-	"	"	0.288	1.06	0.375	0.925
55.5	-	"	"	0.278	1.03	0.401	1.00
63	-	"	"	0.245	1.29	0.487	1.3
68.6	-	"	"	0.216	1.58	0.570	1.62
83.5	-	0.495	0.473	0.121	1.84	0.920	3.09
38.9	-	"	"	0.340	0.909	0.244	0.55
45.9	-	"	0.470	0.313	0.93	0.303	0.715
55.1	-	"	"	0.276	1.20	0.397	0.992
61.4	-	"	"	0.249	1.26	0.470	1.241
77.9	-	"	"	0.162	1.76	0.745	2.460

TABLE 3. 33. Series D. Component B.

$\frac{\beta}{1+\beta}$	Y_{bo}	P_{bi}	P_{bo}	$\overline{K}_{gb}$	NRU_b	$NChU_b$
0.512	0.356	0.458	0.317	1.02	0.278	0.667
0.515	0.35	"	0.311	1.08	0.292	0.704
0.50	0.363	0.470	0.323	0.930	0.280	0.655
0.507	0.332	0.462	0.294	1.045	0.339	0.835
"	0.306	"	0.271	1.13	0.400	1.03
"	0.295	"	0.261	1.095	0.427	1.118
"	0.256	"	0.227	0.847	0.525	1.473
"	0.223	"	0.198	1.055	0.616	1.855
0.505	0.119	0.464	0.105	2.01	1.00	4.12
"	0.372	"	0.329	0.955	0.256	0.592
"	0.343	0.461	0.302	0.950	0.309	0.762
"	0.300	"	0.264	1.265	0.418	1.08
"	0.263	"	0.236	1.19	0.495	1.37
"	0.168	"	0.148	1.88	0.795	2.78

TABLE 3. 34. Series E. Component A.

C	C′	$\frac{\alpha}{1+\alpha}$	P_{ai}	P_{ao}	$\bar{K}_{ga}$	NRU_a	$NChU_a$
23.0	25	0.48	0.47	0.396	0.883	0.129	0.263
30.1	29	"	"	0.376	1.04	0.172	0.364
33.8	35	"	"	0.365	1.15	0.197	0.423
36.2	42	"	"	0.356	1.21	0.216	0.473
49.6	51	0.49	0.462	0.305	1.64	0.357	0.804
57.0	60	0.475	0.477	0.282	1.815	0.401	0.878
60.0	63	"	"	0.269	1.97	0.435	1.03
71.6	76.5	"	"	0.210	2.99	0.600	1.621
31.8	33	"	0.474	0.375	1.10	0.180	0.334
33.7	34	"	"	0.369	1.13	0.194	0.362
37.1	40	0.50	0.451	0.338	1.15	0.226	0.517
41.5	44	"	"	0.322	1.32	0.267	0.623
49.2	51	"	"	0.294	1.59	0.337	0.823
62.1	63	"	"	0.240	2.24	0.485	1.305

TABLE 3. 35. Series E. Component B.

$\frac{\beta}{1+\beta}$	Y_{bo}	P_{bi}	P_{bo}	$\bar{K}_{gb}$	NRU_b	$NChU_b$
0.52	0.411	0.434	0.359	0.987	0.144	0.326
"	0.385	"	0.337	1.215	0.200	0.471
"	0.375	"	0.325	1.345	0.231	0.545
"	0.362	"	0.319	1.36	0.245	0.600
0.51	0.322	0.446	0.282	1.68	0.364	0.905
0.525	0.251	0.431	0.220	2.34	0.520	1.505
"	0.234	"	0.205	2.58	0.570	1.71
"	0.160	"	0.140	4.07	0.815	2.99
"	0.360	0.430	0.314	1.545	0.251	0.606
"	0.362	"	0.316	1.43	0.245	0.590
0.50	0.387	0.453	0.338	1.15	0.226	0.517
"	0.369	"	0.322	1.32	0.267	0.623
"	0.337	"	0.294	1.59	0.337	0.823
"	0.275	"	0.240	2.24	0.485	1.305

TABLE 3. 36. Series F. Component A.

C	C'	$\frac{\alpha}{1+\alpha}$	P_{ai}	P_{ao}	$\bar{K}_{ga}$	NRU_a	$NChU_a$
23.4	26.5	0.510	0.448	0.406	1.16	0.129	0.263
27.2	29	"	"	0.399	1.24	0.152	0.320
34.2	37	"	"	0.394	1.095	0.206	0.436
38.1	39	"	"	0.371	1.54	0.234	0.506
48.3	48	"	0.445	0.340	2.21	0.297	0.703
56.7	62	"	"	0.283	3.38	0.416	1.075
71.6	74.5	"	"	0.234	4.3	0.657	2.01
22.5	24	"	"	0.398	1.26	0.133	0.297
23.6	26.5	"	"	0.392	1.36	0.101	0.239
24.5	26.5	0.488	0.462	0.401	1.38	0.129	0.273
28.7	31	"	"	0.364	1.99	0.158	0.335
33.2	35.5	"	"	0.324	2.86	0.188	0.409
58.3	62	"	"	0.280	3.5	0.415	1.04

TABLE 3. 37. Series F. Component B.

$\frac{\beta}{1+\beta}$	Y_{bo}	P_{bi}	P_{bo}	$\bar{K}_{gb}$	NRU_b	$NChU_b$
0.52	0.41	0.428	0.357	1.215	0.147	0.334
"	0.395	"	0.344	1.44	0.178	0.412
"	0.368	"	0.320	1.53	0.238	0.57
"	0.351	"	0.306	1.57	0.256	0.667
0.50	0.356	0.453	0.314	1.92	0.297	0.703
"	0.302	"	0.266	2.95	0.421	1.075
0.488	0.252	0.464	0.223	3.78	0.640	1.54
"	0.452	"	0.399	1.045	0.118	0.245
0.52	0.408	0.440	0.362	1.331	0.161	0.353
"	0.405	"	0.360	1.315	0.164	0.367
"	0.389	"	0.345	1.54	0.204	0.46
"	0.372	"	0.33	1.575	0.238	0.555
"	0.254	"	0.226	3.25	0.52	0.970

TABLE 3. 38. Series G. Component A.

C	C′	$\frac{\alpha}{1+\alpha}$	P_{ai}	P_{ao}	$\bar{K}_{ga}$	NRU_a	$NChU_a$
13.5	17.2	0.51	0.448	0.406	1.16	0.079	0.163
16.4	25	"	"	0.399	1.24	0.0843	0.204
18.6	24	"	"	0.394	1.095	0.1082	0.231
26.4	33	"	"	0.371	1.54	0.178	0.372
36.2	34	"	0.445	0.340	2.21	0.228	0.529
51.6	49.5	"	"	0.283	3.38	0.370	0.942
63	65.5	"	"	0.234	4.3	0.506	1.415
16.6	19.0	"	"	0.398	1.26	0.092	0.199
19.2	20.5	"	"	0.392	1.36	0.107	0.230
21.7	29.0	0.488	0.462	0.401	1.38	0.119	0.248
33.8	35.0	"	"	0.364	1.99	0.201	0.440
45.2	48.5	"	"	0.324	2.86	0.294	0.680
56.1	60	"	"	0.280	3.5	0.402	1.000

TABLE 3. 39. Series G. Component B.

$\frac{\beta}{1+\beta}$	Y_{bo}	P_{bi}	P_{bo}	$\bar{K}_{gb}$	NRU_b	$NChU_b$
0.490	0.458	0.465	0.411	1.465	0.102	0.210
"	0.467	"	0.419	1.105	0.084	0.172
"	0.461	"	0.414	1.165	0.095	0.198
"	0.437	"	0.392	1.505	0.143	0.305
"	0.392	0.464	0.350	2.28	0.235	0.524
"	0.344	"	0.301	3.06	0.337	0.802
"	0.209	"	0.187	5.71	0.67	2.05
"	0.467	"	0.418	1.105	0.081	0.169
"	0.461	"	0.412	1.225	0.096	0.199
0.512	0.424	0.441	0.377	1.56	0.133	0.293
"	0.381	"	0.339	2.24	0.225	0.518
"	0.334	"	0.297	3.2	0.328	0.810
"	0.282	"	0.250	3.96	0.455	1.22

TABLE 3. 40 Series H. Component A.

C	C'	$\frac{\alpha}{1+\alpha}$	P_{ai}	P_{ao}	$\overline{K}_{ga}$	NRU_a	$NChU_a$
39.2	41.0	0.509	0.469	0.332	1.2	0.252	0.568
40.4	40.5	"	"	0.328	1.2	0.263	0.600
44.0	44	"	"	0.316	1.25	0.294	0.682
53.0	50	"	"	0.277	1.31	0.391	0.965
63.6	61	"	0.465	0.231	1.545	0.515	1.38
71.8	67	"	"	0.191	1.82	0.543	1.91
74.9	72	"	"	0.174	1.82	0.700	2.33
42.9	40	0.51	0.468	0.321	1.23	0.279	0.685
44.9	42.9	"	"	0.314	1.11	0.296	0.742
49.7	47.0	"	"	0.295	1.225	0.346	0.905
56.0	53	"	"	0.269	1.31	0.411	1.13
62.9	59	"	"	0.238	1.44	0.500	1.455

TABLE 3. 41. Series H. Component B.

$\frac{\beta}{1+\beta}$	Y_{bo}	P_{bi}	P_{bo}	$\overline{K}_{gb}$	NRU_b	$NChU_b$
0.491	0.39	0.486	0.351	1.125	0.237	0.570
"	0.385	"	0.346	1.135	0.249	0.557
"	0.372	"	0.334	1.18	0.277	0.63
"	0.330	"	0.296	1.24	0.368	0.889
"	0.285	0.483	0.254	1.43	0.472	1.23
"	0.239	"	0.213	1.53	0.587	1.68
"	0.222	"	0.197	1.665	0.635	1.88
0.49	0.378	0.494	0.343	1.19	0.269	0.603
"	0.371	"	0.336	1.07	0.286	0.648
"	0.353	"	0.320	1.14	0.320	0.746
"	0.325	"	0.294	1.245	0.391	0.940
"	0.290	"	0.263	1.34	0.465	1.19

TABLE 3. 42. Series C'. Component A.

C	C'	$\frac{\alpha}{1+\alpha}$	P_{ai}	P_{ao}	$\overline{K}_{ga}$	NRU_a	$NChU_a$
47.1	-	0.487	0.49	0.316	0.815	0.307	0.62
52.1	-	"	"	0.286	0.845	0.382	0.89
60.4	-	"	"	0.260	0.975	0.450	1.15
63.1	-	0.495	0.484	0.241	1.004	0.497	1.33
69.3	-	"	"	0.211	1.145	0.585	1.68
70.4	-	0.509	0.475	0.198	1.14	0.623	1.88
78.0	-	"	"	0.150	1.18	0.665	2.66
70.4	-	"	"	0.198	0.83	0.623	1.88
47.9	-	0.513	0.471	0.295	0.825	0.337	0.833
54.5	-	"	"	0.269	0.895	0.404	1.10
63.5	-	"	"	0.229	1.02	0.518	1.46
75.1	-	"	"	0.17	1.295	0.715	2.35
71.4	-	"	0.473	0.191	1.035	0.645	1.98
69.8	-	"	"	0.199	0.950	0.617	1.865

TABLE 3. 43. Series C'. Component B.

$\frac{\beta}{1+\beta}$	Y_{bo}	P_{bi}	P_{bo}	$\overline{K}_{gb}$	NRU_b	$NChU_b$
0.513	0.326	0.468	0.288	0.930	0.35	0.865
"	0.287	"	0.253	0.990	0.446	1.18
"	0.257	"	0.227	1.125	0.52	1.465
0.505	0.259	0.474	0.229	1.050	0.519	1.45
"	0.224	"	0.198	1.200	0.615	1.85
0.491	0.249	0.490	0.222	0.939	0.514	1.62
"	0.213	"	0.190	1.16	0.655	2.0
"	0.252	"	0.226	0.74	0.553	1.54
0.487	0.365	0.496	0.325	0.753	0.307	0.702
"	0.337	"	0.301	0.765	0.342	0.84
"	0.294	"	0.262	0.895	0.453	1.16
"	0.232	"	0.207	1.11	0.608	1.755
"	0.253	0.498	0.227	0.89	0.553	1.525
"	0.262	"	0.235	0.81	0.527	1.435

TABLE 3. 44. Series I. Component A.

C	C′	$\frac{\alpha}{1+\alpha}$	P_{ai}	P_{ao}	$\overline{K}_{ga}$	NRU_a	$NChU_a$
21.2	30	0.326	0.653	0.543	0.157	0.077	0.277
23.4	32	0.324	0.656	0.54	0.159	0.086	0.319
25.7	28	0.323	0.657	0.533	0.170	0.097	0.394
34.5	35	0.320	0.660	0.51	0.209	0.136	0.682
42.1	44	"	"	0.484	0.238	0.175	1.18
43.9	50	"	"	0.476	0.221	0.186	1.465

TABLE 3. 45. Series I. Component B.

C	$\frac{\beta}{1+\beta}$	Y_{bo}	P_{bi}	P_{bo}	$\overline{K}_{gb}$	NRU_b	$NChU_b$
43.7	0.674	0.214	0.318	0.188	0.795	0.390	0.600
50.0	0.676	0.197	0.315	0.173	0.830	0.450	0.700
53.7	0.677	0.181	0.314	0.159	0.918	0.521	0.800
70.3	0.680	0.120	0.311	0.1055	1.30	0.840	1.335
89.3	"	0.048	"	0.042	2.07	1.520	2.38
93.5	"	0.03	"	0.0263	2.19	1.840	3.14

TABLE 3. 46. Series J. Component A.

C	C′	$\frac{\alpha}{1+\alpha}$	P_{ai}	P_{ao}	$\overline{K}_{ga}$	NRU_a	$NChU_a$
86.5	88	0.685	0.30	0.049	2.96	1.58	2.14
90	94	0.686	0.299	0.038	3.12	1.56	2.60
90.6	98	0.669	0.315	0.038	2.94	1.59	2.76
97.9	100	"	"	0.009	4.2	2.58	4.67
100	100	0.671	0.313	0			

TABLE 3. 47. Series J. Component B.

C	$\frac{\beta}{1+\beta}$	Y_{bo}	P_{bi}	P_{bo}	$\bar{K}_{gb}$	NRU_b	$NChU_b$
42.5	0.315	0.567	0.652	0.485	0.347	0.162	1.03
43.7	0.314	0.563	0.653	0.483	0.406	0.167	0.71
46.3	0.331	0.521	0.637	0.447	0.382	0.206	1.83
48.5	"	0.510	"	0.437	0.360	0.221	2.39
49.0	0.329	0.510	0.639	0.437	0.312	0.223	3.34

TABLE 3. 48. Series M. Component A.

C	C'	$\frac{\alpha}{1+\alpha}$	P_{ai}	P_{ao}	$\bar{K}_{ga}$	NRU_a	$NChU_a$
9.8	8.5	0.324	0.62	0.580	0.195	0.033	0.109
13.7	14	"	"	0.571	0.256	0.048	0.163
12.55	12.5	"	"	0.574	0.206	0.041	0.145
21.8	22.5	"	"	0.555	0.266	0.073	0.165
22.4	24	0.339	0.60	0.528	0.352	0.085	0.245
27.7	34	"	"	0.514	0.425	0.109	0.341
30.8	37.5	"	"	0.504	0.466	0.124	0.418

TABLE 3. 49. Series M. Component B.

C	$\frac{\beta}{1+\beta}$	Y_{bo}	P_{bi}	P_{bo}	$\bar{K}_{gb}$	NRU_b	$NChU_b$
20.9	0.676	0.275	0.298	0.244	0.925	0.156	0.238
28.6	"	0.255	"	0.227	1.23	0.229	0.352
26.3	"	0.261	"	0.232	1.06	0.208	0.319
42.2	"	0.217	"	0.193	1.34	0.371	0.321
43.6	0.661	0.224	0.308	0.196	1.59	0.382	0.451
54.0	"	0.191	"	0.167	2.0	0.512	0.764
60.7	"	0.168	"	0.148	2.32	0.614	0.940

TABLE 3. 50 Series N. Component A.

C	C′	$\frac{\alpha}{1+\alpha}$	P_{ai}	P_{ao}	$\bar{K}_{ga}$	NRU_a	$NChU_a$
54	48	0.687	0.284	0.151	3.34	0.535	0.81
55.4	57	0.707	0.265	0.147	2.98	0.505	0.71
56.3	60	0.701	0.271	0.137	3.07	0.580	0.87
63.9	68	"	"	0.117	3.59	0.712	1.08
66.6	71	"	0.272	0.109	3.25	0.775	1.175
78.1	82	"	"	0.075	4.67	1.067	1.635
92	93	"	"	0.029	7.04	1.765	2.82
94	96	"	"	0.023	7.02	1.945	3.13

TABLE 3. 51. Series N. Component B.

C	$\frac{\beta}{1+\beta}$	Y_{bo}	P_{bi}	P_{bo}	$\bar{K}_{gb}$	NRU_b	$NChU_b$
21.4	0.313	0.633	0.622	0.553	0.472	0.076	0.300
21.3	0.293	0.655	0.641	0.572	0.422	0.072	0.312
23.8	0.299	0.641	0.635	0.560	0.433	0.082	0.365
27.1	"	0.631	"	0.551	0.475	0.094	0.460
28.2	"	0.626	0.636	0.550	0.416	0.099	0.489
33.3	"	0.610	"	0.535	0.530	0.121	0.700
39.2	"	0.588	"	0.516	0.587	0.147	1.19
39.9	"	0.585	"	0.513	0.550	0.151	1.35

TABLE 3. 52. Reactor V. Series L.

Suspending Medium - Water.

L	θ	F_i	F_{iSTP}	Y_{ai}	Y_{ao}	C	π	T_R °C	F_o	C′
1	24	53.1	50.1	0.533	0.476	19.2	76.5	18	46.6	25
2	24	32.2	30.4	"	0.459	25.7	"	"	28.2	25
3	92	6.89	6.50	"	0.414	38.2	"	"	5.68	35
4	24	55.6	52.5	"	0.506	10.3	"	"	51.5	15
5	32	25.8	24.4	0.512	0.472	14.8	"	"	23.7	20
6	36	14.7	13.5	"	0.462	17.2	75.4	"	13.7	25
7	24	68.5	63.0	"	0.503	3.54	"	"	64.6	11

TABLE 3. 53. Reactor II. Series Q.

Suspending Medium - Water.

Q	θ	F_i	F_{iSTP}	Y_{ai}	Y_{ao}	C	π	T_R °C	F_o	C′
1	24	41.2	38.7	0.485	0.464	8.1	76.2	18	38.6	13
2	20	63.3	59.5	"	0.466	7.35	"	"	59.7	11
3	28	27.0	25.4	"	0.465	7.75	"	"	25.5	11
4	80	7.55	7.1	0.489	0.441	17.6	76.1	"	6.70	22.5
5	32	22.3	21.0	"	0.470	7.4	"	"	20.8	13
6	32	36.4	34.2	"	0.474	7.2	"	"	34.3	11
7	24	50.0	47.0	"	0.480	3.54	"	"	48.1	8
8	24	61.2	57.5	"	0.488	0.4	"	"	60.0	3
9	28	43.5	41.1	0.482	0.476	2.38	76.4	17	42.2	5
10	32	19.45	18.4	"	0.472	3.92	"	"	18.9	5

TABLE 3. 54. Reactor V. Series K.

Suspending Medium - Decalin.

K	θ	F_i	Y_{ai}	Y_{ao}	π	T_R °C	F_o
1	24	80.9	0.528	0.395	76	17	58.1
2	28	48.3	"	0.364	"	"	35.4
3	36	25.4	"	0.323	"	"	17.4
4	80	5.92	"	0.270	"	"	38.4
5	20	65.1	0.514	0.375	"	"	49.8
6	32	34.9	"	0.321	"	"	24.4

TABLE 3. 55. Reactor II. Series O.

Suspending Medium - Decalin.

O	θ	F_i	Y_{ai}	Y_{ao}	π	T_R °C	F_o
1	20	72.5	0.483	0.433	75	18	65.5
2	24	55.9	0.493	0.431	"	"	48.6
3	28	46.9	"	0.431	"	"	40.8
4	32	25.9	0.485	0.395	75.7	"	21.4
5	36	22.0	"	0.385	"	"	16.9
6	60	11.6	"	0.349	"	"	8.3
7	92	6.27	"	0.310	"	"	4.55
8	32	30.4	0.50	0.412	74.7	"	26.1

TABLE 3. 56. Reactor II. Series P.

Suspending Medium - Decalin.

P	θ	T°C	F_i	F_{iSTP}	Y_{ai}	Y_{ao}	F_o	π	T_R °C	C	C′
1	32	75	30.4	28.0	0.500	0.412	26.1	74.5	18	29.9	29
2	32	100	31.4	28.9	"	0.391	25.4	"	"	36.8	37
3	28	125	30.4	28.0	"	0.370	23.8	"	"	41.2	44
4	32	50	30.8	28.6	0.489	0.450	28.0	75.1	19	14.7	18
5	32	25	31.2	28.9	"	0.483	30.5	"	"	2.38	5

TABLE 3. 57. Series K.

Π_{gi}	Π_{go}	Π_{gm}	F_{iSTP}	F_i^M	A_{glm}	N_C^*	$\frac{Z}{F_{iSTP}}$	$\frac{V_R}{F_i^M}$
1.073	0.978	1.026	76.1	3.4	1.74	0.755	1.47	0.291
"	"	"	45.5	2.03	1.24	0.527	2.47	0.488
"	"	"	23.9	1.07	0.715	0.327	4.70	0.926
"	"	"	5.56	0.249	0.22	0.088	20.2	3.98
"	"	"	61.4	2.74	1.50	0.615	1.83	0.361
"	"	"	32.9	1.47	0.99	0.422	3.42	0.675

TABLE 3. 58. Series K. Component A.

C	C′	$\frac{\alpha}{1+\alpha}$	P_{ai}	P_{ao}	$\overline{K}_{ga}$	NRU_a	$NChU_a$
41.6	47	0.472	0.576	0.386	0.524	0.270	0.570
48.8	53.5	"	"	0.356	0.538	0.333	0.769
57.4	63	"	"	0.316	0.617	0.419	0.988
67.0	70	"	"	0.264	0.635	0.540	1.39
43.4	47	0.486	0.550	0.367	0.490	0.274	0.624
55.5	60	"	"	0.314	0.567	0.388	0.955

TABLE 3. 59. Series K. Component B.

$\frac{\beta}{1+\beta}$	Y_{bo}	P_{bi}	P_{bo}	$\overline{K}_{gb}$	NRU_b	$NChU_b$
0.528	0.324	0.507	0.317	0.636	0.331	0.843
"	0.289	"	0.283	0.670	0.415	1.12
"	0.243	"	0.238	0.805	0.541	1.59
"	0.184	"	0.180	0.815	0.430	2.47
0.514	0.340	"	0.323	0.550	0.282	0.758
"	0.284	"	0.278	0.605	0.311	1.165

TABLE 3. 60 Series O.

η_{gi}	η_{go}	η_{gm}	F_{iSTP}	F_i^M	A_{glm}	N_C^*	$\frac{Z}{F_{iSTP}}$	$\frac{V_R}{F_i^M}$
0.988	0.965	0.982	67.1	3.00	1.68	0.870	0.558	0.112
"	"	"	51.7	2.31	1.43	0.755	0.727	0.145
"	"	"	43.4	1.94	1.275	0.634	0.865	0.173
1.008	0.975	0.992	24.2	1.08	0.84	0.481	1.55	0.311
"	"	"	20.6	0.92	0.695	0.447	1.82	0.364
"	"	"	10.8	0.482	0.39	0.303	3.47	0.695
"	"	"	5.80	0.258	0.244	0.195	6.46	1.30
0.990	0.957	0.974	28.0	1.25	0.95	0.558	1.34	0.268

TABLE 3. 61. Series O. Component A.

C	C'	$\frac{\alpha}{1+\alpha}$	P_{ai}	P_{ao}	$\overline{K}_{ga}$	NRU_a	$NChU_a$
18.3	21	0.517	0.482	0.418	0.566	0.105	0.228
22.2	26	0.507	0.492	0.416	0.615	0.125	0.272
22.2	28	"	"	0.416	0.577	0.125	0.272
30.8	34	0.515	0.488	0.385	0.715	0.186	0.429
33.6	35	"	"	0.375	0.834	0.209	0.488
43.5	46	"	"	0.341	1.06	0.286	0.699
52.2	55	"	"	0.302	1.2	0.377	0.985
29.9	29	0.50	0.495	0.385	0.800	0.181	0.414

TABLE 3. 62 Series O. Component B.

$\frac{\beta}{1+\beta}$	Y_{bo}	P_{bi}	P_{bo}	$\overline{K}_{gb}$	NRU_b	$NChU_b$
0.483	0.470	0.516	0.453	0.498	0.093	0.189
0.493	0.448	0.506	0.433	0.565	0.115	0.243
"	0.448	"	0.433	0.531	0.115	0.243
0.485	0.430	0.518	0.418	0.649	0.168	0.352
"	0.421	"	0.411	0.719	0.180	0.389
"	0.386	"	0.376	0.945	0.254	0.569
"	0.350	"	0.341	1.042	0.328	0.775
0.50	0.412	0.495	0.394	0.73	0.181	0.396

3. 2. Catalyst Concentration and % Conversion.

As the catalyst properties were not under examination the removal of any catalytic influence on conversion was desirable.

It can be predicted from equation 1.2.49

$$\frac{1}{\bar{K}_{ga}} = \frac{1}{K_{ga}} + \frac{A_{gl}}{K_{ra}A_{ls}}$$

that above a certain ratio of solid/liquid surface area to gas liquid surface area, the reaction on the catalyst surface should cease to have appreciable influence on reaction rate. This was tested at constant inlet gas flow rate and composition by examining the effect, on % ethylene conversion, of changing the catalyst concentration.

Results - Tables 3.2 and 3.15.

Fig. 3.3. shows the effect on conversion of increasing the liquid solid/gas liquid surface area ratio at constant inlet gas flow rate and composition. The % conversion of ethylene increases until $A_{ls}/A_{gl} \simeq 3$. It then attains an approximately constant value. It is thus inferred from equation 1.2.49 that under such conditions, $\bar{K}_{ga}$ is virtually a mass transfer coefficient. It may be said that at an inlet flow rate of 30 litres/hr. and a reactant ratio of 1:1 the % ethylene (hydrogen) conversion is unaffected by catalyst concentrations leading to A_{ls}/A_{gl} ratios > 3.

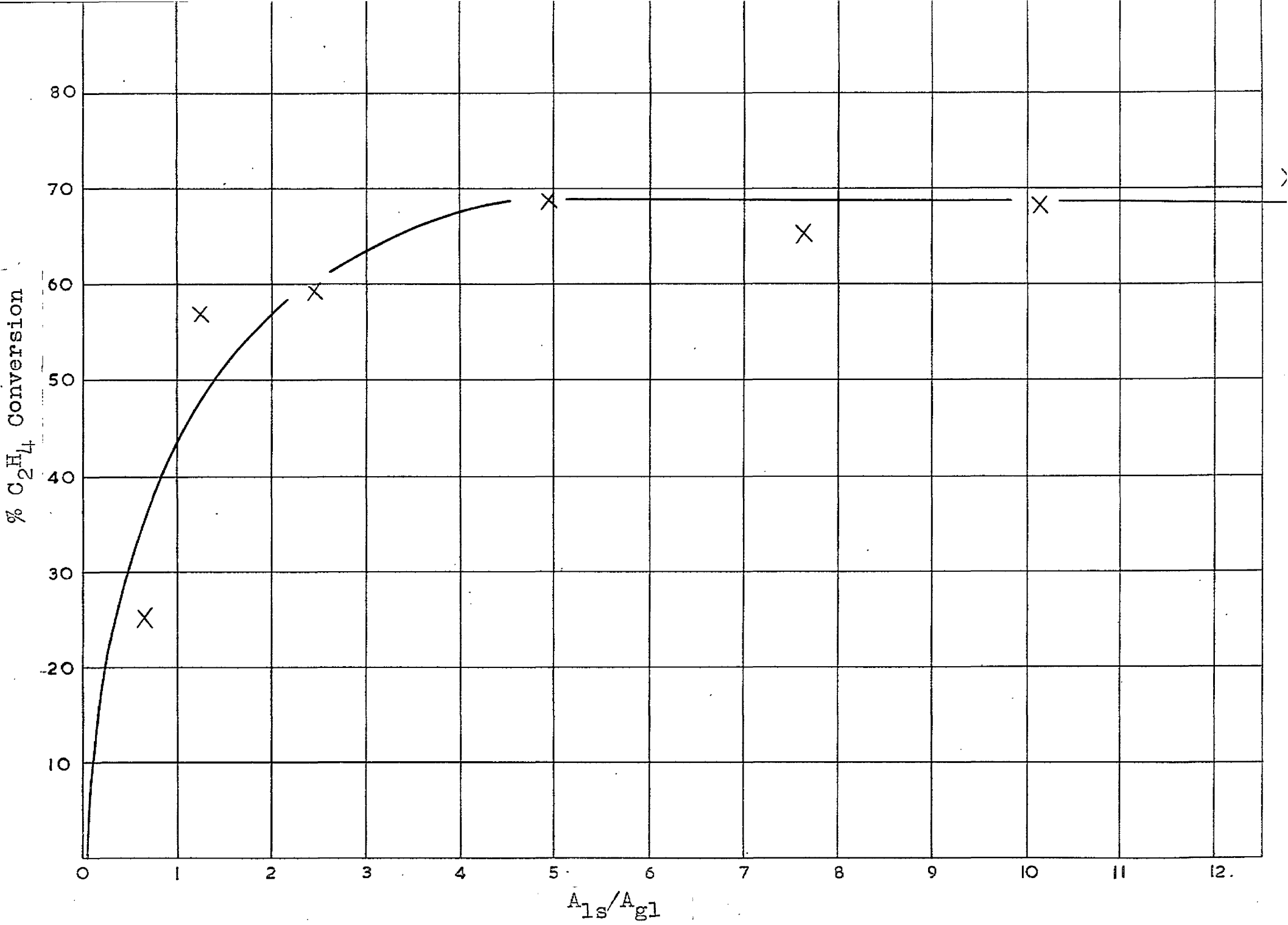
% C_2H_4 Conversion
80
70
60
50
40
30
20
10
0
1
2
3
4
5
6
7
8
9
10
11
12.
A_{ls}/A_{gl}

FIG. 3.3.

At an inlet flow rate of 70 litres/hr. $A_{gl} \simeq$ 2.0cm^2/cm^3 (Appendix 2) and since the minimum value of A_{ls}/A_{gl} for constant reaction rate is 3.0, and A_{ls} value of 6.0 cm^2/cm^3 is required. It may be shown that (Appendix 3) the specific surface of the catalyst is 247 cm^2/gm. Thus a concentration of 0.025 gms/cc. is required to give an A_{ls} value of $\simeq$ 6.00 cm^2/cm^3. By such reasoning, a catalyst concentration of 2.5 gms/100 cc. of slurry was considered the minimum catalyst concentration to ensure the removal of the influence of surface reaction on overall reaction rate. Information on gas hold up in the reactor was not obtainable because of the slurry recirculation. It was estimated that the value of A_{ls} at high gas flow rates was 0.9 of its value when no gas was flowing. In view of this, the influence of A_{ls} in determining reaction rate was assumed to be negligible over the experimental range. Calderbank (10) also states that excess catalyst removes any influence the catalyst has on reaction rate.

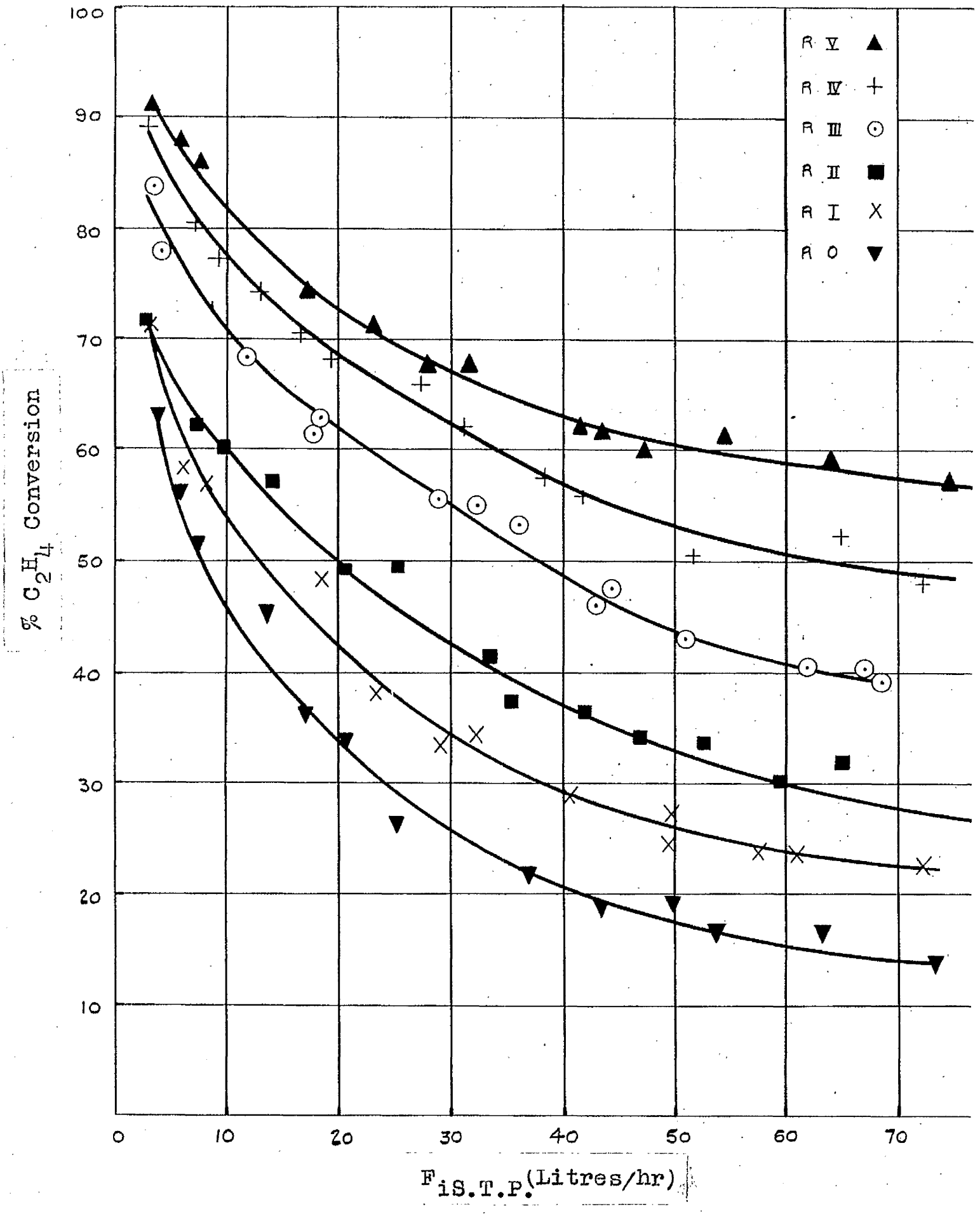
R V
R IV
R III
R II
R I
R 0
% C_2H_4 Conversion
100
90
80
70
60
50
40
30
20
10
0
10
20
30
40
50
60
70
$F_{iS.T.P.}$(Litres/hr)

FIG. 3.4.

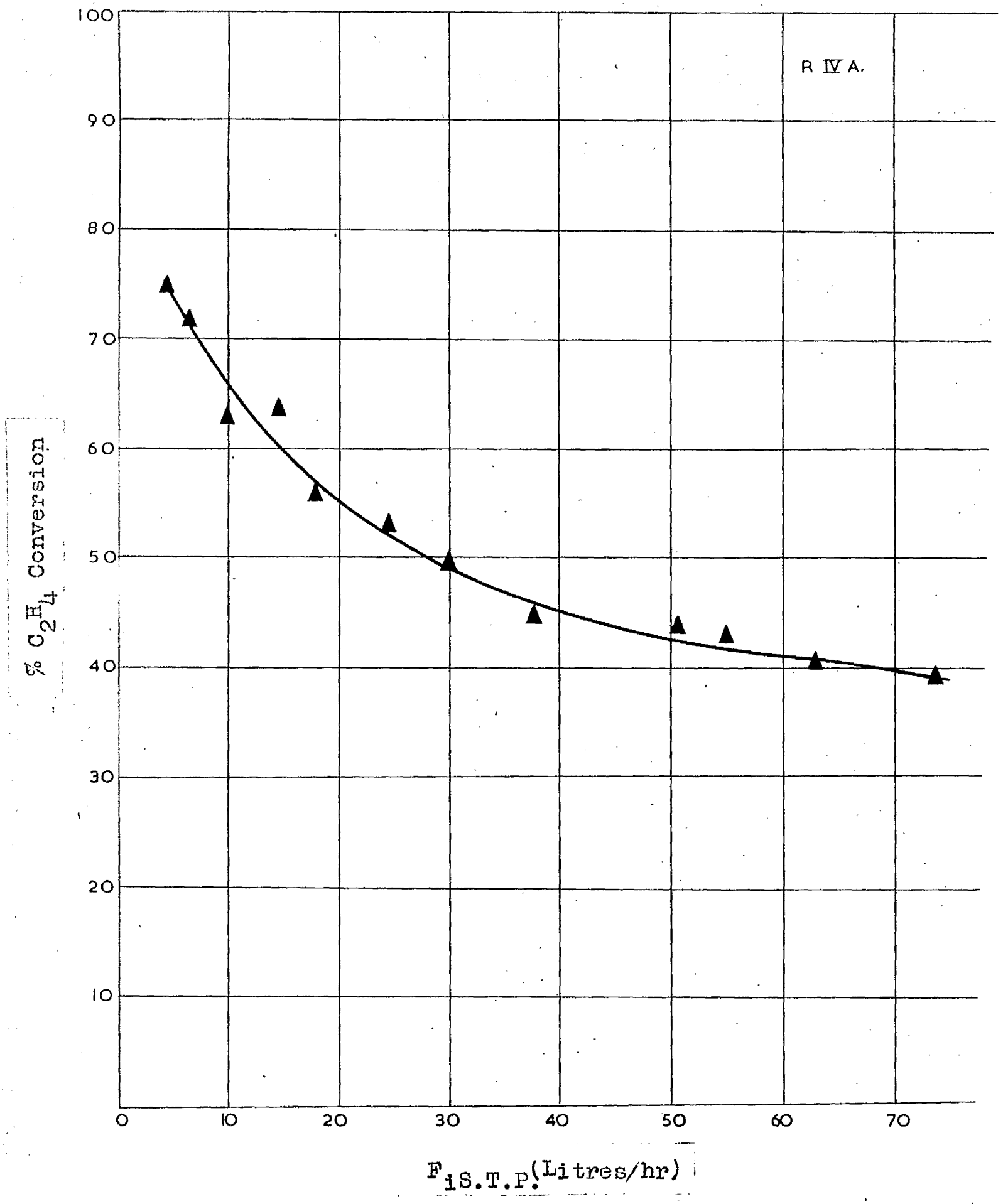
R IV A.
% C_2H_4 Conversion
100
90
80
70
60
50
40
30
20
10
0
10
20
30
40
50
60
70
$F_{i\,S.T.P.}$ (Litres/hr)

FIG. 3.5.

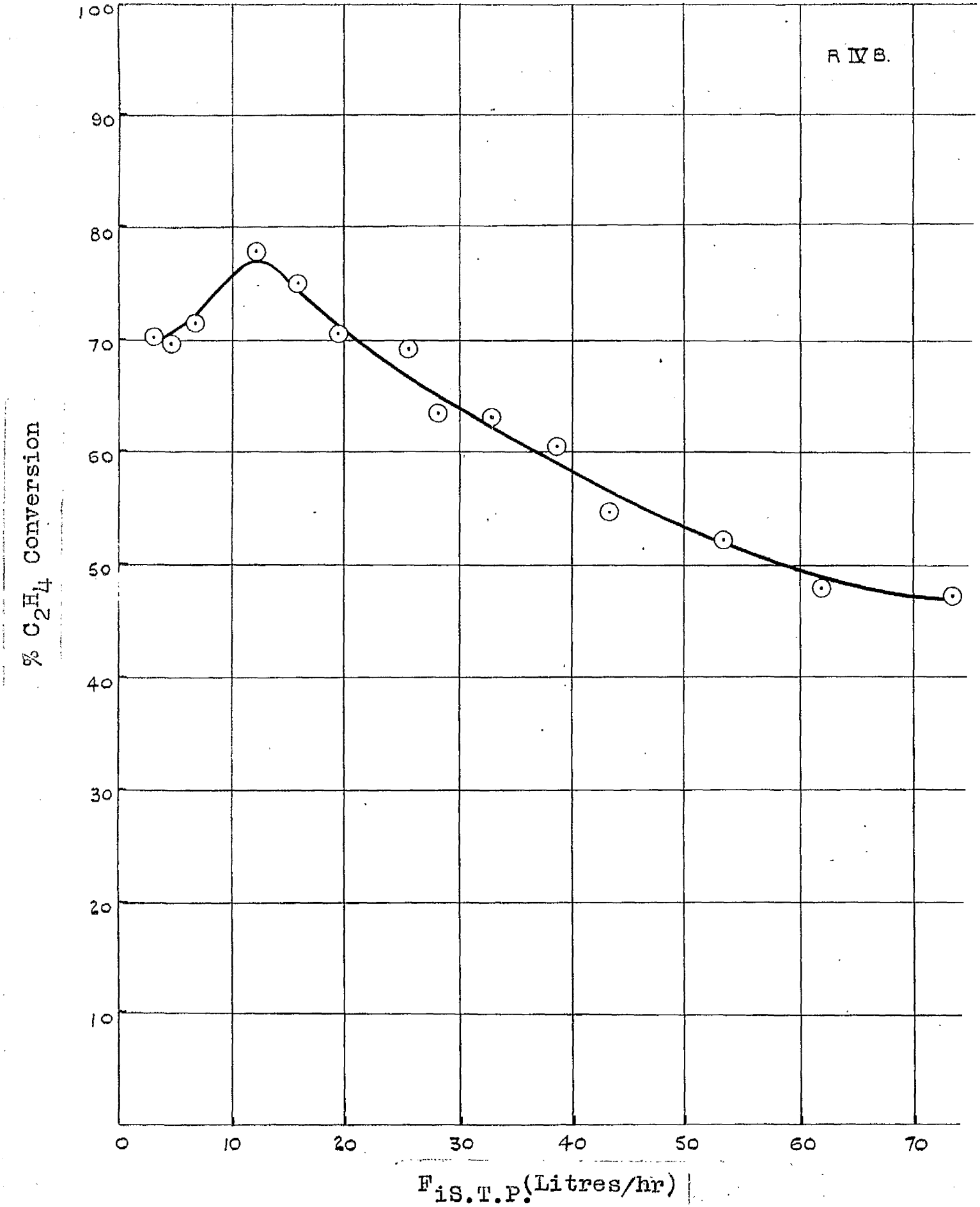
R IV B.
% C_2H_4 Conversion
100
90
80
70
60
50
40
30
20
10
0
10
20
30
40
50
60
70
$F_{iS.T.P.}$ (Litres/hr)

FIG. 3.6.

3. 3. The Effect of Flow Rate and Reactor Size on Reactant Conversion.

At constant gas inlet composition the effect of varying gas inlet flow rate on % ethylene conversion was noted for reactors V - O.

Results - see tables 3. 28, 30, 32, 34, 36, 38.

The various plots of % ethylene conversion vs. gas flow rate are shown in Fig. 3. 4. (as C_2H_4: H_2 = 1:1, similar plots would be obtained if % hydrogen conversion were used).

From Fig. 3. 4. it can be seen that conversion increases with decreasing inlet flow rate. The % conversion also appears to decrease with decreasing reactor volume at any flow rate.

Results from reactor IV A conflict with this;- table 3. 40 Fig. 3. 5. If conversion varies with reactor volume, corresponding conversions appear low. Another reactor dimension which might govern conversion is length. Conversions in the various reactors at selected flow rates are shown below.

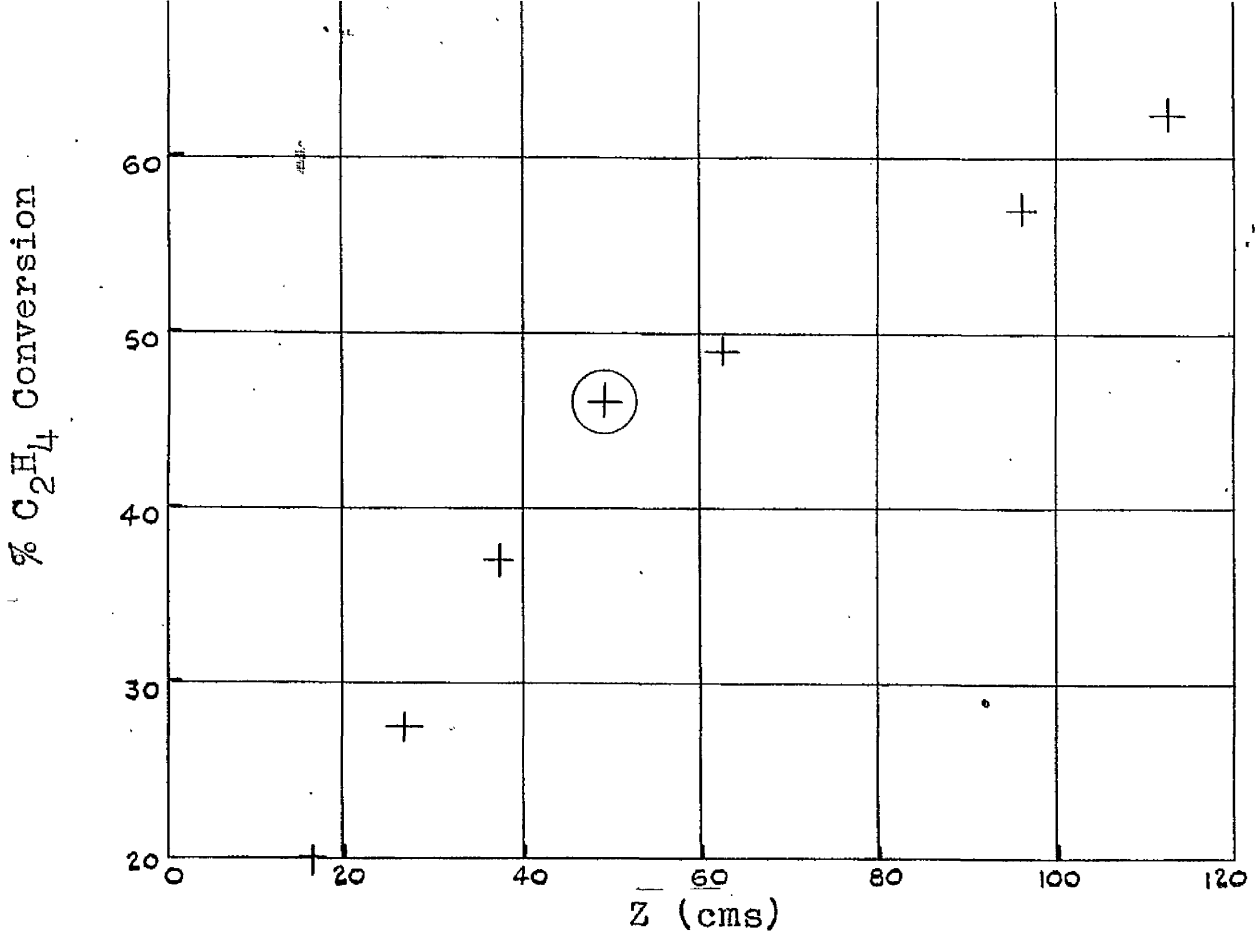
% C_2H_4 Conversion
60
50
40
30
20
0
20
40
60
80
100
120
Z (cms)

FIG. 3.8.

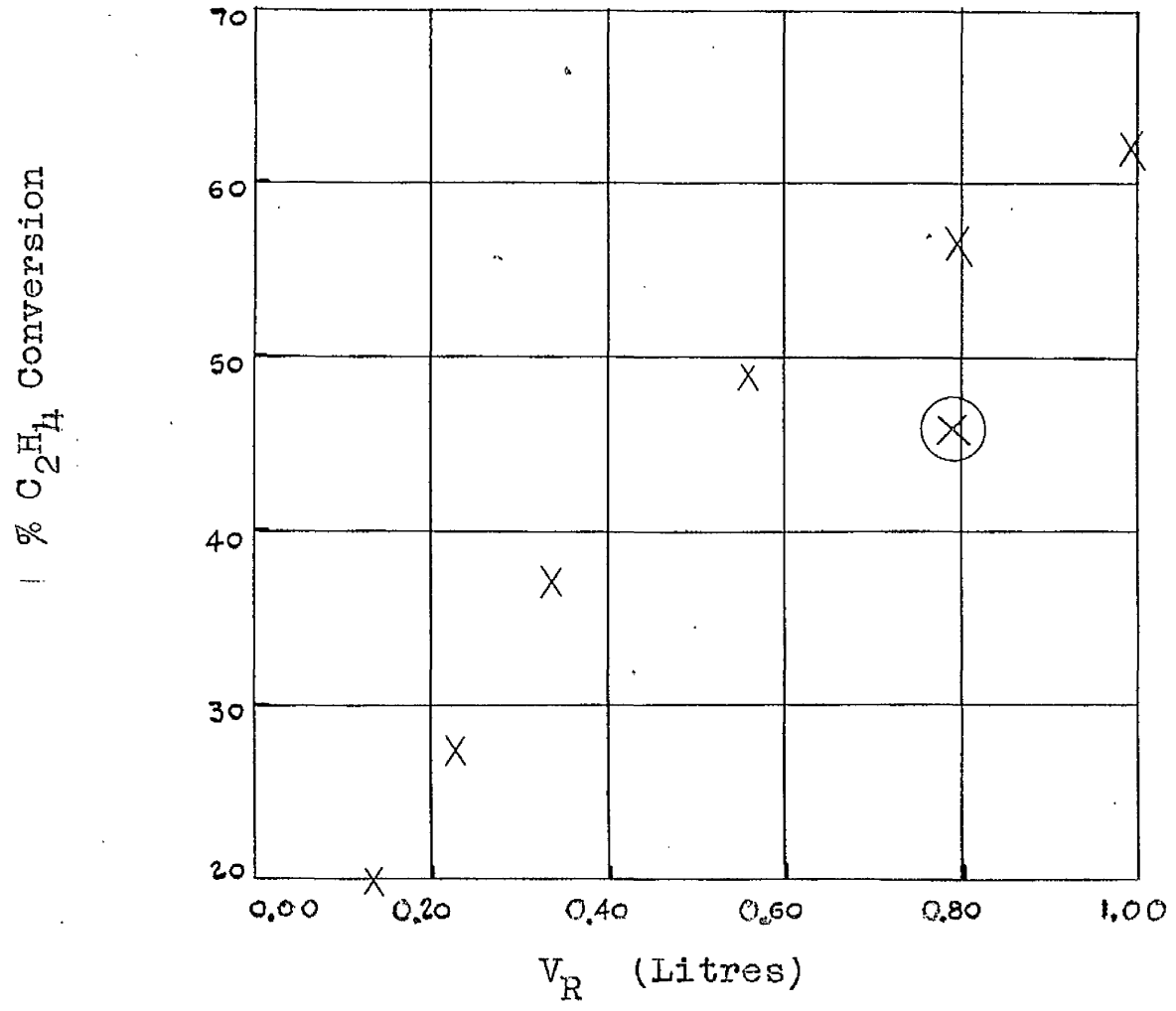
% C_2H_4 Conversion
70
60
50
40
30
20
0.00
0.20
0.40
0.60
0.80
1.00
V_R (Litres)

FIG. 3.7

Reactor	V_R	F_{iSTP} = 70 Z	40 C	40 C	10 C
V	0.990	112	58	62.5	82.5
IV	0.790	86	49	57	77
III	0.560	62	39.5	49	71
II	0.335	37.5	30.5	37	61
I	0.230	26.5	22.5	27.5	56.5
0	0.140	16.5	14	20	47.5
IV A	0.790	49.5	40	46	66.5

In Figs. 3. 7. and 3. 8. plots of % ethylene conversion *vs.* V_R and Z respectively are shown at a flow rate of 40 litres/hr. Similar plots may be obtained at the other flow rates. The point corresponding to reactor IV A does not lie on the conversion *vs.* V_R plot while it appears to lie on the conversion *vs.* Z plot.

It therefore appears justifiable to say that conversion is a function of reactor length rather than volume. Due to experimental difficulties, this point was not investigated more fully. It is also obvious that the rate of increase of conversion with reactor length decreases with increasing reactor length.

Results for reactor IV B in which there is no slurry recirculation are given in table 3. 42. A

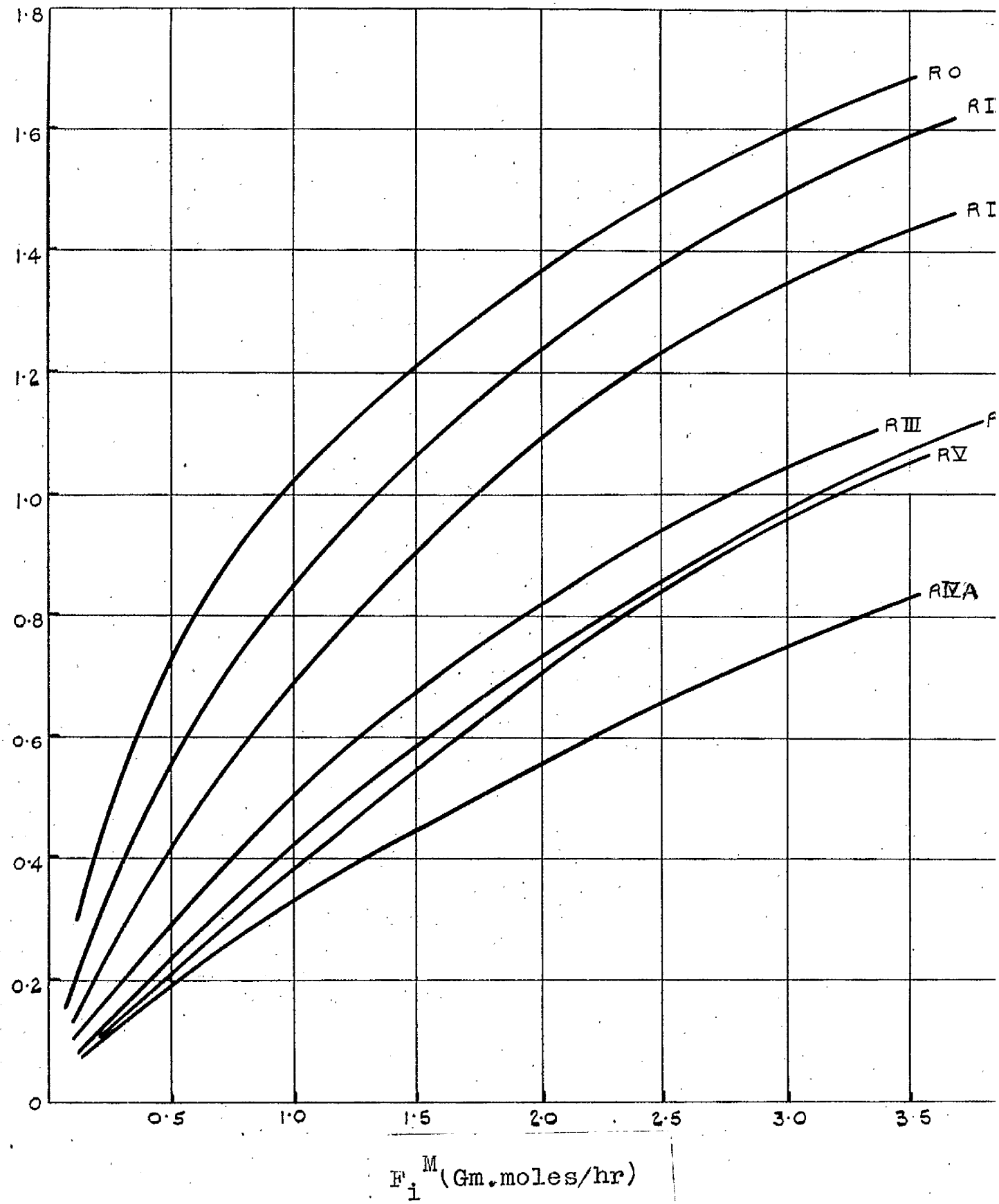
1·8
1·6
1·4
1·2
1·0
0·8
0·6
0·4
0·2
0
0·5
1·0
1·5
2·0
2·5
3·0
3·5
R O
R I
R I
R III
R V
R IV A
N_c^M (Gm.moles/hr litre)
F_i^M (Gm.moles/hr)

FIG. 3.9.

plot of % ethylene conversion *vs.* flow rate is shown in Fig. 3. 6. This reactor has identical dimensions with reactor IV. The % conversion results obtained from the two reactors are identical except at very low flow rates, where conversions in reactor IV B fall. It is believed that there is insufficient turbulence created by bubbles at low gas flow rates to keep the catalyst in suspension. Thus the value of A_{ls} falls causing the conversion to drop in the manner discussed in 3. 2. It appears that slurry recirculation has no effect on conversion except at very low gas flow rates.

3. 4. The Effect of Flow Rate and Reactor Size on Space Time Yield (S.T.Y.).

The S.T.Y. is a measure of the productivity of a reactor - high S.T.Ys. are desirable.

From the plots of S.T.Y. (N_C^*) v F_i^M for different reactor sizes (Fig. 3. 9.) it would appear that S.T.Y's. decrease with decreasing flow rate and increase with decreasing reactor length.

Reactor IV A appears to be the only exception to this, the S.T.Y. being lower than might be expected. Taking length as the controlling dimension, S.T.Y's may be compared at similar flow rates. The trend showing increase of S.T.Y. is clearly shown

at all flow rates except in the case of reactor IV A where S.T.Y's. are considerably lower than might be expected.

From the available information, it is concluded that, for a given diameter of reactor, S.T.Y. increases with decreasing length and increasing flow rate. From rather scanty information, it appears that S.T.Y. is less for a short fat reactor than a long thin one of the same volume at any given flow rate.

Much more experimental work, not possible with present equipment, is required. The information on the short fat reactor was obtained using the same diameter distributor as with the narrow diameter set. The investigation of a series of fat reactors with suitable gas distributors is necessary to elucidate this point. A detailed study would enable optimi-:sation studies on the length, & shape of the slurried bed reactor to be made. The effect of inlet gas composition on S.T.Y. is discussed later.

---

3. 5. The Effect on Conversion of Varying Gas Inlet Composition.

Experiments were conducted in reactors V and II with inlet gas compositions of $C_2H_4:H_2$ = 2:1 and 1:2.

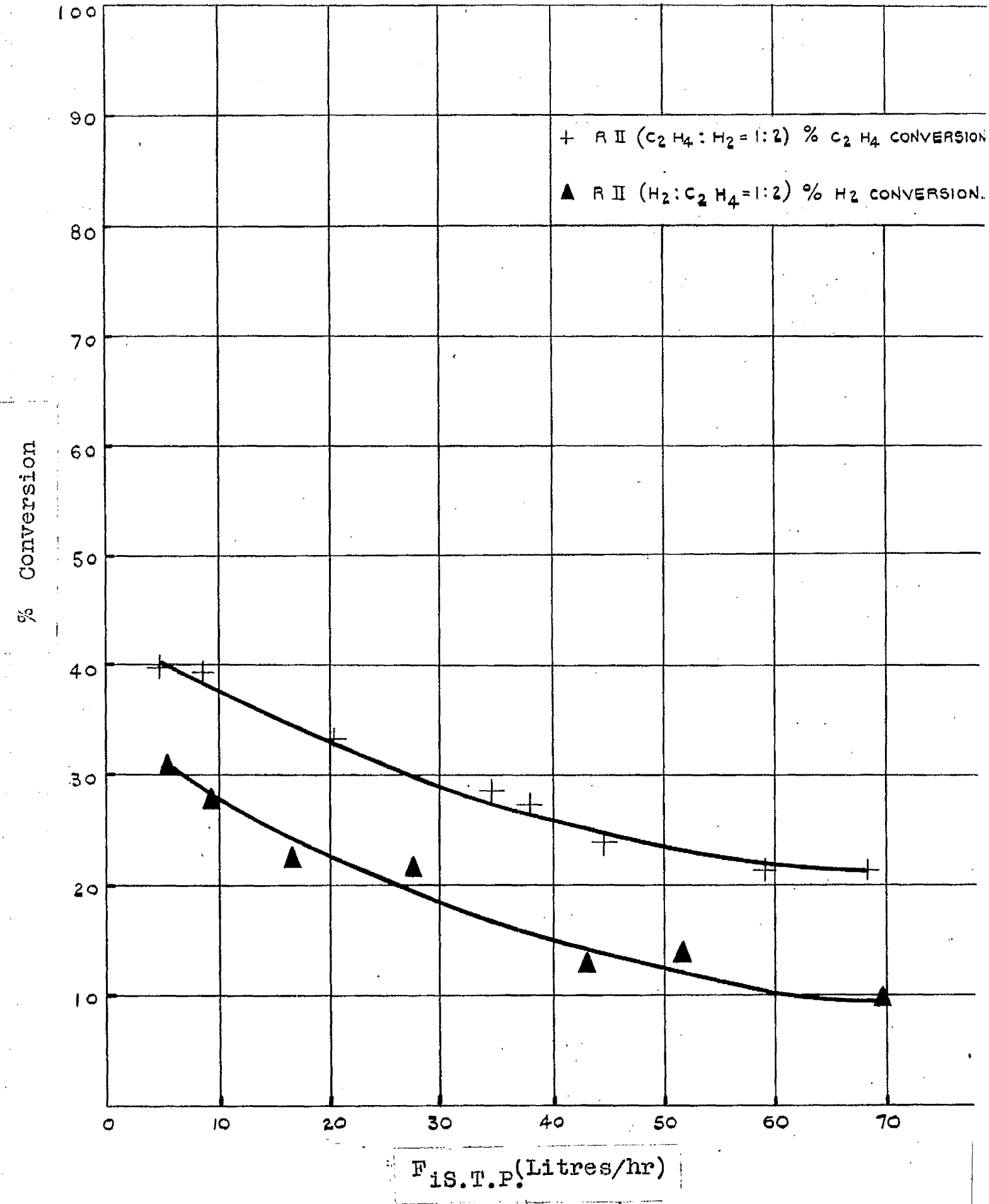
100
90
80
70
60
50
40
30
20
10
0
10
20
30
40
50
60
70
% Conversion
+ R II ($C_2H_4 : H_2 = 1:2$) % C_2H_4 CONVERSION
▲ R II ($H_2 : C_2H_4 = 1:2$) % H_2 CONVERSION.
$F_{iS.T.P.}$(Litres/hr)

FIG. 3. 10.

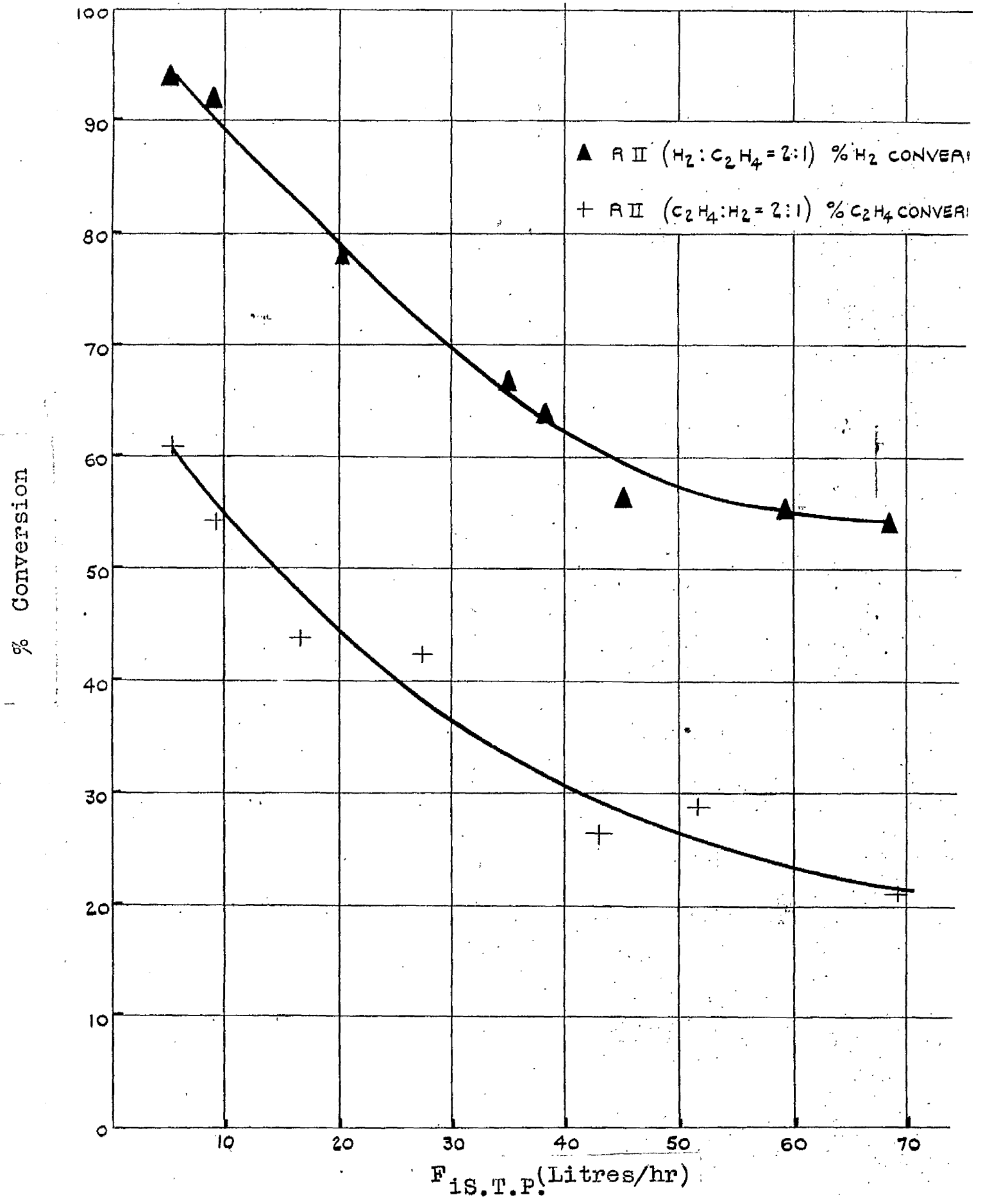
▲ R II (H2 : C2H4 = 2:1) % H2 CONVER
+ R II (C2H4 : H2 = 2:1) % C2H4 CONVER
% Conversion
100
90
80
70
60
50
40
30
20
10
0
10
20
30
40
50
60
70
F i S.T.P. (Litres/hr)

FIG. 3.11.

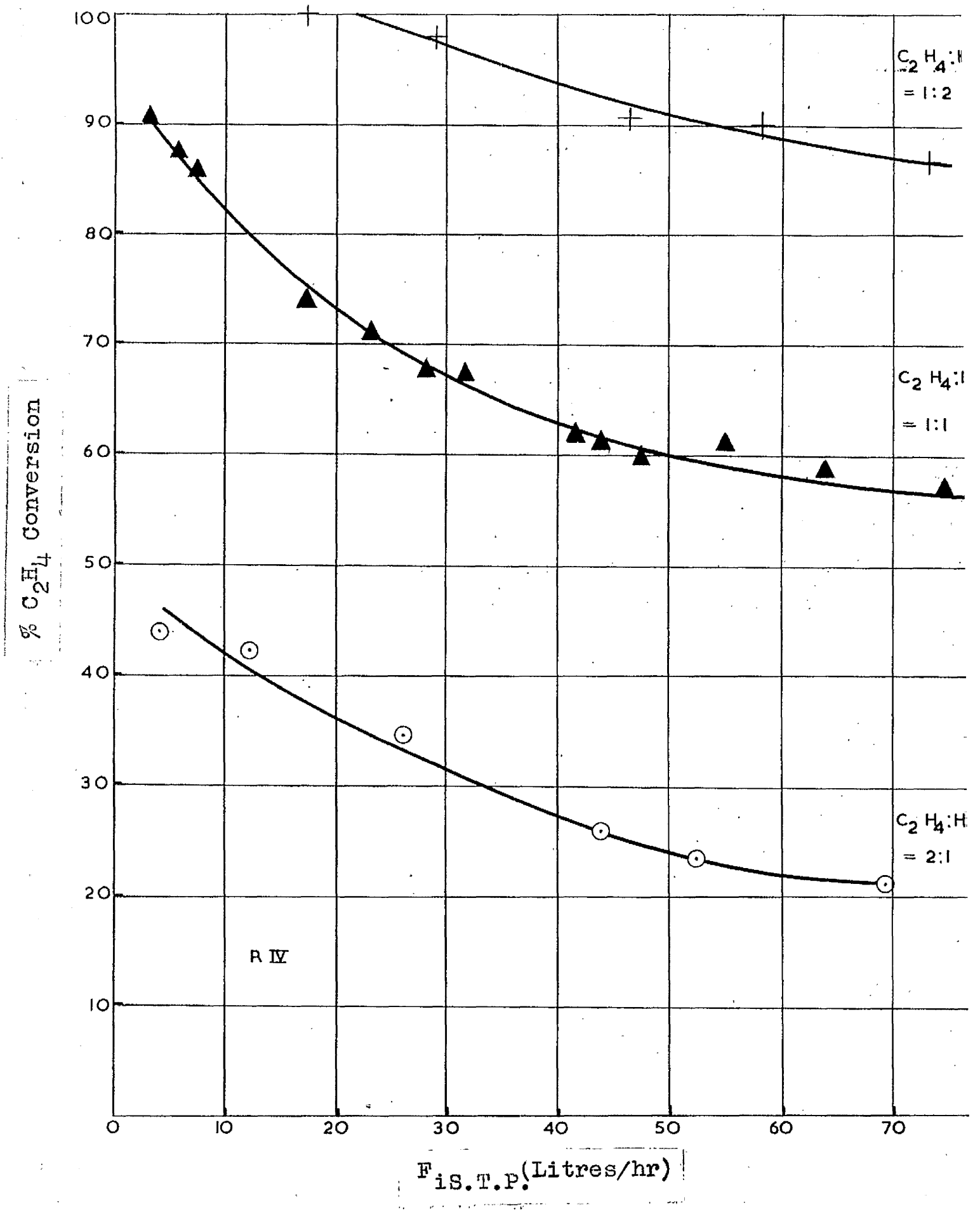
% C_2H_4 Conversion
100
90
80
70
60
50
40
30
20
10
0
10
20
30
40
50
60
70
$F_{i S.T.P.}$ (Litres/hr)
C_2H_4:H = 1:2
C_2H_4:H = 1:1
C_2H_4:H = 2:1
R IV

FIG. 3.12.

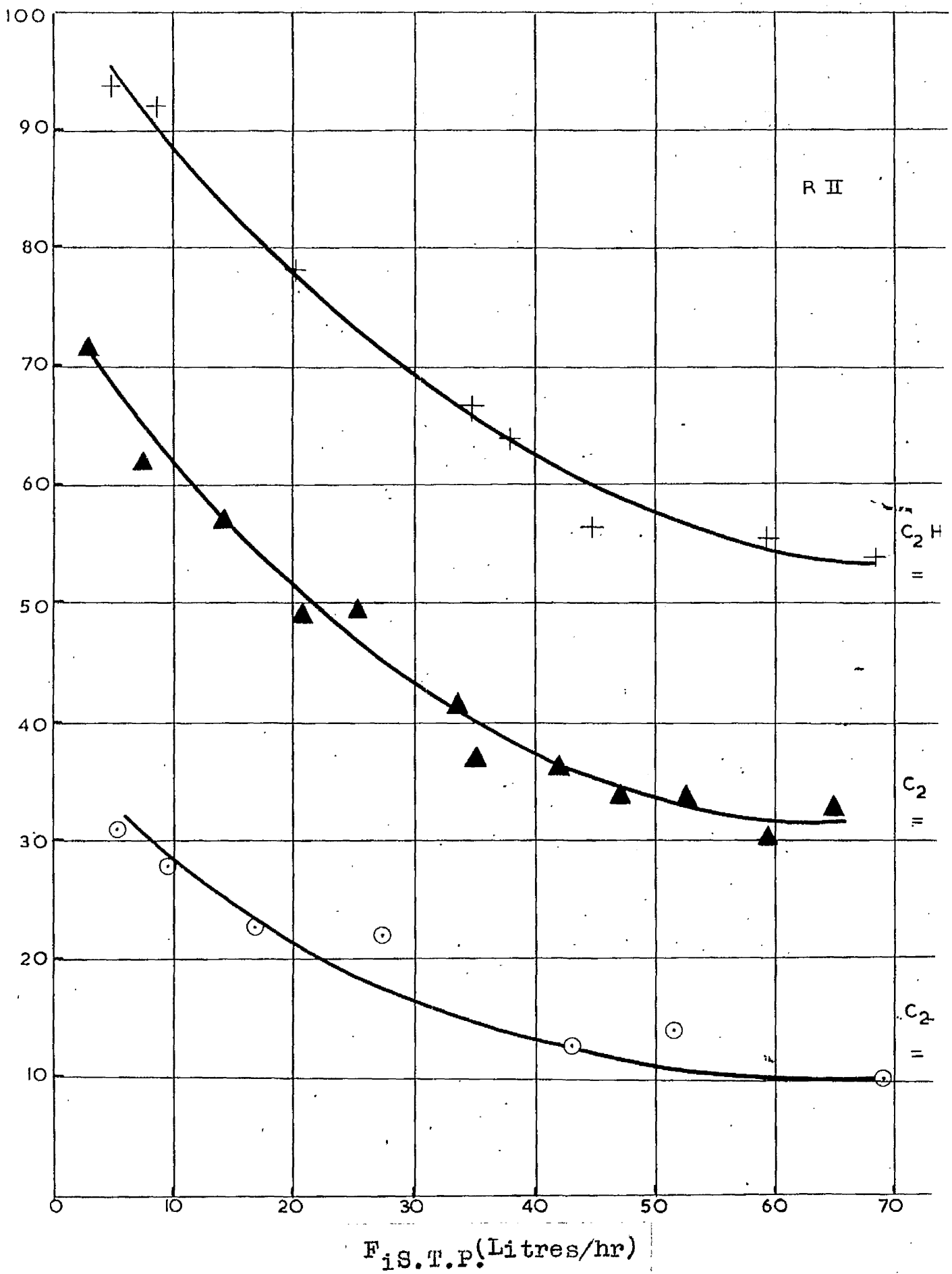
% C_2H_4 Conversion
100
90
80
70
60
50
40
30
20
10
0
10
20
30
40
50
60
70
$F_{is.T.P.}$(Litres/hr)
R II
C_2H_4
C_2H_6
C_2H_2

FIG. 3.13.

In experiments conducted in reactors V and II with an inlet gas composition of C_2H_4:H_2 = 1:1, conversion figures are similar whether based on hydrogen or ethylene. If the transport processes in a slurried bed reactor are identical for C_2H_4 and H_2 it might be expected that % conversion of ethylene when C_2H_4: H_2 = 1:2 would equal % conversion of hydrogen when H_2: C_2H_4 = 1:2. Also the % conversion of C_2H_4 (C_2H_4: H_2 = 2:1) would equal % conversion of H_2 (H_2: C_2H_4 = 2:1)

The results are presented in tables 3. 24 - 27 and 3. 48 - 51.

From Figs. 3. 10 and 3. 11 it is seen that in reactor II % conversion C_2H_4 (C_2H_4: H_2 = 1:2) > % conversion H_2 (H_2: C_2H_4 = 1:2) and % conversion H_2 (H_2: C_2H_4 = 2:1) > % conversion C_2H_4(C_2H_4: H_2=2:1), at corresponding gas flow rates. Similar plots may be obtained with reactor V.

In reactors V, II % C_2H_4 conversion increases with H_2 concentration in inlet gas stream - Figs. 3. 12 and 3. 13.

The S.T.Y. at any flow rate in both reactors increaseswith increase in H_2 inlet concentration up to an inlet gas composition of C_2H_4 : H_2 = 1:1 and remains constant up to

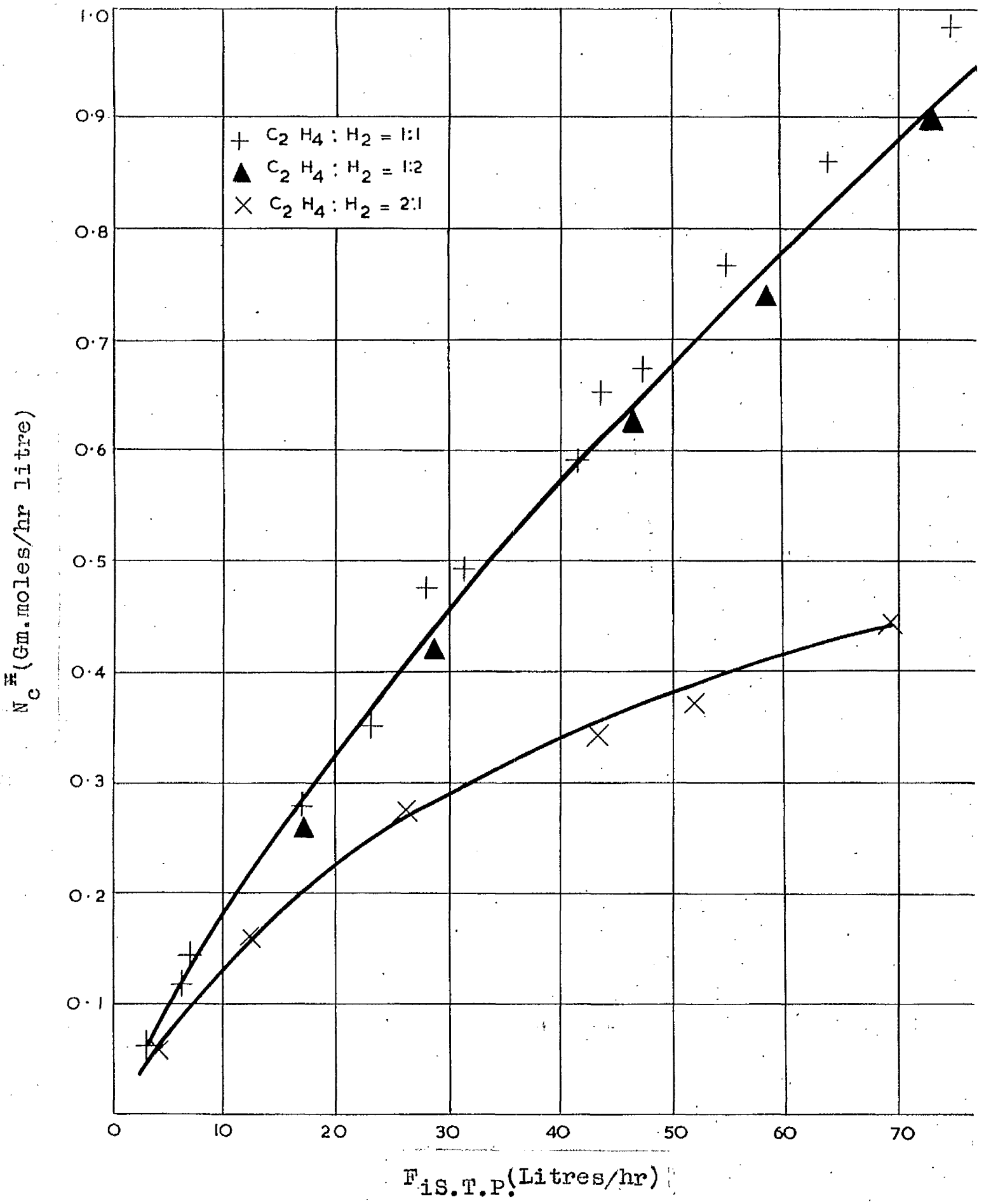
+ C2 H4 : H2 = 1:1
▲ C2 H4 : H2 = 1:2
× C2 H4 : H2 = 2:1
1·0
0·9
0·8
0·7
0·6
0·5
0·4
0·3
0·2
0·1
0
10
20
30
40
50
60
70
Nc (Gm. moles/hr litre)
FiS.T.P. (Litres/hr)

FIG. 3. 14.

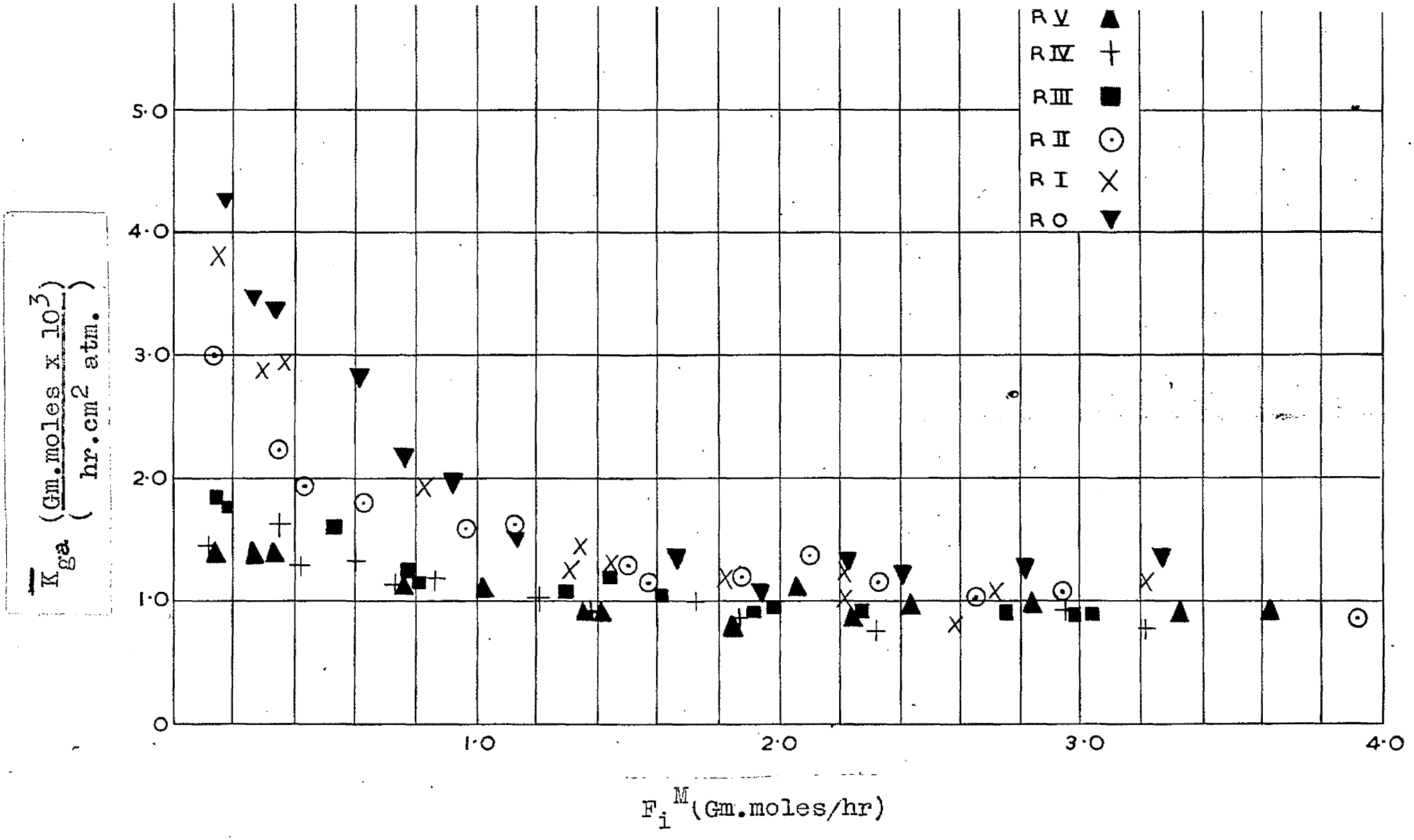
RV
RIV
RIII
RII
RI
RO
5·0
4·0
3·0
2·0
1·0
0
1·0
2·0
3·0
4·0
$\bar{K}_{ga}$ $\left(\frac{\text{Gm.moles} \times 10^3}{\text{hr.cm}^2 \text{ atm.}}\right)$
F_i^M (Gm.moles/hr)

FIG. 3.15

C_2H_4 : H_2 = 1:2. For reactor V this is shown in Fig.3.14.

The inference of this experimental work is that the transport mechanisms for hydrogen and ethylene are not identical. The resistances to hydrogen transport are greater and high concentrations of H_2 produce steeper concentration gradients which facilitate hydrogen transport through these resistances.

---

3. 6. <u>The Overall Process Coefficient $\bar{K}_g$ and No. of Reactor Units, N.R.U.</u>

The overall process coefficient $\bar{K}_g$ for both C_2H_4 and H_2 has been evaluated for each set of experimental conditions. In Fig. 3.15 the values of $\bar{K}_{ga}$ are plotted against F_i^M for reactors [V] to [O] when the inlet gas composition is C_2H_4 : H_2 = 1:1. The values of $\bar{K}_{ga}$ tend to increase with decreasing reactor size and gas flow rates. A decrease in $\bar{K}_{ga}$ at very high gas flow rates could be explained by a decrease in A_{ls} causing $\frac{A_{gl}}{K_{ra}A_{ls}}$ to become significant in equation 1.2.49. No such explanation is available for the observed behaviour of the system. It is concluded that some complexity in the hydrodynamics of the system, possibly related to high turbulence and interference in boundary layer conditions, can explain the increase in $\bar{K}_{ga}$ in the smaller reactors.

$\bar{K}_{ga}$ and $\bar{K}_{gb}$ have also been evaluated at gas inlet ratios of $C_2H_4 : H_2 = 1:2$ and $2:1$. The values differ from those obtained when $C_2H_4 : H_2 = 1:1$ but may be shown to exhibit the same trends.

From equation 1.2.41, N.R.U. is a function of gas inlet composition and of conversion. From equation 1.2.39

$$\frac{Z}{F_i^M} = \frac{1}{\pi_{gm}\,\bar{K}_{ga}\,A_{glm}\gamma} \cdot N.R.U_a$$

Since $\bar{K}_{ga}$ and A_{glm} may be shown to vary with flow, a plot of $\frac{Z}{F_i^M}$ vs. $N.R.U_a$ (reactors $[V] - [O]$, $C_2H_4 : H_2 = 1:1$) would not be expected to yield a straight line, though a correlation of some sort might be expected and is indeed obtained Fig. 3.16.

In view of this a log-log plot of $\frac{Z}{F_{i\ S.T.P}}$ vs. $N.R.U_a$ was made and a near straight line correlation obtained - Fig. 3.17 ($F_{i\ S.T.P.}$ is closely related to F_i^M)

Similar plots are obtainable with results obtained from inlet gas compositions of $C_2H_4 : H_2 = 1:2$ and $2:1$ Thus a method has been evolved whereby, for specific inlet conditions, the performance of a reactor may be predicted from the performance of one of different length. The relationship indicated by this graph cannot be

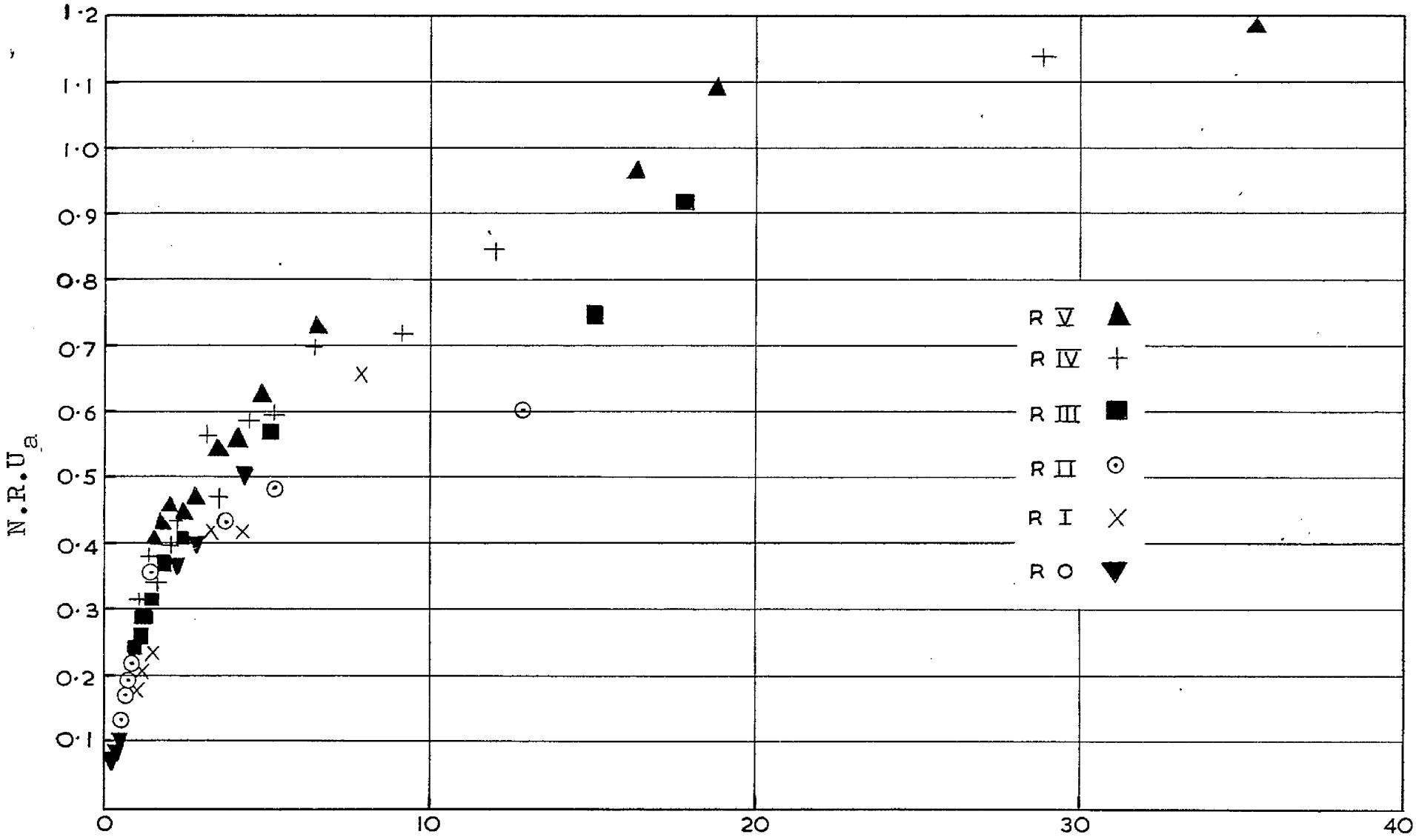

$$\frac{Z}{F_i S.T.P.}$$

FIG. 3.16.

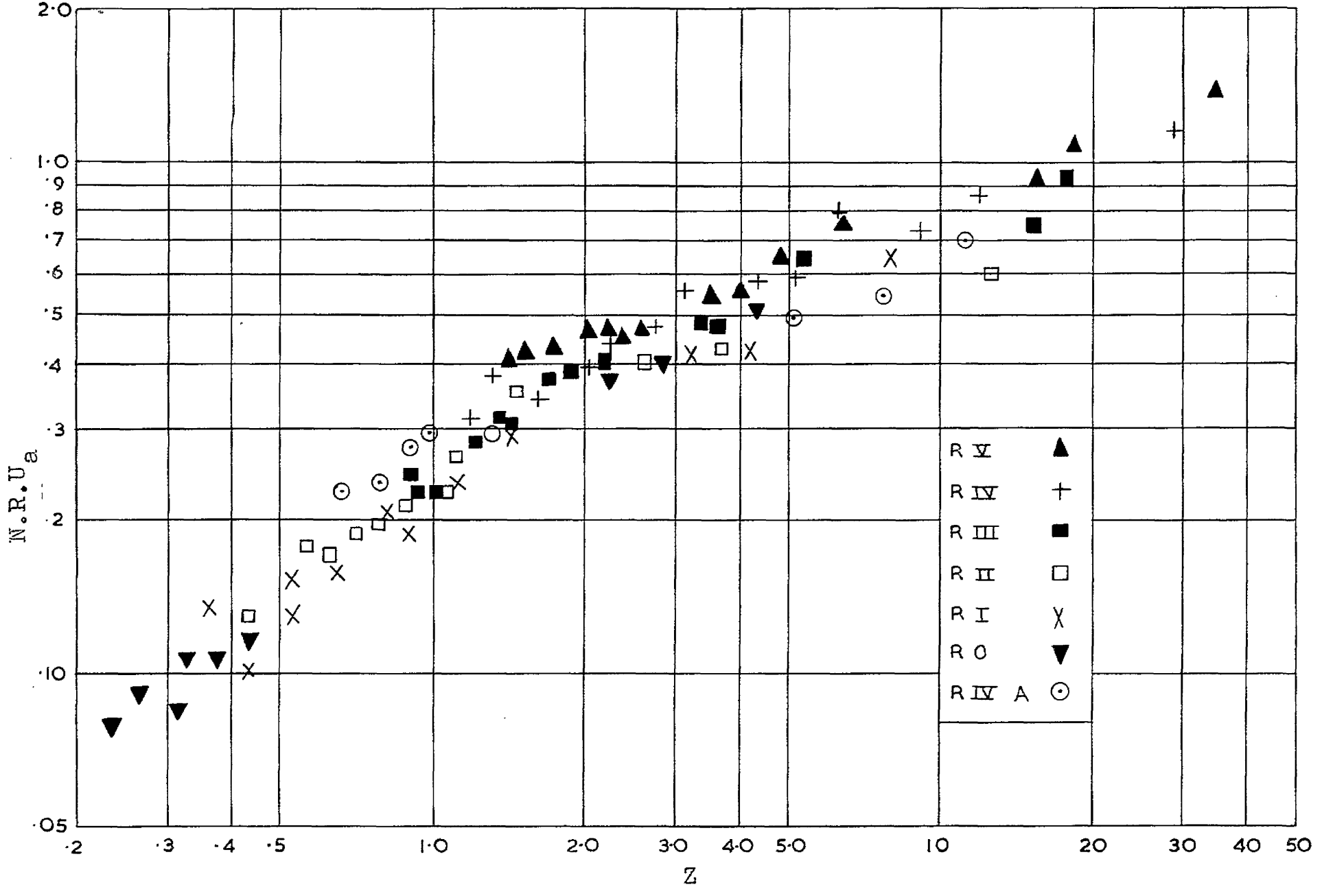

Fig. S.T.P.

FIG. 3.17.

explained simply by equation 1.2.39. The functions $\overline{K}_{ga}$ and A_{glm} included in this equation are complex and the type of relation indicated experimentally between $\frac{Z}{F_i \text{ S.T.P.}}$ and $N.R.U_a$ may be justifiable theoretically from 1.2.39. This is not attempted here. Further work on the properties of $\overline{K}_{ga}$ and the effect of reactor diameter could make the method valuable for the scale up of slurried bed reactors.

---

3. 7. Relationship of K_g, K_l, N.R.U., and N.Ch.U.

It can be seen from equation 1.2.57 -

$$\frac{V_R}{F_i^M \, N.Ch.U} = \frac{1}{\pi_{gm}^2 K_l A_{ls}} + \frac{N.R.U}{N.Ch.U} \cdot \frac{1}{K_g A_{glm} \pi_{gm}}$$

that a plot of $\frac{V_R}{F_i^M \, N.Ch.U}$ vs. $\frac{N.R.U.}{N.Ch.U.} \cdot \frac{1}{A_{glm} \pi_{gm}}$

should ideally produce a line of gradient $\frac{1}{K_g}$ and intercept $\frac{1}{\pi_{gm}^2 K_l A_{ls}}$. The functions $\frac{V_R}{F_i^M \, N.Ch.U}$ and $\frac{N.R.U.}{N.Ch.U.} \cdot \frac{1}{A_{glm} \pi_{gm}}$ were calculated for all runs done in reactors [V] - [O] and [IVB] at 75°C and a 1:1 inlet reactant ratio. In Figs. 3.18 - 3.25, the plots for ethylene are shown. Similar plots may be obtained for hydrogen. In practice $\frac{1}{K_{ga}}$ would not be expected to

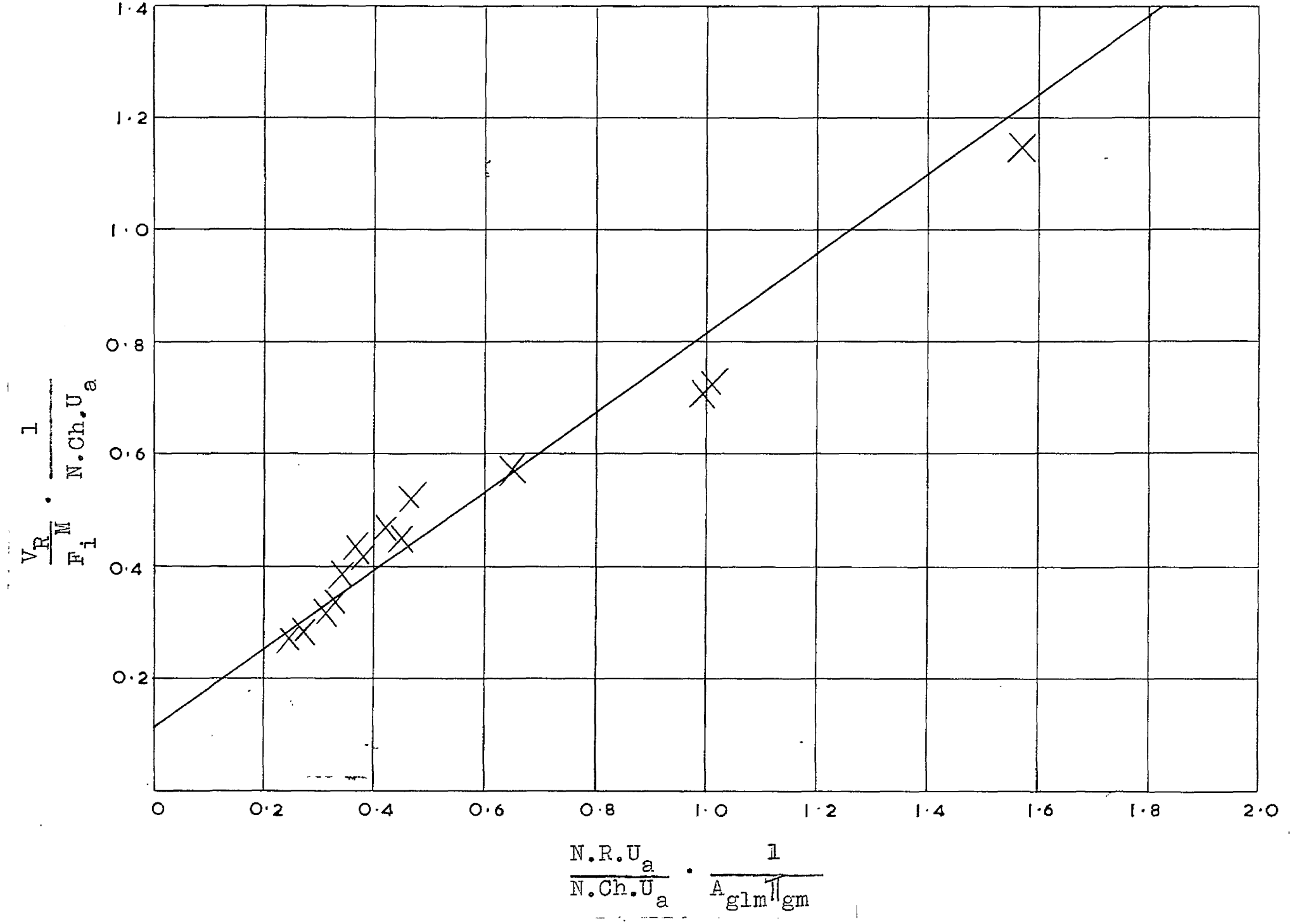
1·4
1·2
1·0
0·8
0·6
0·4
0·2
0
0·2
0·4
0·6
0·8
1·0
1·2
1·4
1·6
1·8
2·0
$\frac{V_R}{F_i M} \cdot \frac{1}{N.Ch.U_a}$
$\frac{N.R.U_a}{N.Ch.U_a} \cdot \frac{1}{A_{glm}\sqrt{\Pi_{gm}}}$

FIG. 3.18

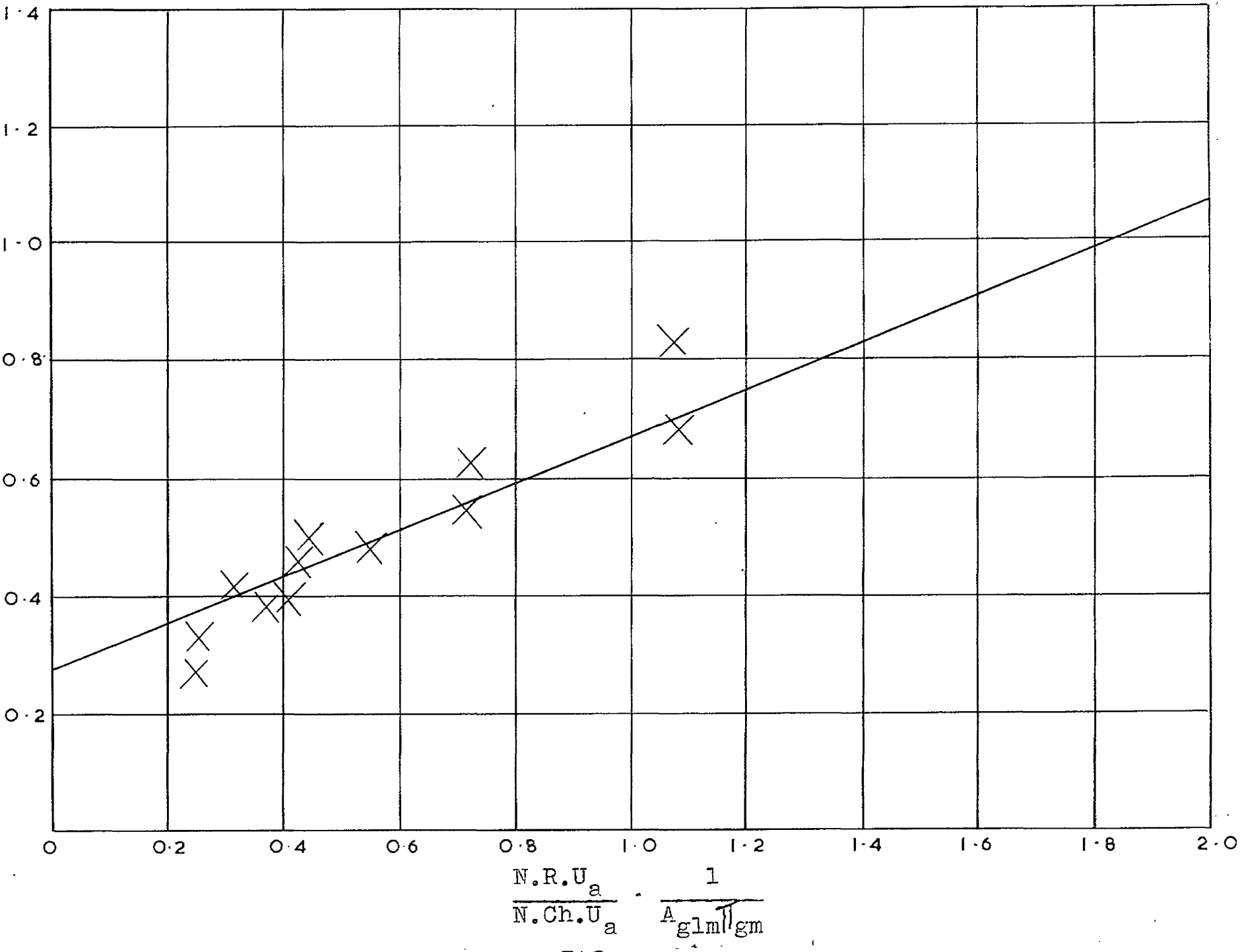
1·4
1·2
1·0
0·8
0·6
0·4
0·2
0
0·2
0·4
0·6
0·8
1·0
1·2
1·4
1·6
1·8
2·0
$\frac{V_R}{F_i} \cdot \frac{1}{M} \cdot \frac{}{N.Ch.U_a}$
$\frac{N.R.U_a}{N.Ch.U_a} \cdot \frac{1}{A_{glm}\eta_{gm}}$

FIG . 3 . 19

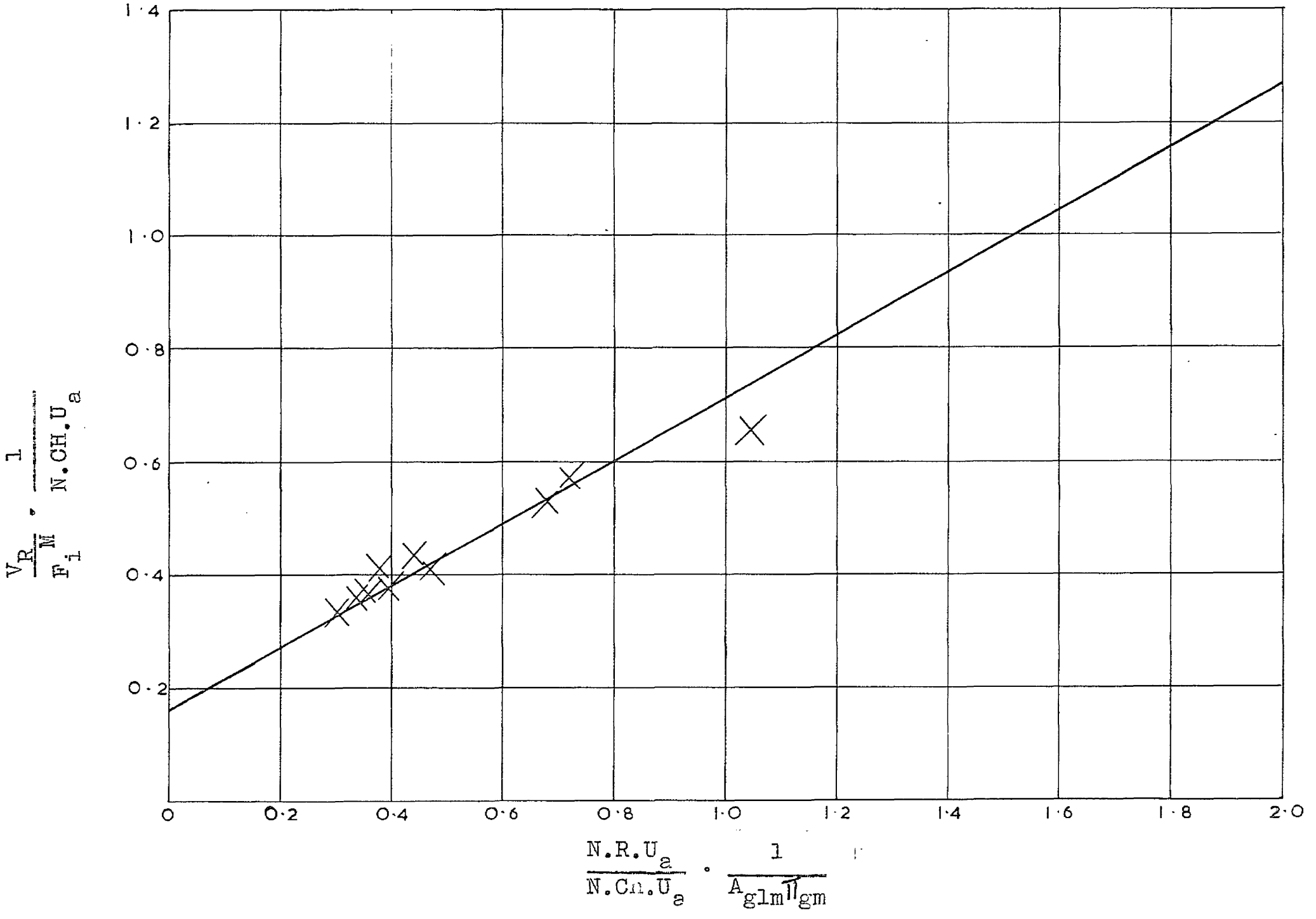
1·4
1·2
1·0
0·8
0·6
0·4
0·2
0
0·2
0·4
0·6
0·8
1·0
1·2
1·4
1·6
1·8
2·0
$\frac{V_R}{F_i} \cdot \frac{1}{M}$
$N.CH.U_a$
$\frac{N.R.U_a}{N.Cm.U_a} \cdot \frac{1}{A_{glm}\eta_{gm}}$

FIG. 3.20

REACTOR II (C_2H_4)

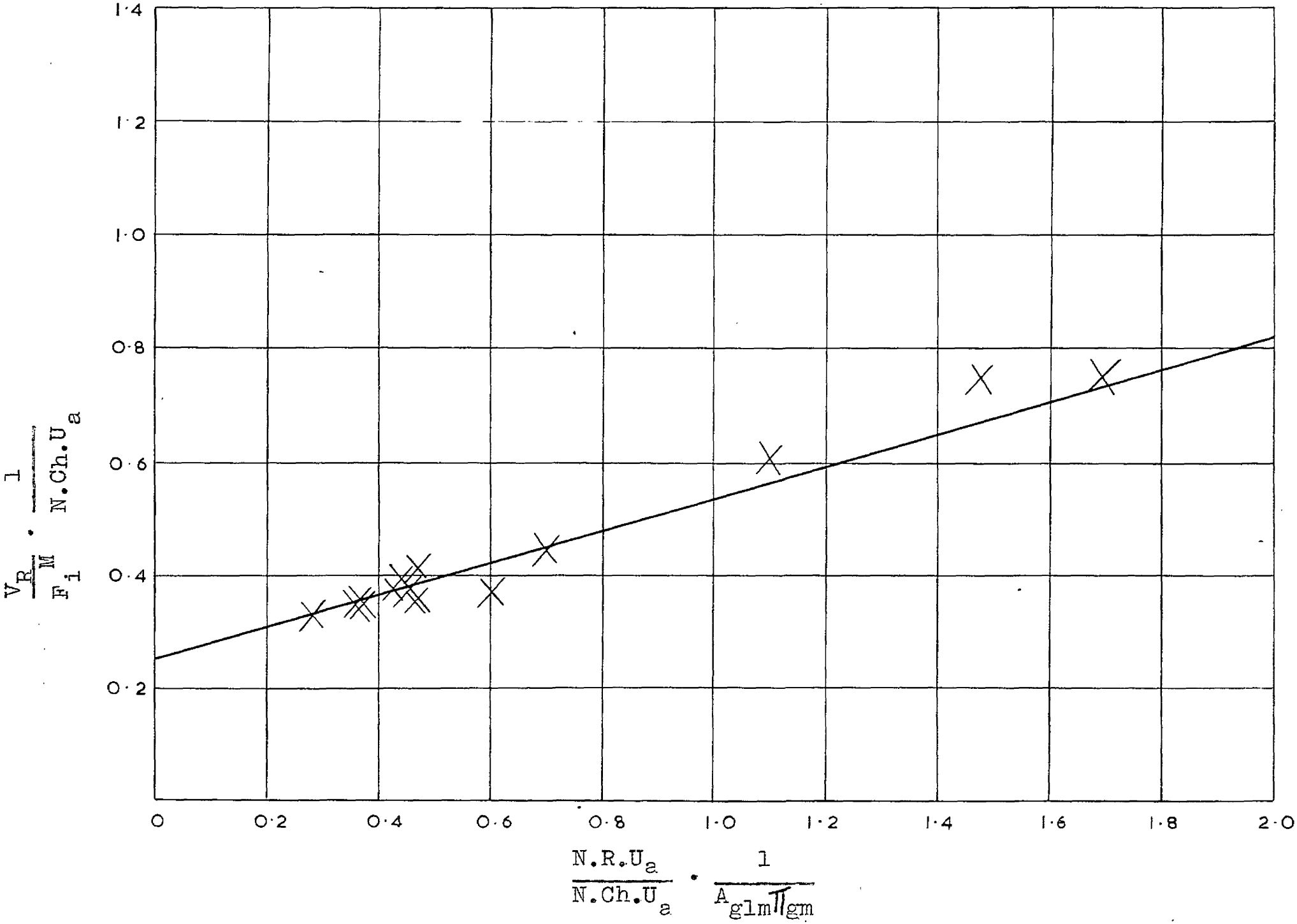

FIG. 3.21

REACTOR 1 (C_2H_4)

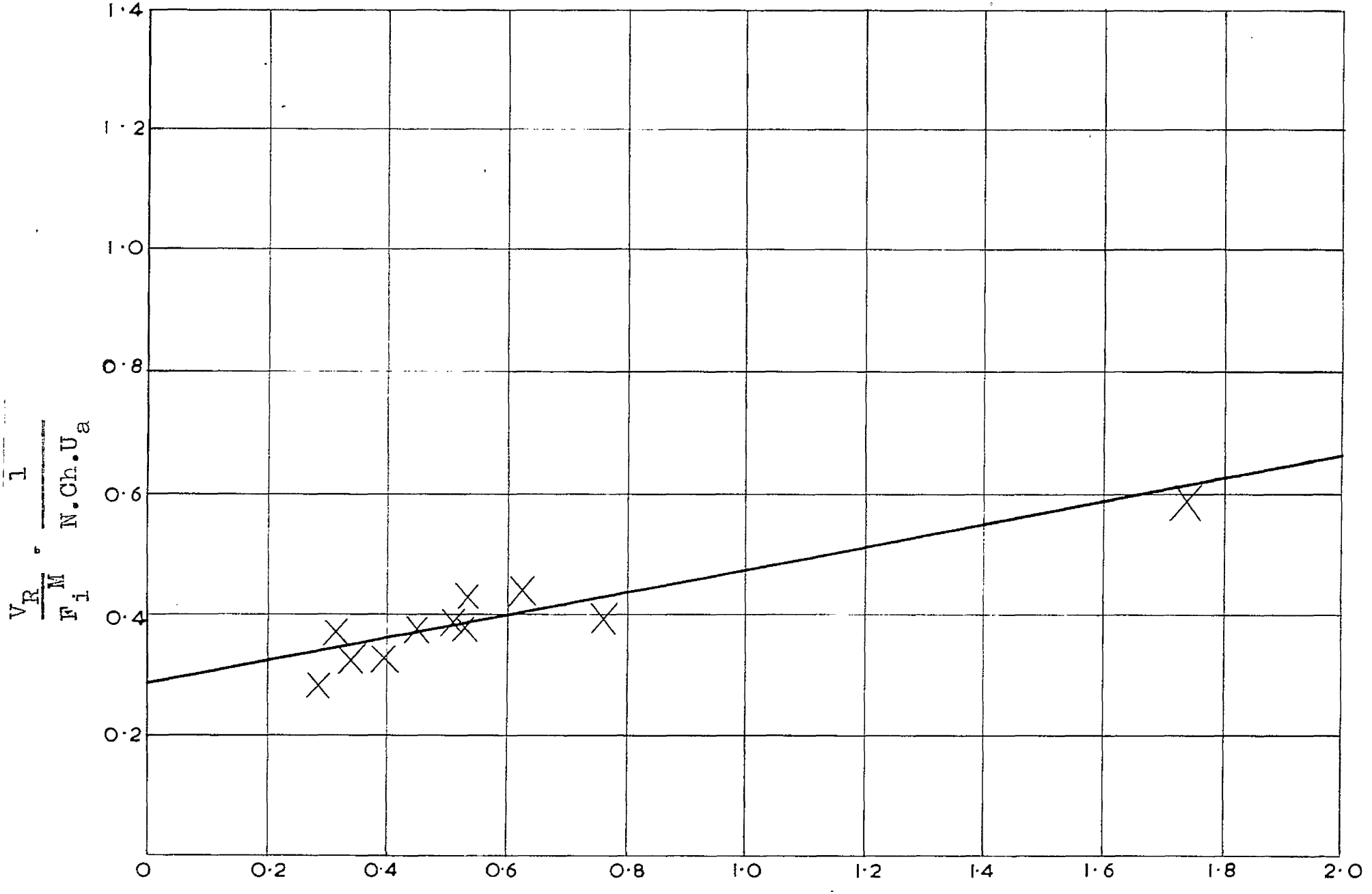

FIG. 3.22

REACTOR O (C_2H_4)

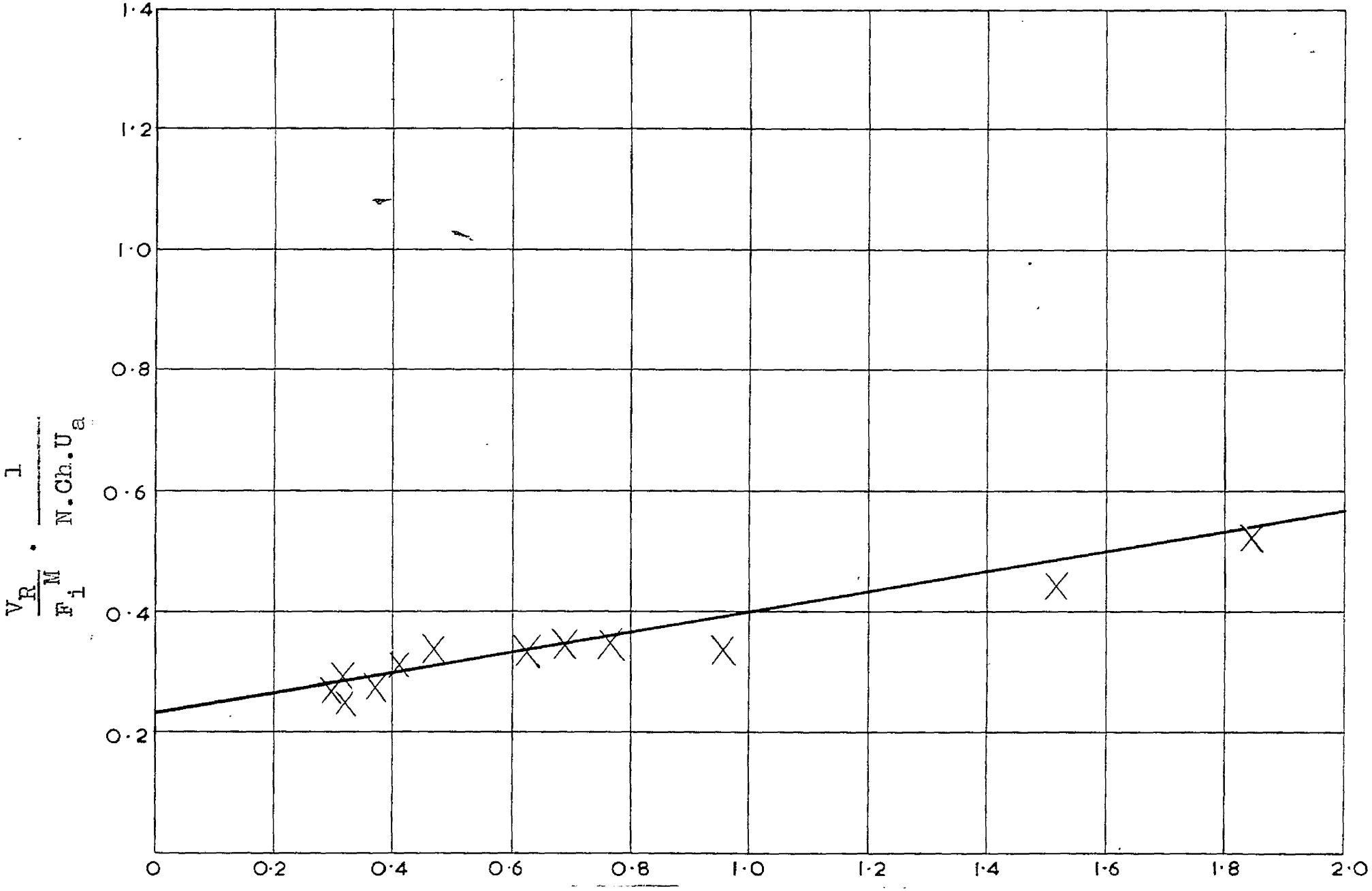

FIG. 3.23

REACTOR IV A (C_2H_4)

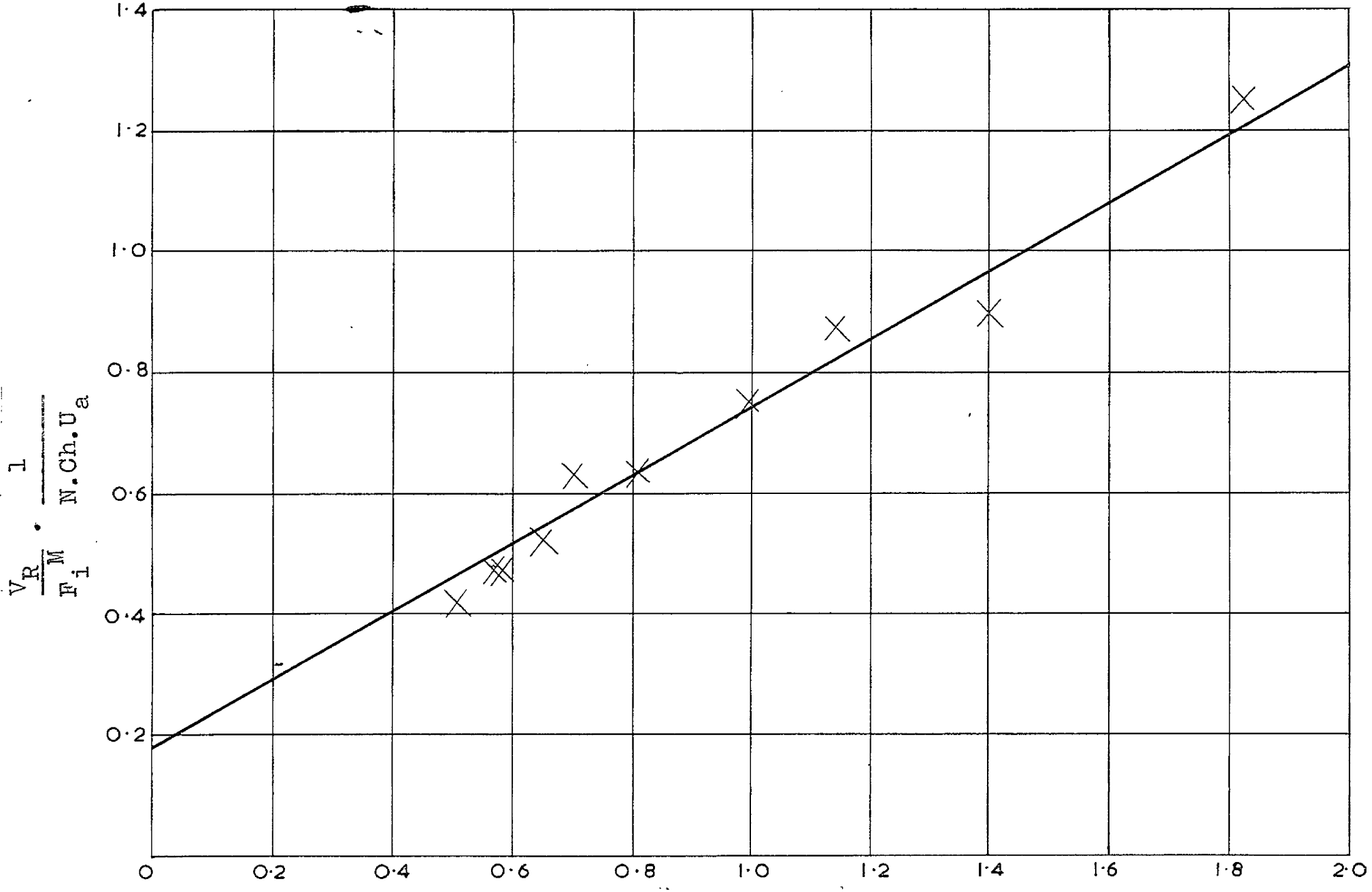

FIG. 3. 24

REACTOR IV B

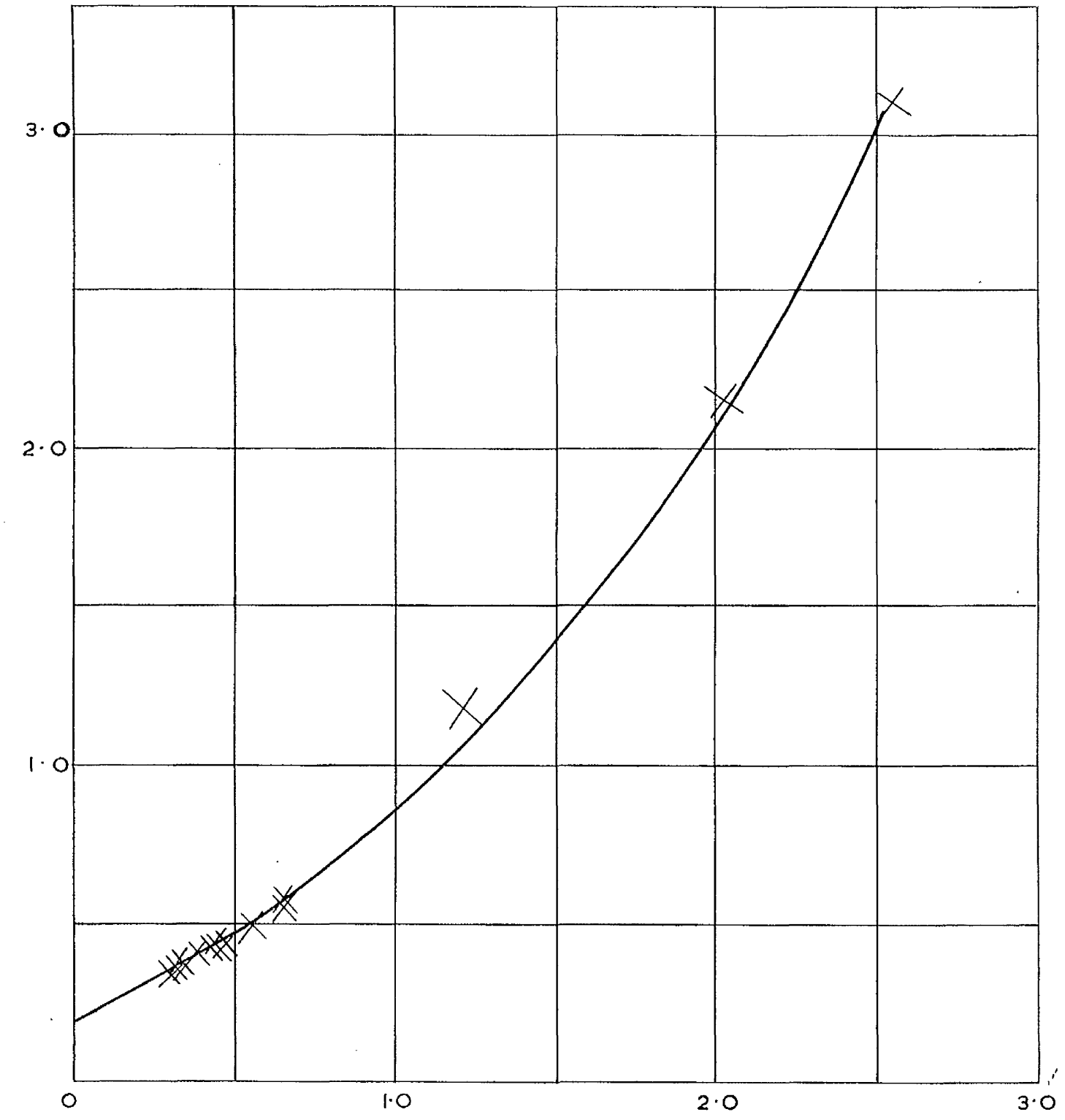

FIG. 3.25

remain constant as the hydrodynamics of the system (F) change. However the data indicates very little change. The mean gradient of each line gives a mean value of $\frac{1}{K_{ga}}$ over the range. The intercept representing $\frac{1}{K_1 A_{1s} \pi_{gm}}$ is obtained by extrapolation from real experimental conditions to a point where either $F_i^M = \infty$ or $V_R = 0$. The result is considered to be valid however, as it is possible to imagine a hypothetical system where even at infinite flow rates A_{1s} remains constant.

The plot obtained for reactor IVB (no slurry recycle) shows a distinct curve upwards at low gas flow rates. This indicates a great diminution of K_{ga} values.

Consider equation 1.2.44

$$\frac{1}{K_{ga}} = \frac{1}{K_{a1}} + \frac{1}{K_{a2}H_a} + \frac{1}{K_{a3}H_a} + \frac{A_{gl}}{K_{a4}H_a A_{1s}}$$

At low gas flow rates there is poor catalyst suspension and $A_{1s} < A_{gl}$ instead of $A_{1s} > A_{gl}$. Thus K_{ga} decreases in size.

The values of K_{ga} and K_1 calculated are shown in table 3.64.

In table 3.63

$$f_1 = \frac{V_R}{F_i^M \, N.Ch.U_a} \qquad f_2 = \frac{N.R.U_a}{N.Ch.U_a} \cdot \frac{1}{A_{glm} \pi_{gm}}$$

ie. the functions used in figs. 3.18 - 3.25.

TABLE 3. 63 (ethylene)

R V		R IV		R III		R II	
f_1	f_2	f_1	f	f_1	f_2	f_1	f_2
0.289	0.270	0.330	0.254	0.334	0.305	0.326	0.288
0.317	0.310	0.416	0.316	0.361	0.335	0.346	0.360
0.339	0.326	0.504	0.447	0.376	0.346	0.376	0.430
0.437	0.365	0.461	0.431	0.373	0.368	0.373	0.452
0.465	0.420	0.825	0.726	0.377	0.397	0.368	0.607
0.460	0.434	0.831	1.072	0.435	0.446	0.605	1.10
0.572	0.650	1.05	2.26	0.53	0.685	0.746	1.48
0.724	6.01	0.272	0.254	0.66	1.05	1.59	4.76
1.15	1.57	0.388	0.372	1.16	2.14	0.34	0.377
0.272	0.248	0.392	0.410	0.335	0.304	0.395	0.448
0.391	0.341	0.485	0.557	0.409	0.381	0.411	0.470
0.420	0.372	0.545	0.713	0.402	0.473	0.358	0.473
0.521	0.464	0.685	1.08	0.576	0.724	0.443	0.704
0.711	0.988			1.545	2.17	0.745	1.69

TABLE 3. 63 Continued.

R I		R O		R IV A		R IV B	
f_1	f_2	f_1	f_2	f_1	f_2	f_1	f_2
0.322	0.344	0.263	0.298	0.422	0.507	0.394	0.32
0.324	0.399	0.284	0.316	0.470	0.565	0.378	0.319
0.388	0.51	0.311	0.410	0.518	0.647	0.402	0.391
0.439	0.625	0.333	0.624	0.752	0.988	0.412	0.415
0.398	0.761	0.346	0.765	0.891	1.39	0.416	0.475
0.585	1.74	0.446	1.51	1.435	2.23	0.486	0.554
0.77	2.99	0.578	2.51	1.715	3.15	0.556	0.655
0.283	0.282	0.249	0.315	0.470	0.580	3.09	2.56
0.371	0.311	0.272	0.372	0.636	0.70	0.349	0.287
0.379	0.525	0.339	0.468	0.634	0.804	0.374	0.335
0.377	0.449	0.346	0.69	0.875	1.14	0.435	0.443
0.428	0.533	0.336	0.957	1.255	1.82	0.485	0.625
0.781	2.26	0.525	1.84			1.17	1.21
						2.14	2.02

Table 3. 64.

R	K_{ga}	$K_1 A_{1s}$	A_{1s}	K_1
V	1.64	6.96	6.17	1.13
IV	2.62	4.45	"	0.72
III	1.83	7.22	"	1.17
II	3.50	5.02	"	0.81
I	5.47	4.39	"	0.71
0	5.95	5.26	"	0.85
IVA	1.82	6.4	"	1.04
IVB	1.74	6.65	"	1.08

The manner in which equation 1.2.57 is derived from 1.2.51 can be criticised. If $K_{ga} \simeq K_{gb}$, the value of the results might be questioned. However, using laborious mathematical processes, it may be shown that the values of K_{ga} and K_{gb} derived from equation 1.2.57 should be identical when the inlet reactant ratio = 1:1, ie. when $P_{ai} = P_{bi}$. The value of K_g obtained represents the smaller of the two. The method employed involves substitution of numerical values of K_{ga} and K_{gb} into 1.2.51. P_a and P_b being known, N_a may be calculated. Using similar assumptions to those made in the theoretical proof, K_{ga} or K_{gb} is then calculated and compared with the true value. The method is not rigorous but it shows that the error incurred in K_g and K_1 by the assumptions decreases as one K_g becomes greater than the other.

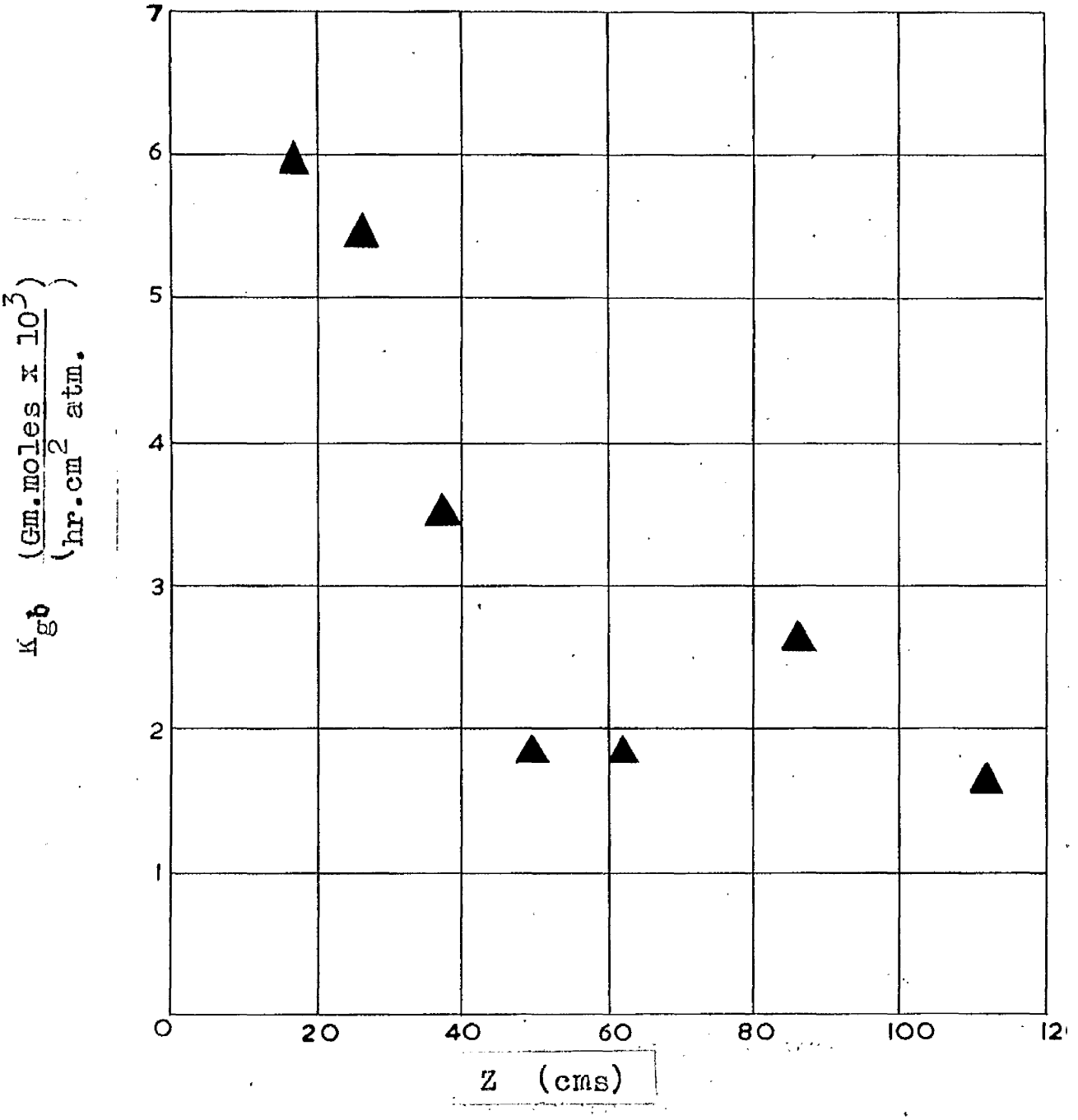
K_{gb} $\left(\frac{\text{Gm.moles} \times 10^3}{\text{hr.cm}^2 \text{ atm.}}\right)$
7
6
5
4
3
2
1
0
20
40
60
80
100
12
Z (cms)

FIG. 3·26

Using this method for evaluating K_g, there is no way of telling which K_g is represented by the calculated value. However, the experimental evidence discussed in 3. 5 indicates that in the experimental model K_{gb}, ie. the overall hydrogen mass transfer coefficient, is the smaller. Thus, in fact, the values of K_{ga} actually represent K_{gb}.

The method is also limited in that it can only be employed when $C_2H_4 : H_2 = 1:1$. When this is not so the results obtained may be shown to be very ambiguous. Thus the results obtained when $C_2H_4 : H_2 = 1:2$ and 2:1 are neglected.

The values of K_{gb} appear to increase with decreasing reactor size - Fig. 3.26. This is surprising as the value might have been expected to be dependent on flow rate only. In Appendix 2 it is demonstrated that at high flow rates bubble coalescence in the large reactors causes A_{gl} to be less than at corresponding flow rates in the smaller reactors. Since this effect was neglected to avoid complications in calculating N.R.U., N.Ch.U. and etc., it may be the explanation of the decrease in K_{gb} values. Calderbank (10) also discusses this phenomenon. It may be inferred that the more relevant values of K_{gb} are those obtained with the smaller reactors.

From equation 1.2.44, the overall mass transfer coefficient is given by:-

$$K_{bg} = \frac{1}{\frac{1}{K_{b1}} + \frac{1}{K_{b2}H_b} + \frac{1}{K_{b3}H_b} + \frac{A_{gl}}{K_{b4}H_b A_{ls}}}$$

When A_{ls} becomes greater than A_{gl}, the fourth term becomes insignificant. Also transport in the bulk liquid is assumed to be very rapid hence K_{b3} is very large and the third term also becomes insignificant. Hence

$$K_{gb} = \frac{1}{\frac{1}{K_{b1}} + \frac{1}{K_{b2}H_b}}$$

The following information is available on the solubilities of ethylene in xylene (44) and hydrogen in xylene (45)

Ethylene at 0°C and 1 atmosphere in xylene

Vols./vol. xylene	gm. moles/ c.c. atmosphere	T°C
5.95	2.65×10^{-4}	0
3.80	1.7×10^{-4}	20
3.03	1.355×10^{-4}	40

Hydrogen at 0°C and 1 atmosphere in xylene

Vols./vol. xylene	gm. moles/ c.c. atmosphere	T°C
0.075	3.35×10^{-6}	0
0.075	3.35×10^{-6}	20
0.085	3.8×10^{-6}	40

These being the only values for solubilities available it was necessary to extrapolate in order to find solubilities at 75°C - Fig. 3.27 - 3.28. At 1 atmosphere and

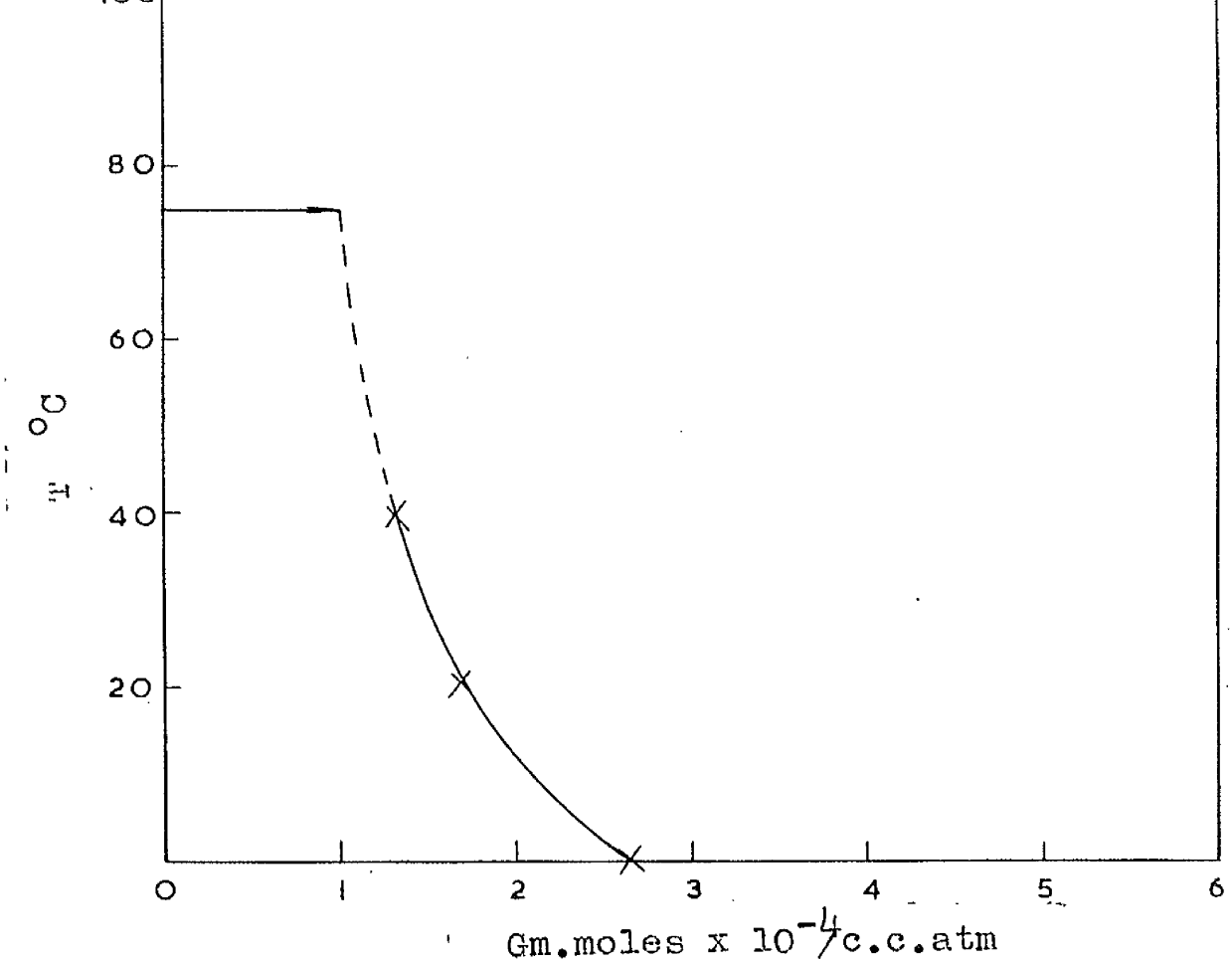

FIG. 3.27 SOLUBILITY OF ETHYLENE IN XYLENE.

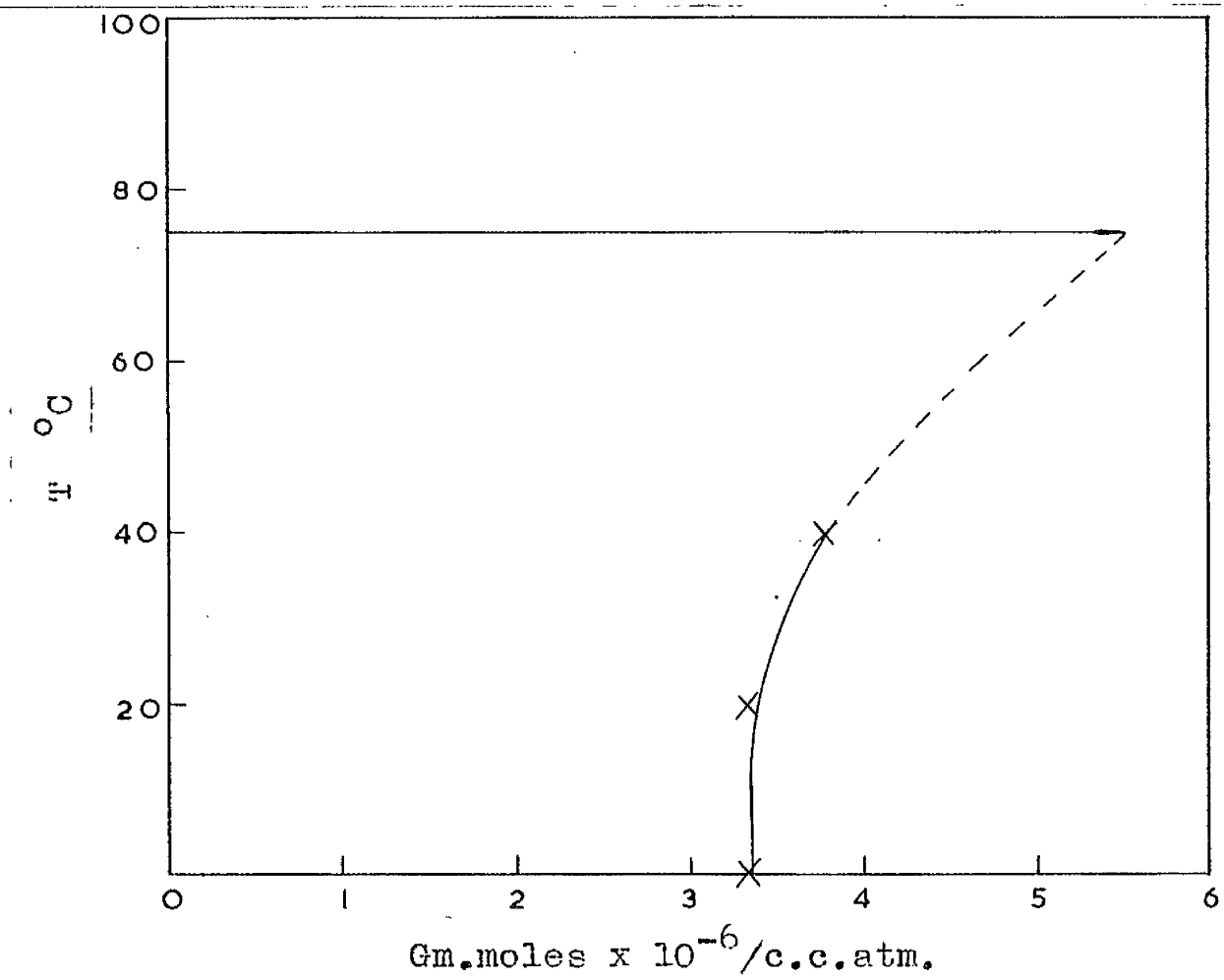

FIG. 3.28. SOLUBILITY OF HYDROGEN IN XYLENE.

75°C the following solubilities were estimated

C_2H_4 = 1 x 10^{-1} gm. moles/litre.atmosphere

H_2 = 5.5 x 10^{-3} gm. moles/litre.atmosphere

Henry's law is here defined as C = HP

C = concentration (gm. moles/litre)

H = Henry's law constant (gm. moles/litre.atm)

P = solute partial pressure (atm.)

The corresponding values of H are

C_2H_4 H_a = 1 x 10^{-1} gm. moles/litre atm.

H_2 H_b = 5.5 x 10^{-3} gm. moles/litre atm.

It is generally agreed that the absorption of a relatively insoluble gas is controlled by mass transfer through a liquid film (46). Both the above gases may be considered to be insoluble, hydrogen being more so. Thus, in the case of hydrogen K_{b1} is considered to be large and

$$K_{gb} = H_b \; K_{b2}$$

i.e. the overall mass transfer coefficient is effectively equal to the product of the liquid film coefficient and the Henry's law constant.

Calculation of K_{b2}.

Calderbank (47) gives the following relationship for mass transfer from a bubble rising through a vertical column of liquid -

$$K_2(Sc)^{\frac{1}{2}} = 0.42\left[\frac{\Delta \rho\, \mu_1 g}{\rho_1^{\,2}}\right]^{\frac{1}{3}} \quad - (A)$$

The Schmidt No., $Sc = \dfrac{\mu_1}{\rho_1 D_g}$

The diffusion coefficient, D_g, of the gas in the liquid can be calculated from the relation given by Wilke and Chang (48)

$$D_g = 7.4 \times 10^{-8} \frac{(\chi M)^{\frac{1}{2}} T}{\mu_1 V^{0.6}} \quad - (B)$$

For hydrogen in xylene at 75°C

M, the solvent molecular wt. = 106

χ, the degree of association of the solvent = 1

μ_1, the solvent viscosity, in centipoises = 0.4

V, the molecular volume of solute = 14.3 c.c./gm.mole

T, the absolute temperature = 348°K

Hence $D_g = \dfrac{7.4 \times 10^{-8} \times 10.4 \times 348}{0.4 \times 4.94} = 1.357 \times 10^{-4} cm^2/sec.$

Similarly for ethylene $D_g = 6.875 \times 10^{-5}$ $cm^2/sec.$

The density of xylene, assuming it to be mainly para and meta isomers, at 75°C, may be calculated (49)

$$\rho_1 = 0.815 \text{ gms./c.c.}$$

The densities of H_2 and C_2H_4 at 75°C are respectively 7.05×10^{-5} gms./c.c. and 9.9×10^{-4} gms./c.c. (50).

Hence $\Delta\rho = 0.815$ and 0.814 respectively. From (A) the respective liquid film coefficients may be calculated at 75°C:-

K_{a2} cm./sec. (C_2H_4)	K_{b2} cm./sec. (H_2)
0.082	0.116

From these, the overall mass transfer coefficients may be calculated

$$K_{ga} = 29.5 \frac{\text{gm. moles}}{\text{hr. cm}^2 \text{ atm.}} \times 10^3$$

$$K_{gb} = 2.3 \frac{\text{gm. moles}}{\text{hr. cm}^2 \text{ atm.}} \times 10^3$$

Thus, the experimental evidence that $K_{ga} > K_{gb}$ is substantiated by theoretical predictions of these quantities. It is only possible to obtain values of K_{gb} experimentally, K_{ga} being "masked".

The value of K_{gb} obtained from reactor 0 is considered

$$K_{gb} = 5.95 \frac{\text{gm. moles}}{\text{hr. cm}^2 \text{ atm.}} \times 10^3$$

This is a factor of $\simeq 3$ greater than the predicted value. Since this latter value is obtained from equations based on work in bubble columns free of suspended solids, it might be expected that mass transfer coefficients predicted thus would be lower than when catalyst is present by analogy with heat transfer where Kölbel (19)(20)(21) found that the presence of solid particles in a bubble column considerably increased heat transfer coefficients.

For a hydrogen overpressure of 1 atmosphere the experimental value of K_{gb} indicates a mass transfer rate of H_2 from the gas bubble of 162×10^{-8} $\frac{\text{gm. moles}}{\text{sec. cm}^2}$. Macrae gives a value of 14.3×10^{-8} $\frac{\text{gm. moles}}{\text{sec. cm}^2}$ for the instantaneous rate of pure hydrogen into pure toluene.(9) Assuming toluene to resemble xylene closely this result differs from the present experimental value by a factor of rather more than 10.

Values of K_1 are shown in table 3.64. There is an entirely random scatter of values, the mean of which is

$$1.015 \ \frac{\text{gm. moles}}{\text{cm}^2 \text{ hr. atm}^2} \times 10^3$$

Assuming the partial pressures of ethylene and hydrogen to be $\frac{1}{2}$ atmosphere, equation 1.2.50 indicates a reaction rate of 0.0435×10^{-5} $\frac{\text{gm. moles}}{\text{sec. c.c.}}$ or since the catalyst concentration is .025 gms./c.c.

$$1.74 \times 10^{-5} \ \frac{\text{gm. moles}}{\text{sec. gm. of catalyst}}$$

While using a different mechanism at 75°C and $\frac{1}{2}$ atm. pressure of H_2, work by Wynkoop and Wilhelm (51) in a fixed bed reactor indicates a reaction rate =

$$1.35 \times 10^{-5} \ \frac{\text{gm. moles}}{\text{sec. c.c.}}$$

A similarity with the experimental rate indicated above can be demonstrated if an overall bed density of

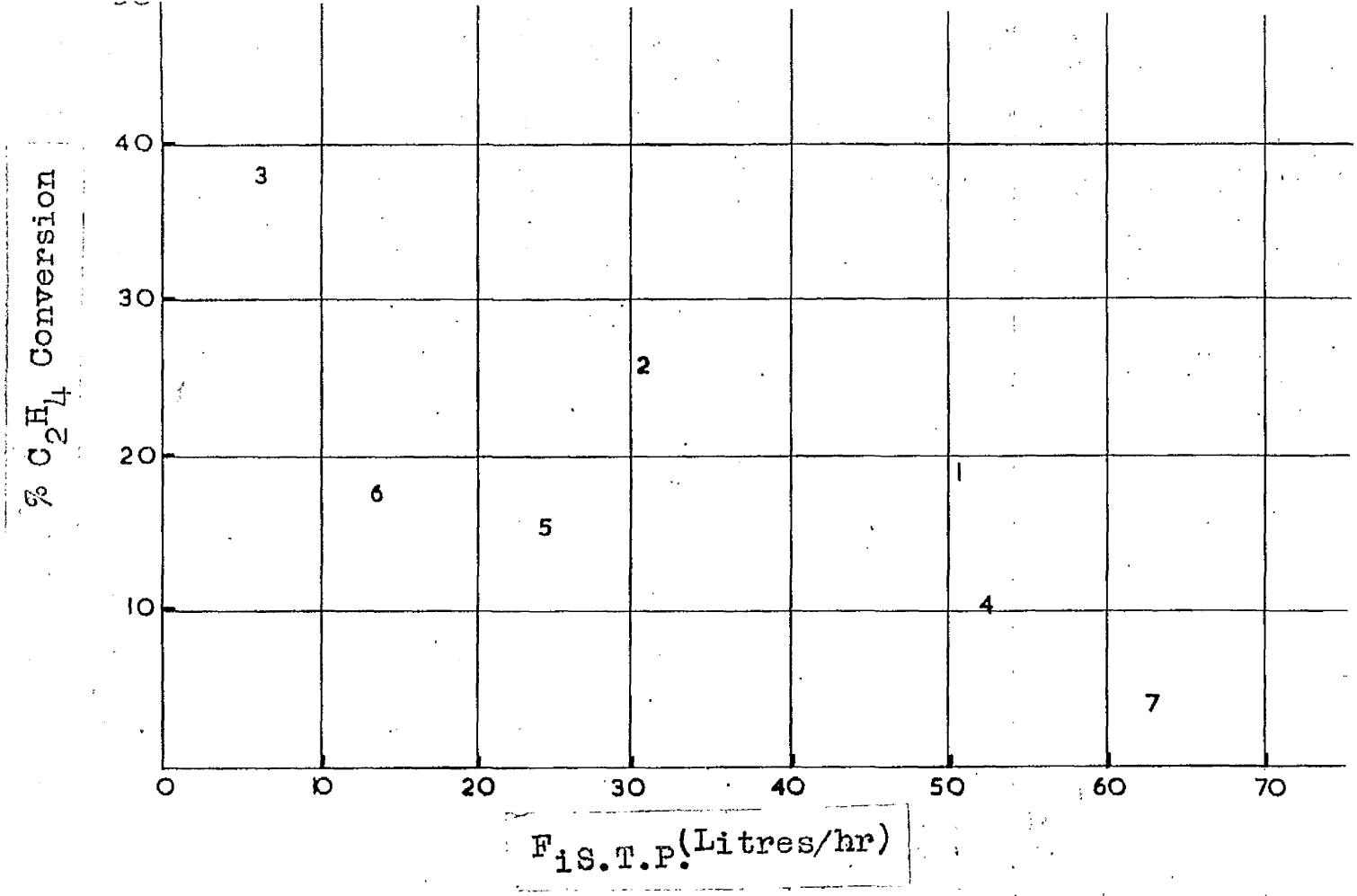

FIG. 3. 29.

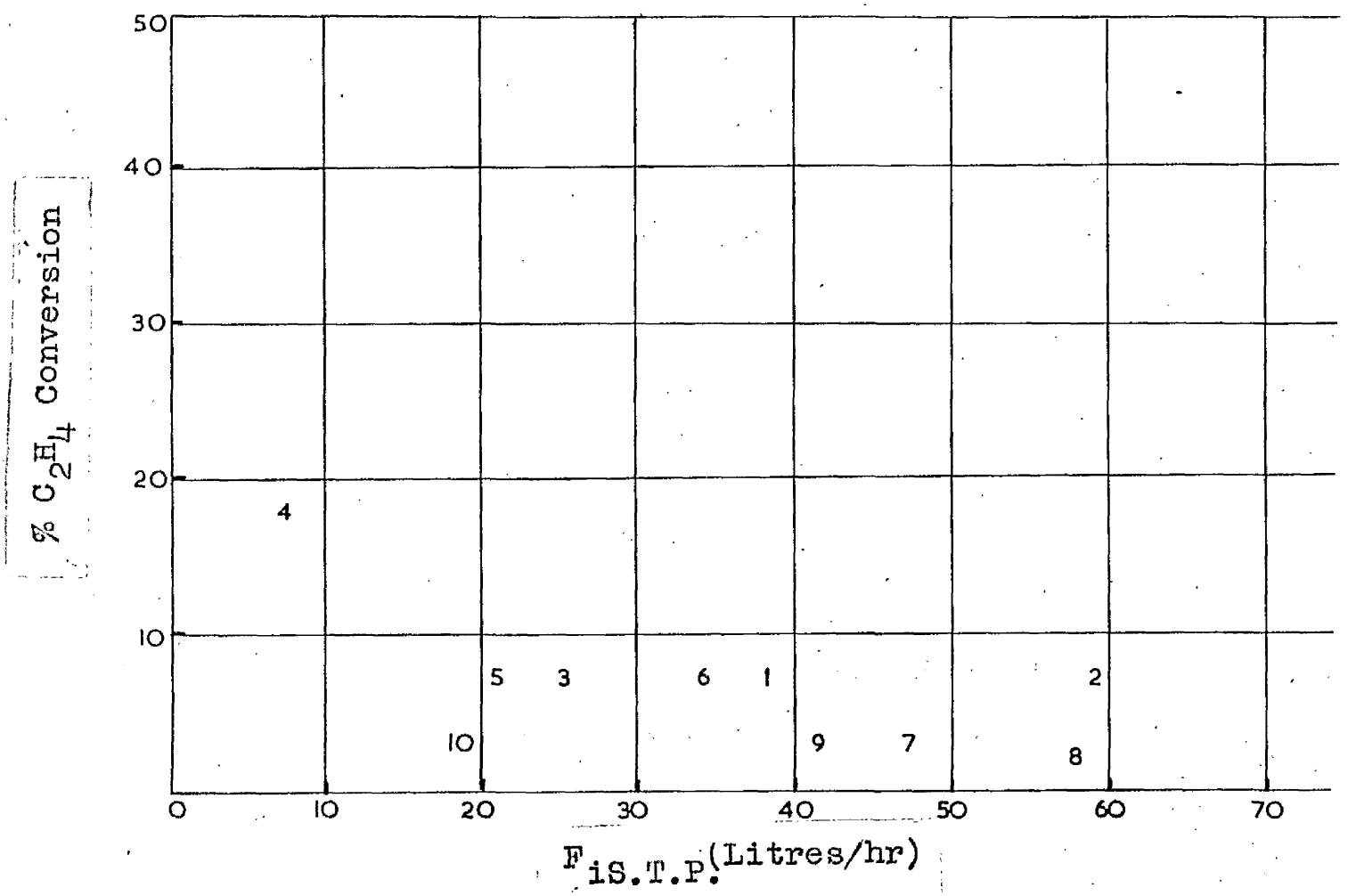

FIG. 3. 30.

1 gm./c.c. is reasoned for the work of Wynkoop. This gives the more interesting rate value of

$$1.35 \times 10^{-5} \quad \frac{\text{gm. moles}}{\text{sec. gm. of catalyst}}$$

It must be emphasised that this value is based on a deduced figure of overall bed density.

Pauls et al. (40) obtained reaction rates for ethylene hydrogenation on Raney nickel of the order of

$$0.55 \times 10^{-5} \quad \frac{\text{gm. moles}}{\text{sec. gm. of catalyst}}$$

Comparison of the above values for reaction rates of ethylene hydrogenation is unjustifiable due to the difference in catalysts and catalytic activites, but the similarity of order of magnitude is interesting.

3. 8. Water as a Catalyst Suspending Medium.

Experiments were carried out in reactors V and II using a water based slurry.

Results - Tables 3.52 - 3.53.

% C_2H_4 conversion vs. gas flow rate plots are shown in figs. 29 - 30.

The catalyst appears to lose its activity fairly rapidly. This results in diminishing conversions. This fact accords with the work of Barford (52) who claimed that water vapour poisons Raney nickel.

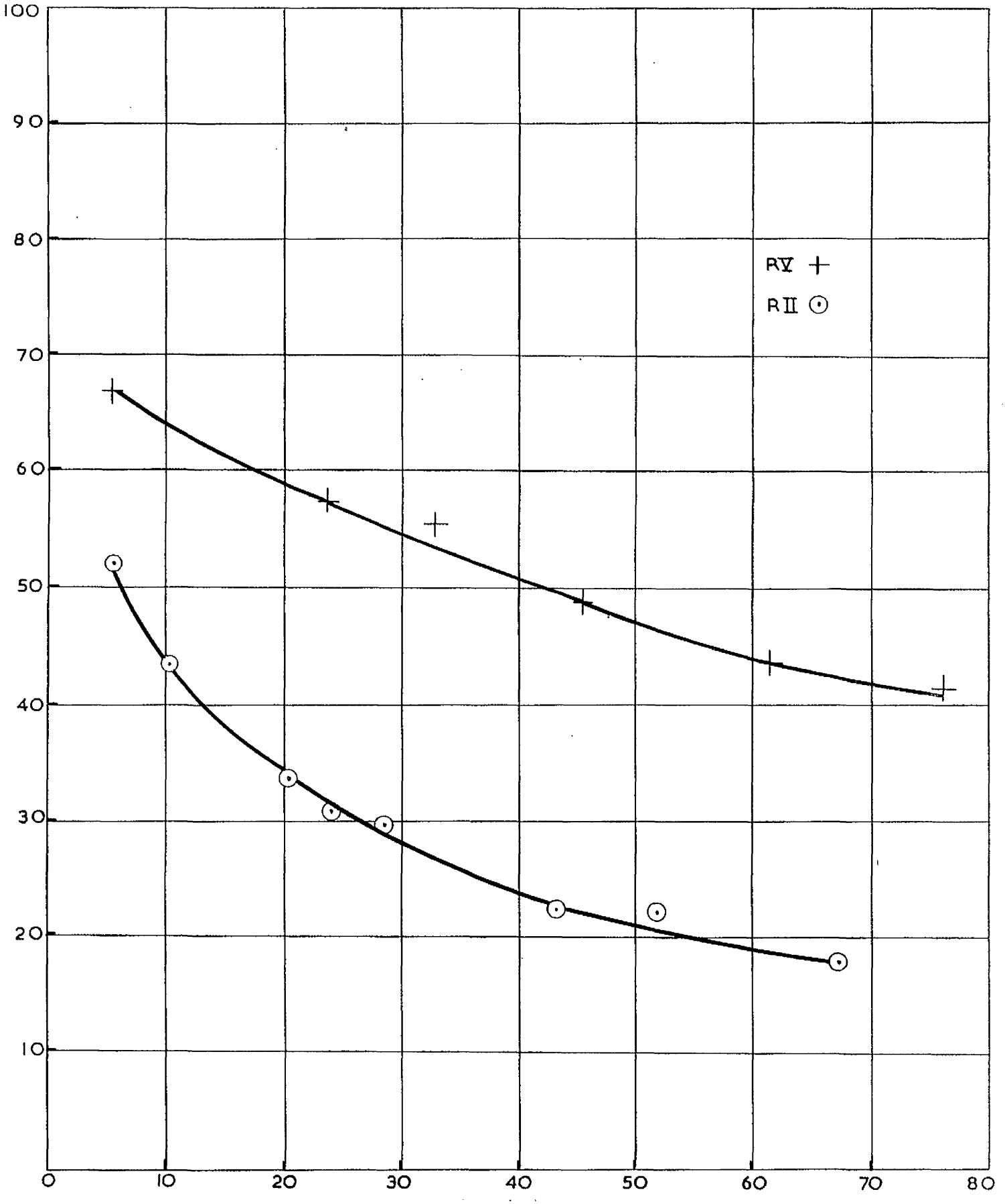
100
90
80
70
60
50
40
30
20
10
0
10
20
30
40
50
60
70
80
RV +
RII ⊙
F iS.T.P.(Litres/hr)

FIG. 3. 31.

As water was of little value as a catalyst suspending medium further work with it was abandoned.

3. 9. Decalin as a Catalyst Suspending Medium.

Experiments were carried out in reactors V and II using a decalin, based slurry.

The results obtained with decalin closely resemble those for xylene. Tables 3. 54 - 62., Fig 3.31 Corresponding conversions, however, are lower in the case of decalin.

Fig. 3. 33 shows the plot of NRU_a vs $\frac{Z}{F_i}$ for decalin. This is similar to that obtained in the case of xylene, although fewer results are available.

TABLE 3. 65.

R V		R II	
f_1	f_2	f_1	f_2
0.510	0.266	0.491	0.278
0.635	0.342	0.534	0.327
0.94	0.725	0.635	0.368
2.87	1.73	0.725	0.520
0.579	0.286	0.745	0.621
0.706	0.400	0.995	1.06
		1.32	1.58
		0.649	0.52

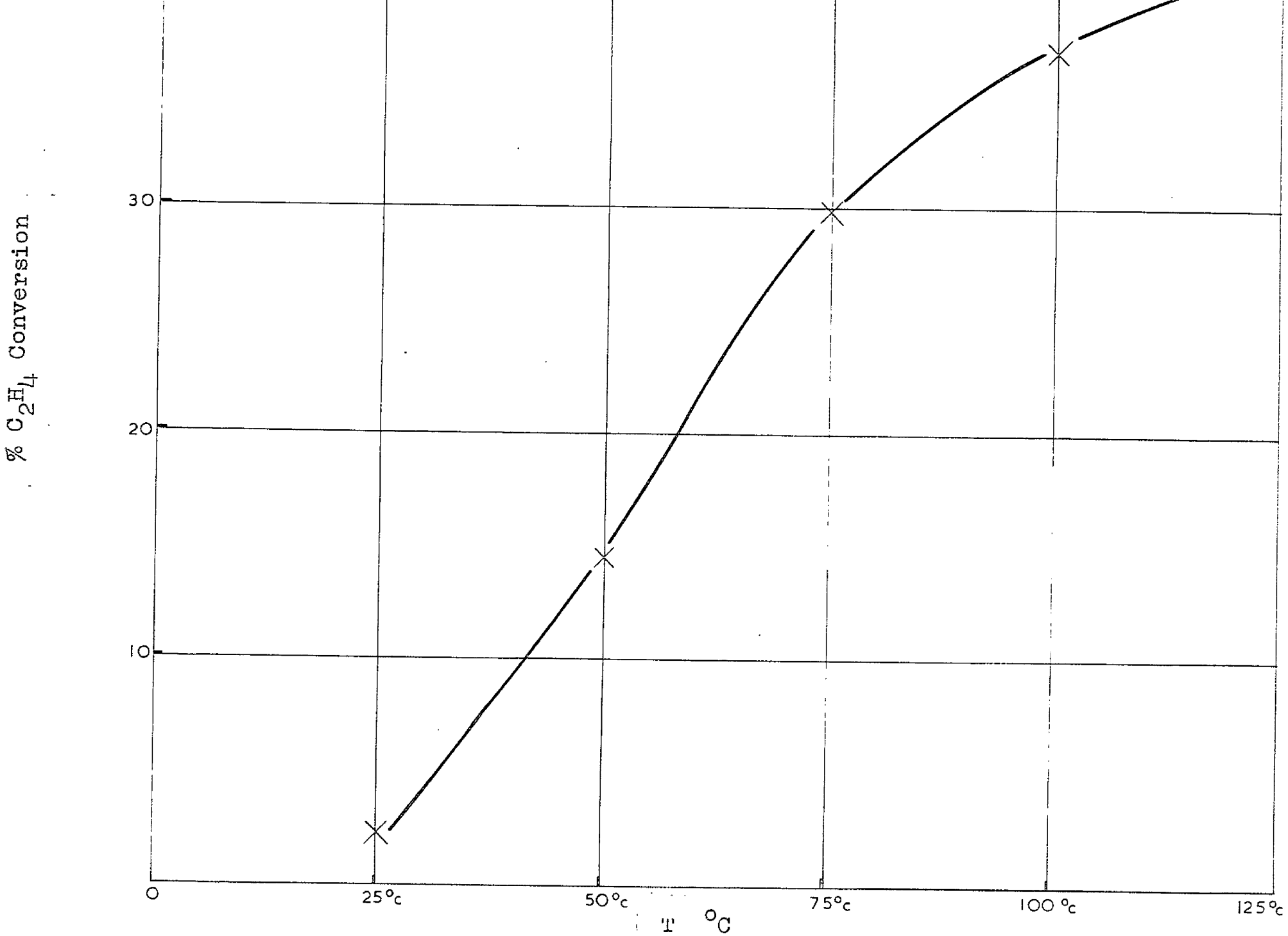

FIG. 3. 32.

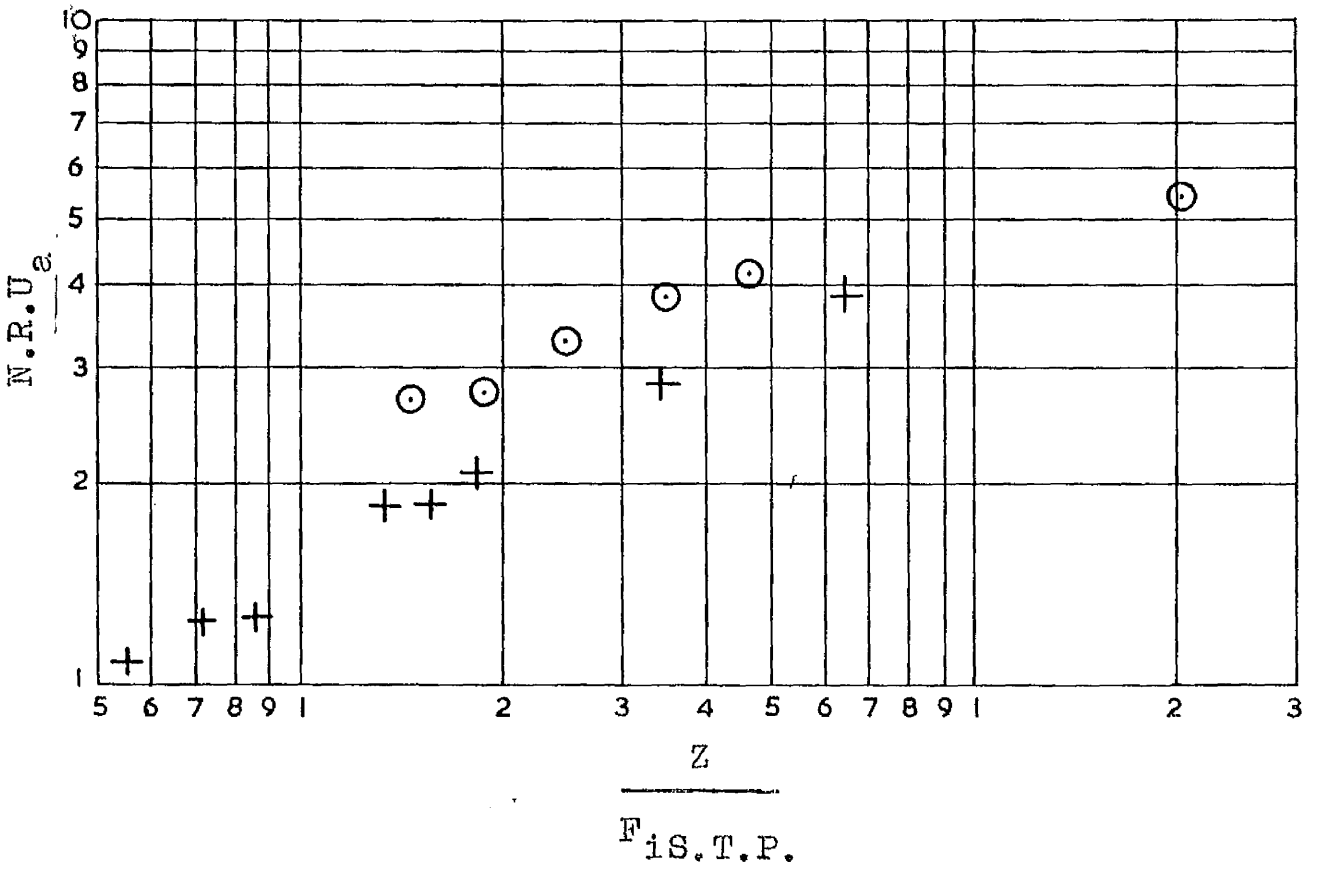

FIG. 3.33.

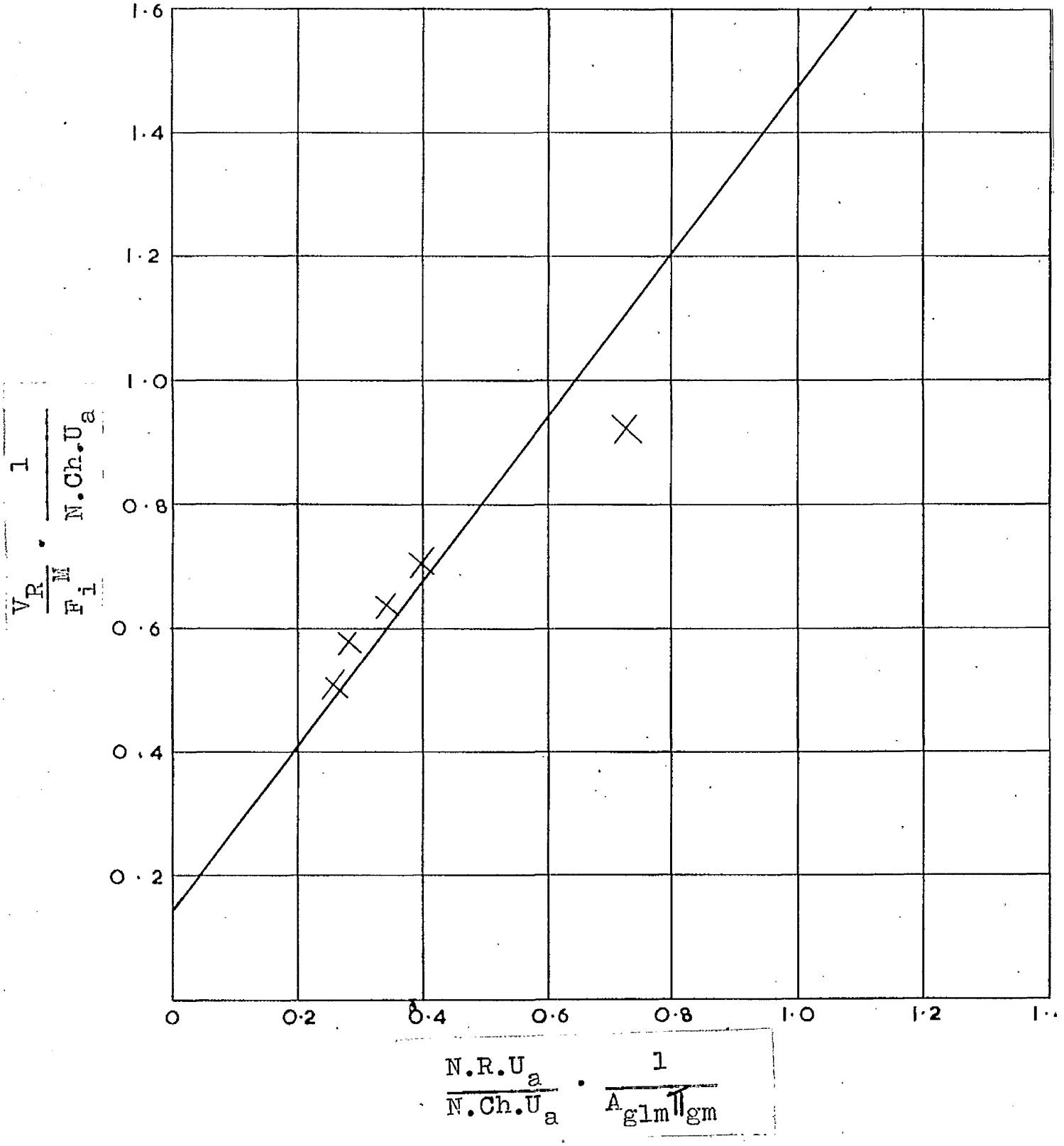
1·6
1·4
1·2
1·0
0·8
0·6
0·4
0·2
0
0·2
0·4
0·6
0·8
1·0
1·2
$\frac{V_R}{F_i} \cdot \frac{1}{\frac{M}{N.Ch.U_a}}$
$\frac{N.R.U_a}{N.Ch.U_a} \cdot \frac{1}{A_{glm}\eta_{gm}}$

FIG. 3.34

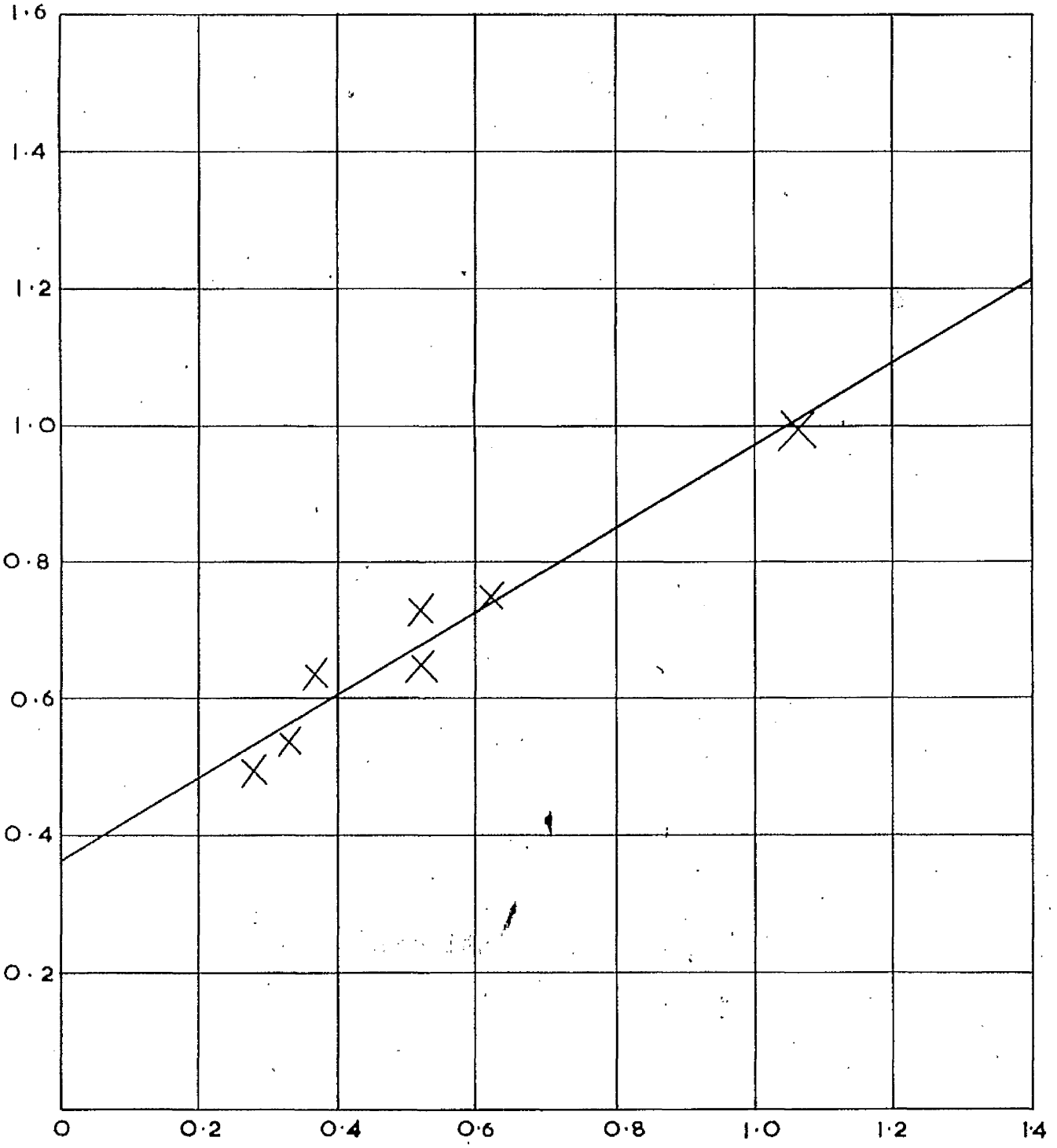
1·6
1·4
1·2
1·0
0·8
0·6
0·4
0·2
0
0·2
0·4
0·6
0·8
1·0
1·2
1·4
$\frac{V_R}{F_1 M} \cdot \frac{1}{N.Ch.U_a}$
$\frac{N.R.U_a}{N.Ch.U_a} \cdot \frac{1}{A_{glm}\sqrt{\pi_{gm}}}$

FIG. 3.35

Figs. 3.34 - 3.35 show plots of

$$\frac{V_R}{F_i^M}, \frac{1}{N.Ch.U} \quad \text{vs.} \quad \frac{N.R.U.}{N.Ch.U.}, \frac{1}{A_{glm}\pi_{gm}}$$ for ethylene.

The values of K_g and K_l are shown in the table below:-

Table 3.66.

R	K_g	$K_l A_{ls}$	A_{ls}	K_l
V	0.74	6.45	6.76	0.955
II	0.65	2.87	6.76	0.425

The K_g values, which are assumed to be those of hydrogen, are less than the corresponding xylene values but show a similar increase in the smaller reactor. The values of K_l show less agreement with one another than the values derived from work in xylene but are of the same order of magnitude as the xylene results.

The fact that the conversions are lower and mass transfer coefficients smaller in decalin than in xylene is attributed to the different physical properties of the liquids

eg. At 25°C	Xylene	Decalin.
Viscosity	0.61 centipoises	1.9 centipoises
Density	0.861 gms./cc.	0.869 gms./cc.

The higher viscosity especially of decalin will affect mass transfer coefficients adversely. The solubilities of the gases in decalin may also be lower although no information is available. Lower solubilities

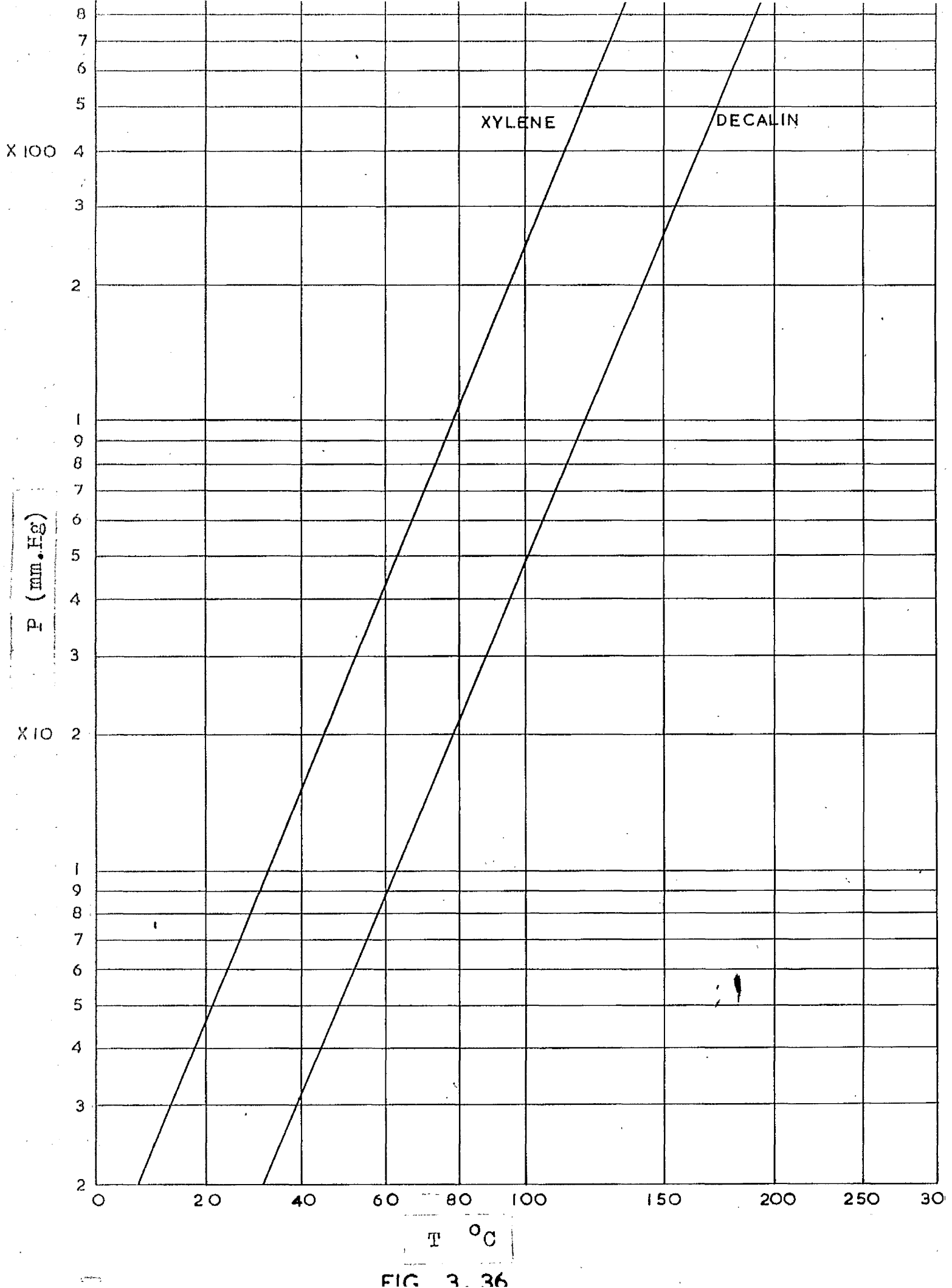
XYLENE
DECALIN
X 100
X 10
P (mm.Hg)
T °C
0
20
40
60
80
100
150
200
250
30

FIG. 3.36

would also affect mass transfer coefficients adversely.

The effect of liquid partial pressure on conversion was studied by varying the temperature of the reactor. With xylene it was impossible to attain operating temperatures appreciably greater than 80°C due to vapour locks forming in the slurry circulation pump. However, it was possible to achieve operating tempera-:tures of 125°C with decalin.

Fig. 3.32 shows the variation of conversion with temperature at a constant reactant gas inlet flow rate. The rate of increase of conversion decreases with temperature. In equation 1.2.45, the rate of reaction is shown to be a function of $(P_a - P_{als})$. If the reaction at the catalyst surface is not rate controlling the P_{als} is very small. Hence $N_a \propto P_a$. As the temperature of the system increases, the vapour pressure of the solvent increases and hence P_a is reduced. Thus the diminution of conversion at high temperatures is explained.

In Fig. 3.36, the partial pressures of xylene and decalin at various temperatures are shown.

It can be said that the lower vapour pressure of decalin must in some measure offset the effect of poor mass transfer on conversion in that liquid.

3. 10. Conclusions.

Using the hydrogenation of ethylene on a Raney nickel catalyst as an experimental model, the following conclusions were reached.

(1) Equation 1.2.49 of the mathematical model suggests that above a certain catalyst concentration the reaction on the catalyst surface will have a negligible effect on the overall reaction rate. Experiments at constant inlet reactant flow rate and various catalyst concentrations showed this prediction to be true.

(2) The experimental results show that conversion is an inverse function of reactant flow rate and is a function of reactor length rather than reactor volume. Slurry recirculation has no beneficial effects on conversion except at very low reactant flow rates. Space time yields are a function of reactant flow rate and an inverse function of reactor length.

(3) A study of the effects of variation of inlet gas composition confirmed the general view (9)(10) that resistances to hydrogen transport are rate controlling.

(4) The effect of reactor length and diameter on conversion and space time yield has not been fully elucidated. It is suggested that a thorough investi-:gation of these effects would be a suitable subject for future work. Optimisation work on slurried bed reactor shape and size would then be possible.

(5) A method of predicting reactor performance has been evolved and is expressed in terms of reactor length, reactant inlet flow rate and number of reactor units (N.R.U.). It is submitted that this method has immediate potential for solving practical problems.

(6) The values for hydrogen mass transfer coefficients calculated using equation 1.2.57 of the mathematical model are not in disagreement with the values predicted using a method suggested elsewhere (47).

The rates, for the chemical reaction occurring at the catalyst surfaces, estimated using equation 1.2.57 show the same order of magnitude as values obtained by other workers (40)(51). However, this is not necessarily significant as comparison of rates of catalytic reactions carried out under different conditions is generally ill-advised..

The validity of the mathematical model has not been disproved by the experimental results, but there are certain effects which have not been fully explained. It is claimed that the mathematical model provides a possible method for scaling up slurried bed reactors for second order chemical reactions by the substitution of basic physico-chemical data, obtained from studies of gas liquid systems and the kinetics of chemical reactions, in equation 1.2.57.

(7) Results indicate that the catalyst suspending medium is of great importance in determining the performance of a slurried bed reactor (eg. Decalin results versus those of xylene). Detailed information over a range of temperatures on gas solubilities and liquid properties is required for a large number of apparently suitable media. Only then for a particular system may the best liquid be chosen.

NOMENCLATURE.

SYMBOL	DESCRIPTION	DIMENSIONS	UNITS
a	Activity	-	-
A_{gl}	Gas-liquid interfacial area/ unit volume of reactor	$\frac{1}{L}$	$\frac{cms^2}{cms^3}$
A_{ls}	Liquid-solid interfacial area/ unit volume of reactor	$\frac{1}{L}$	$\frac{cms^2}{cms^3}$
C	% Reactant conversion (chemical analysis)	-	-
C'	% Reactant conversion (volume reduction)	-	-
C_{gl}	Concentration at gas liquid interface	$\frac{M}{L^3}$	$\frac{gm.moles}{litre}$
C_l	Concentration in bulk liquid (1)	$\frac{M}{L^3}$	$\frac{gm.moles}{litre}$
C_l'	Concentration in bulk liquid (2)	$\frac{M}{L^3}$	$\frac{gm.moles}{litre}$
C_{ls}	Concentration at liquid solid interface	$\frac{M}{L^3}$	$\frac{gm.moles}{litre}$
C^*	Molal concentration of occupied active centres on catalyst surface	$\frac{M}{L^2}$	$\frac{gm.moles}{cm^2}$
C_t^*	Total concentration of active centres on catalyst surface	$\frac{M}{L^2}$	$\frac{gm.moles}{cm^2}$
C_v^*	Molal concentration of vacant active centres on catalyst surface	$\frac{M}{L^2}$	$\frac{gm.moles}{cm^2}$
D_g	Diffusion coefficient of gas	$\frac{L^2}{T}$	$\frac{cm^2}{sec.}$
F	Volumetric flow rate	$\frac{L^3}{T}$	$\frac{litres}{hr.}$
F_{STP}	Volumetric flow rate at S.T.P.	$\frac{L^3}{T}$	$\frac{litres}{hr.}$
$F.M$	Molar flow rate	$\frac{M}{T}$	$\frac{gm.moles}{hr.}$
F_x	Molar flow rate when conversion is x	$\frac{M}{T}$	$\frac{gm.moles}{hr.}$

SYMBOL.	DESCRIPTION	DIMENSIONS	UNITS
f	Fugacity	$\frac{M}{LT^2}$	Atm.
f_o	Fugacity at standard state	$\frac{M}{LT^2}$	Atm.
f'	Fugacity of pure component	$\frac{M}{LT^2}$	Atm.
G	Catalyst concentration	$\frac{M}{L^3}$	$\frac{\text{gms. x } 10^2}{\text{cms}^3}$
H	Henry's law constant	$\frac{T^2}{L^2}$	$\frac{\text{gm.moles}}{\text{litre atm.}}$
H.Ch.U.	Height of a chemical unit	L	cms.
H.R.U.	Height of a reactor unit	L	cms.
H.T.U.	Height of a transfer unit	L	cms.
K	Equilibrium constant	-	-
K_p	" "	$\frac{LT^2}{M}$	Atm.^{-1}
K_x	" "	-	-
K_y	" "	-	-
K_f	Forward rate constant	$\frac{M}{L^3T}$	$\frac{\text{gm.moles}}{\text{litre hr.}}$
K_b	Backward rate constant	$\frac{M}{L^3T}$	$\frac{\text{gm.moles}}{\text{litre hr.}}$
K_{sf}	Forward surface rate constant	$\frac{1}{T}$	$\frac{10^3}{\text{hr.}}$
K_{sb}	Backward surface rate constant	$\frac{1}{T}$	$\frac{10^3}{\text{hr.}}$
K_s	Surface equilibrium constant	-	-
K_1'	Forward surface rate constant	$\frac{T}{L}$	$\frac{\text{gm.moles}}{\text{cm}^2\text{hr.atm}^2}$

SYMBOL	DESCRIPTION	DIMENSIONS	UNITS
K_2'	Backward surface rate constant	$\frac{T^3}{M}$	$\frac{gm.moles}{cm^2 hr.atm.}$
K_1	Forward surface rate constant	$\frac{T}{L}$	$\frac{gm.moles \times 10^3}{cm^2 hr.atm^2}$
$K_{a1}K_{b1}$ K_{c1}	Mass transfer coefficient	$\frac{T}{L}$	$\frac{gm.moles \times 10^3}{hr.\ cm^2\ atm.}$
$K_{a2}K_{b2}$ K_{c2}	" " "	$\frac{L}{T}$	$\frac{cm.}{hr.}$
$K_{a3}K_{b3}$ K_{c3}	" " "	$\frac{L}{T}$	$\frac{cm.}{hr.}$
$K_{a4}K_{b4}$ K_{c4}	" " "	$\frac{L}{T}$	$\frac{cm.}{hr.}$
K_g	Overall mass transfer coefficient	$\frac{T}{L}$	$\frac{gm.moles \times 10^3}{hr.cm^2\ atm.}$
$\bar{K}_g$	Overall process coefficient	$\frac{T}{L}$	$\frac{gm.moles \times 10^3}{hr.cm^2\ atm.}$
K_r	Reaction coefficient	$\frac{T}{L}$	$\frac{gm.moles \times 10^3}{hr.cm^2\ atm.}$
K'	Proportionality factor	-	-
N_a	Instantaneous reaction rate	$\frac{M}{L^3T}$	$\frac{gm.\ moles}{litre\ hr.}$
N_a'	" " "	$\frac{M}{T}$	$\frac{gm.\ moles}{hr.}$
$N_c^{\text{Æ}}$	Overall reaction rate (space time yield)	$\frac{M}{L^3T}$	$\frac{gm.\ moles}{litre\ hr.}$
N.Ch.U.	No. of Chemical Units	-	-
N.R.U.	No. of Reactor Units	-	-
N.T.U.	No. of Transfer Units	-	-
P.	Gas bulk partial pressure	$\frac{M}{LT^2}$	Atm.
P_{gl}	Gas liquid interfacial partial pressure	$\frac{M}{LT^2}$	Atm.

SYMBOL	DESCRIPTION	DIMENSIONS	UNITS.
P_1	Liquid bulk partial pressure (1)	$\frac{M}{LT^2}$	Atm.
P_1'	Liquid bulk partial pressure (2)	$\frac{M}{LT^2}$	Atm.
P_{1s}	Liquid solid interfacial partial pressures	$\frac{M}{LT^2}$	Atm.
P^M	Equilibrium gas bulk partial pressures	$\frac{M}{LT^2}$	Atm.
r_f	Forward reaction rate	$\frac{M}{TL^3}$	$\frac{\text{gm.moles}}{\text{hr. litre}}$
r_b	Back reaction rate	$\frac{M}{TL^3}$	$\frac{\text{gm.moles}}{\text{hr.litre}}$
r	Overall reaction rate	$\frac{M}{TL^3}$	$\frac{\text{gm.moles}}{\text{hr.litre}}$
r_{sf}	Forward surface reaction rate	$\frac{M}{TL^2}$	$\frac{\text{gm.moles}}{\text{hr. cm}^2}$
r_{sb}	Back surface reaction rate	$\frac{M}{TL^2}$	$\frac{\text{gm.moles}}{\text{hr. cm}^2}$
r_s	Overall surface reaction rate	$\frac{M}{TL^2}$	$\frac{\text{gm.moles}}{\text{hr. cm}^2}$
S	Adsorption equilibrium constant	$\frac{LT^2}{M}$	Atm.^{-1}
T	Reaction temperature	$\frac{L^2}{T^2}$	$^oC.$
T_R	Room temperature	$\frac{L^2}{T^2}$	$^oC.$
V_R	Reactor volume	L^3	$\text{litre}\left(\frac{\text{cms}^3}{10^3}\right)$
X	Fractional molar conversion	-	-
Y	Mole fraction	-	-
Z	Reactor height	L	cms.
α	Ratio of partial pressures $\frac{P_{bi}}{P_{ai}}$	-	-

SYMBOL	DESCRIPTION	DIMENSIONS	UNITS.
α'	Ratio of partial pressures $\frac{P_b}{P_a}$	-	-
β	$\frac{1}{\alpha}$	-	-
β'	$\frac{1}{\alpha'}$	-	-
δ	Ratio of partial pressures $\frac{P_{blsi}}{P_{alsi}}$	-	-
δ'	" " $\frac{P_{bls}}{P_{als}}$	-	-
γ	Reactor cross sectional area	L^2	$\frac{cms.^2}{10^3}$
π	Atmospheric pressure	$\frac{M}{LT^2}$	cms. Hg
π_g	Total gas pressure	$\frac{M}{LT^2}$	Atm.
π_l	Liquid head	$\frac{M}{LT^2}$	cms. Hg
π_s	Partial pressure of solvent	$\frac{M}{LT^2}$	cms. Hg
ρ_s	Density of solvent	$\frac{M}{L^3}$	gms/c.c.
ϕ	Function of standard fugacities	$\frac{M}{LT^2}$	Atm.
μ	Viscosity of solvent	$\frac{M}{LT}$	Poises
ψ_f	Forward Adsorption rate constant	$\frac{LT}{M}$	$\frac{10^3}{atm.hr.}$
ψ_r	Reverse adsorption rate constant	$\frac{1}{T}$	$\frac{10^3}{hr.}$
θ	Time of experiment	T	Minutes
SUFFIXES	a, b, c - components $A(C_2H_4)$ $B(H_2)$ and $C(C_2H_6)$	-	-
"	i, o, m - inlet, outlet and mean respectively	-	-

APPENDICES 1, 2 and 3.

APPENDIX 1.

Calculation of the equilibrium constants K and K_P for the reaction $C_2H_4 + H_2 \longrightarrow C_2H_6$.

The method used was suggested elsewhere (52).

The heat of reaction is given by

$$\Delta H_{R_{TO}} = \sum_{P} N \Delta H_f - \sum_{R} N \Delta H_f$$

For this reaction, heats of formation are (52), at 18°C and 1 atm.

H_2 ΔH_f = 0 cals/gm. mole

C_2H_4 ΔH_f = 12,496 cals/gm. mole

C_2H_6 ΔH_f = 20,236 cals/gm. mole.

Hence $\Delta H_{R_{291}}$ = - 32,732 cals/gm. mole.

The reaction takes place at 75°C and 1 atm.

$$\text{Now } \Delta H_{R_T} = \Delta H_{R_{TO}} + \int_{To}^{T} \Delta Cp dT$$

For this reaction, the average molal heat capacities are (55)

H_2	6.5 cals/gm. mole °C	
C_2H_4	11.2 cals/gm. mole °C	
C_2H_6	13.2 cals/gn. mole °C	

Thus ΔCp = - 4.5 cals/gm. mole °C

Hence $\Delta H_{R_{348}} = \Delta H_{R_{291}} + (-4.5)(57)$

= - 32,989 cals/gm. mole.

For C_2H_4, H_2 and C_2H_6, third law entropies are (56)

C_2H_4	31.2	cals/gm. mole degree
H_2	52.5	cals/gm. mole degree
C_2H_6	55.0	cals/gm. mole degree

Thus for the reaction $\Delta S_{291}^{o} = -28.7$ cals/gm. mole degree

$$\text{Now } \Delta S_{348} = \Delta S_{291} + \int_{To}^{T} \frac{\Delta Cp}{T} dT$$

$$= -28.7 + (-4.5) \cdot \ln \frac{348}{298}$$

$$= -29.4 \text{ cals/gm. mole degree.}$$

$$\text{Now } \Delta G_{348} = \Delta H_{348} - T\Delta S_{348}$$

$$\Delta G_{348} = -32,989 - 348 \times 29.4$$

$$= -22,820 \text{ cals/gm. mole}$$

$$\text{Also } \Delta G = -RT \ln K$$

$$\therefore \ln K = \frac{22,820}{1.98 \times 348} = 33$$

This leads to a value of 2×10^{14} for K, ie. K is large and equilibrium conversion will be high.

A value of $K = 2 \times 10^{14}$ is reported elsewhere (57)

$$\text{Now } K = K_p K_\alpha \phi$$

It has already been shown that $\phi = 1$ and has units of atmospheres.

$$K_\alpha = \frac{\left[\frac{f'}{P_T}\right]_{C_2H_6}}{\left[\frac{f'}{P_T}\right]_{H_2} \left[\frac{f'}{P_T}\right]_{C_2H_4}}$$

$\frac{f'}{P_T}$ may be read off a fugacity ratio - reduced pressure chart (58).

$\underline{C_2H_4}$ 75°C 1 atm.

$T_R = \frac{T}{Tc} = \frac{348}{263.1}$ 1.325

$P_R = \frac{P}{Pc} = \frac{1}{50.07}$ 0.0197

$\frac{f'}{P_T}$ = 1.00

$\underline{H_2}$ 75°C 1 atm.

$T_R = \frac{T}{Tc} = \frac{348}{41.1} = 8.46$

$P_R = \frac{P}{Pc} = \frac{1}{20.8} = 0.048$

$\frac{f'}{P_T}$ = 1.00

$\underline{C_2H_6}$ 75°C 1 atm.

$T_R = \frac{T}{Tc} = \frac{298}{240.73} = 1.45$

$P_R = \frac{P}{Pc} = \frac{1}{48.2}$ 0.0218

$\frac{f'}{P_T}$ = 1.00

$K_\alpha = \frac{(1.00)}{(1.00)(1.00)} = 1.00$

Hence $K_p = 2.0 \times 10^{14}$ atm.$^{-1}$.

APPENDIX 2.

The method employed to measure the surface area of bubbles in the reactor was first used by Calderbank (59).

A parallel beam of light is passed from a light source along a tube, through the reactor column, and thence to a photoelectric cell. Bubbles passing through the light beam appear as black particles and cause a diminution in the intensity of the light incident on the photoelectric cell. The cell is connected to an electronic measuring system which records the amount of incident light over a fixed time. This time is regulated by an electric timing switch between the light source and a constant voltage supply system. The experimental arrangement used is shown in Fig. A. 2. 1.

The following equation enables the bubble surface area per unit volume to be calculated:-

$$\log_{10} \frac{I_o}{I} = \frac{A_{gl} L}{9.210}$$

where I_o = amount of light passing through column in absence of bubbles.

I = amount of light passing at some gas flow rate, F.

A_{gl} = bubble surface area/unit volume of reactor cm^2/cm^3.

L = light path length through column. cm.

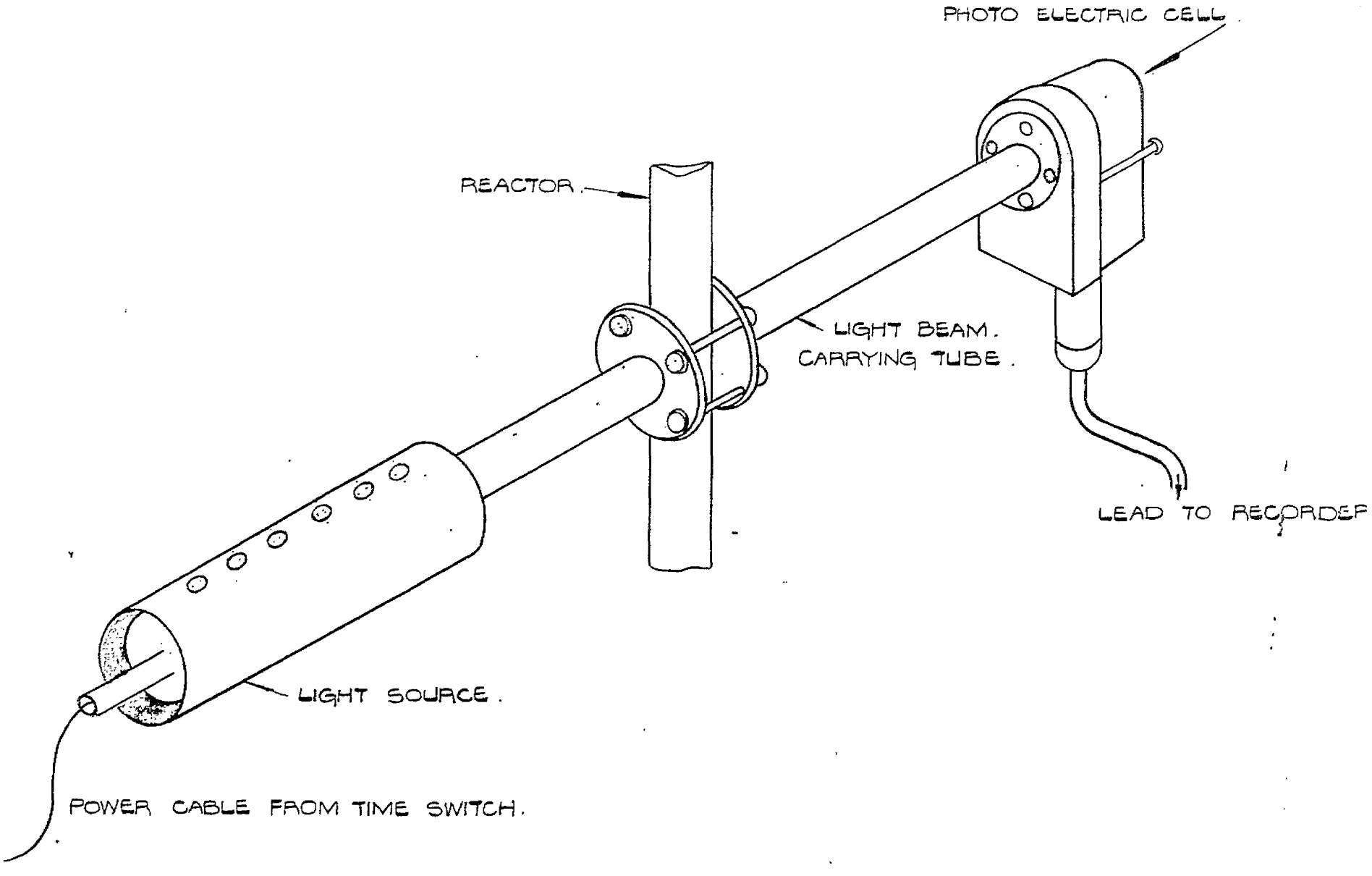

FIG. A. 2.1. BUBBLE SIZE MEASURING APPARATUS.

Due to the nature of the experiment, it was necessary to operate each reactor in the absence of catalyst. When possible, measurements were made at both top and bottom of the reactor. Reactor II was the smallest reactor in which measurements could be made.

θ = setting of timing clock (seconds)

The results obtained are shown in the following tables and graphs:-

REACTOR V.

$C_2H_4 : H_2 = 1:1$
Path length = 3.3 cm.
Ht. from column base = 95.5 cm.
I_o = 218
θ = 100
T_R = 17°C π = 74.5 cm.

F_i	I	A_{gl}
85.0	90	1.105
77.5	90	1.105
68.0	92	1.05
52.5	99	0.955
43.0	102	0.920
35.0	105	0.887
20.0	128	0.648
12.5	160	0.377
6.25	184	0.209
1.5	208	0.062

$C_2H_4 : H_2 = 1:1$
Path length = 3.3 cm.
Ht. from column base = 20 cm.
I_o = 233
θ = 100
T_R = 15°C π = 74.5 cm.

F_i	I	A_{gl}
85.0	48	1.92
76.0	61	1.63
67.5	62	1.61
53.5	78	1.33
42.5	83	1.26
31.0	95	1.095
20.5	140	0.62
13.5	158	0.472
6.5	188	0.263
2.0	210	0.129

REACTOR IV.

C_2H_4 : H_2 = 1:1
Path length = 3.3 cm.
Ht.from column base = 70 cm.
I_o = 223
θ = 100
T_R = 17.5°C π = 74.5 cm.

F_i	I	A_{gl}
87.5	72	1.375
77.5	81	1.235
72.5	84	1.190
55	90	1.100
45	98	1.00
36	105	0.915
24	112	0.836
18.5	136	0.600
17.0	145	0.525
12.0	160	0.405
6.0	190	0.198
1.5	210	0.078

C_2H_4 : H_2 = 1:1
Path length = 3.3 cm.
Ht.from column base = 22.5 cm.
I_o = 236
θ = 100
T_R = 19°C π = 73.9 cm.

F_i	I	A_{gl}
90.0	35	2.320
76.0	46	1.990
66.0	57	1.725
57.0	72	1.59
46.0	92	1.145
42.0	95	1.100
32.5	101	1.030
31.0	95	1.100
22.5	130	0.725
13.5	153	0.525
5.0	198	0.212
2.5	205	0.173

REACTOR III.

C_2H_4 : H_2 = 1:1
Path length = 3.3 cm.
Ht. from column base = 45.5 cm.
I_o = 230
θ = 100
T_R = 18°C π = 75.2 cm.

F_i	I	A_{gl}
87.5	49	1.88
78.5	51	1.835
70.0	60	1.63
52.0	84	1.22
40.0	98	1.04
28.0	108	0.92
36.0	100	1.01
19.0	130	0.692
13.0	158	0.464
7.5	189	0.243
1.25	214	0.089

C_2H_4 : H_2 = 1:1
Path length = 3.3 cm.
Ht. from column base = 18 cm.
I_o = 220
θ = 100
T_R = 18°C π = 75.2 cm.

F_i	I	A_{gl}
87.5	39	2.10
76.5	47	1.88
70.0	58	1.62
59.0	68	1.43
47.5	70	1.39
38.0	80	1.24
29.0	96	1.005
16.0	130	0.642
9.0	162	0.372
6.0	179	0.254
1.5	196	0.139

REACTOR II.

C_2H_4 : H_2 = 1:1
Path length = 3.3 cm.
Ht.from column base = 19.5 cm.
I_o = 218
θ = 100
T_R = 18°C Π = 75.6 cm.

F_i	I	A_{gl}
87.5	43	1.97
81.0	52	1.74
74.0	58	1.615
66.0	62	1.525
52.5	69	1.40
44.0	80	1.215
36.0	88	1.10
26.0	104	0.90
17.5	132	0.608
11.0	161	0.368
7.0	185	0.201
2.0	205	0.078

REACTOR IV A.

C_2H_4 : H_2 = 1:1
Path length = 5.6 cm.
Ht.from column base = 30 cm.
I_o = 215
θ = 160
T_R = 20°C Π = 75.5 cm.

F_i	I	A_{gl}
72.5	50	1.045
59.0	66	0.845
52.5	72	0.785
45.5	85	0.665
40.0	91	0.615
34.0	92	0.609
26.5	112	0.465
18.0	135	0.333
16.5	130	0.358
11.0	146	0.272
5.5	175	0.149
3.0	205	0.100

REACTOR V.

C_2H_4 : H_2 = 2:1
Path length = 3.3 cm.
Ht.from column base = 95.5 cm.
I_o = 219
θ = 100
T_R = 17°C π = 74.5 cm.

F_i	I	A_{gl}
74.5	89	1.09
64	93	1.04
54	99	0.965
41	101	0.940
33	109	0.850
20	128	0.653
11	166	0.341
3.0	200	0.114

C_2H_4 : H_2 = 1:2
Path length = 3.3 cm.
Ht.from column base = 95.5 cm.
I_o = 238
θ = 100
T_R = 17°C π = 74.6 cm.

F_i	I	A_{gl}
79	91	1.165
67	89	1.195
56	103	1.02
44	108	0.96
35	113	0.905
26	119	0.843
17	135	0.690
8	189	0.282
2	210	0.156

C_2H_4 : H_2 = 2:1
Path length = 3.3 cm.
Ht.from column base = 20 cm.
I_o = 223
θ = 100
T_R = 15°C π = 74.5 cm.

F_i	I	A_{gl}
75	53	1.74
63	64	1.51
51.5	77	1.29
40	85	1.17
31	86	1.15
22.5	134	0.62
11.5	161	0.395
3.0	205	0.103

C_2H_4 : H_2 = 1:2
Path length = 3.3 cm.
Ht. from column base = 20 cm.
I_o = 227
θ = 100
T_R = 15°C π = 74.5 cm.

F_i	I	A_{gl}
78	51	1.81
68	53	1.76
58.5	69	1.44
44.5	87	1.17
31	94	1.07
23	144	0.552
10.5	156	0.458
1.5	205	0.128

REACTOR II.

C_2H_4 : H_2 = 2:1
Path length = 3.3 cm.
Ht. of tube from column base = 19.5 cm.
I_o = 215
θ = 100
T_R = 18°C π = 75.5 cm.

F_i	I	A_{gl}
76.5	46	1.87
63	54	1.68
52.5	70	1.36
41	77	1.25
33	91	1.04
18	134	0.57
9	178	0.232
3	200	0.092

C_2H_4 : H_2 = 1:2
Path length = 3.3 cm.
Ht. of tube from column base = 19.5 cm.
I_o = 230
θ = 100
T_R = 18°C π = 75.5 cm.

F_i	I	A_{gl}
78	49	1.88
70	56	1.72
58	73	1.39
47.5	79	1.30
32	101	1.00
21	132	0.68
12	169	0.38
7	190	0.234
2	210	0.114

REACTOR V.

DECALIN.

C_2H_4 : H_2 = 1:1
Path length = 3.3 cm.
Ht. of tube from column base = 95.5 cm.
I_o = 221
θ = 100
T_R = 17°C π = 74.6 cm.

F_i	I	A_{gl}
77	70	1.4
63	83	1.19
52	98	0.985
41.5	103	0.925
32.5	110	0.850
19	131	0.635
9.5	174	0.293
2.5	208	0.078

WATER.

C_2H_4 : H_2 = 1:1
Path length = 3.3 cm.
Ht. of tube from column base = 95.5 cm.
I_o = 228
θ = 100
T_R = 17°C π = 74.6 cm.

F_i	I	A_{gl}
76	97	1.04
60	97	1.04
49.5	108	0.908
38	112	0.865
27.5	128	0.703
15	158	0.446
9	178	0.304
1.5	208	0.117

REACTOR V.

DECALIN.

C_2H_4 : H_2 = 1:1
Path length = 3.3 cm.
Ht. of tube from column base = 20 cm.
I_o = 231
θ = 100
T_R = 16°C Π = 74.5 cm.

F_i	I	A_{gl}
76.5	49	1.89
63	56	1.72
52	77	1.33
43.5	82	1.26
31	110	0.90
22	138	0.63
12	174	0.349
2.0	212	0.109

WATER.

C_2H_4 : H_2 = 1:1
Path length = 3.3 cm.
Ht. of tube from column base = 20 cm.
I_o = 218
θ = 100
T_R = 16°C Π = 74.5 cm.

F_i	I	A_{gl}
75	51	1.77
62	55	1.67
51	78	1.25
39	85	1.14
27	113	0.80
17.5	121	0.715
8.0	168	0.322
2.5	195	0.14

REACTOR II.

DECALIN.

C_2H_4 : H_2 = 1:1
Path length = 3.3 cm.
Ht. of tube from column base = 19.5 cm.
I_o = 220
θ = 100
T_R = 18°C Π = 75.5 cm.

F_i	I	A_{gl}
74	49	1.82
62	56	1.66
55	71	1.37
43	85	1.15
31	95	1.02
23	135	0.595
9	180	0.248
1.5	205	0.089

WATER.

C_2H_4 : H_2 = 1:1
Path length = 3.3 cm.
Ht. of tube from column base = 19.5 cm.
I_o = 225
θ = 100
T_R = 18°C Π = 75.5 cm.

F_i	I	A_{gl}
77	50	1.83
65.5	55	1.71
53	72	1.38
42	84	1.2
30	103	0.95
19.5	131	0.66
10	165	0.38
2.0	203	0.129

Fig. A 2. 2 shows a plot of the specific surface, A_{gl} vs. flow rate using results obtained at reactor bases. Fig. A 2. 3 shows corresponding results obtained at reactor tops.

It is seen, in the case of the larger reactors at high flow rates, that the specific area at the reactor top is less than would be expected. This may be explained by reference to Fig. A 2. 4. It can be seen in A 2. 4. 5 and A 2. 4. 6 that large agglomerations of bubbles tend to occur. These photographs show conditions existing at the reactor top at medium and high flow rates. This agglomerating of bubbles, or "slugging", causes the diminution of the specific surface. Agglomeration of bubbles appears to occur only in the taller reactors at higher flow rates. It was decided to ignore its effects as no correction factor for it is immediately evident. Furthermore conversion will normally have reduced the volume of gas passing through the reactor upper section and this should diminish the slugging tendency. It was assumed for the purposes of this work that the no. of bubbles/unit volume is the same at the reactor top as the bottom and any change in interfacial area/unit volume is entirely due to reduction in volume caused by conversion. The

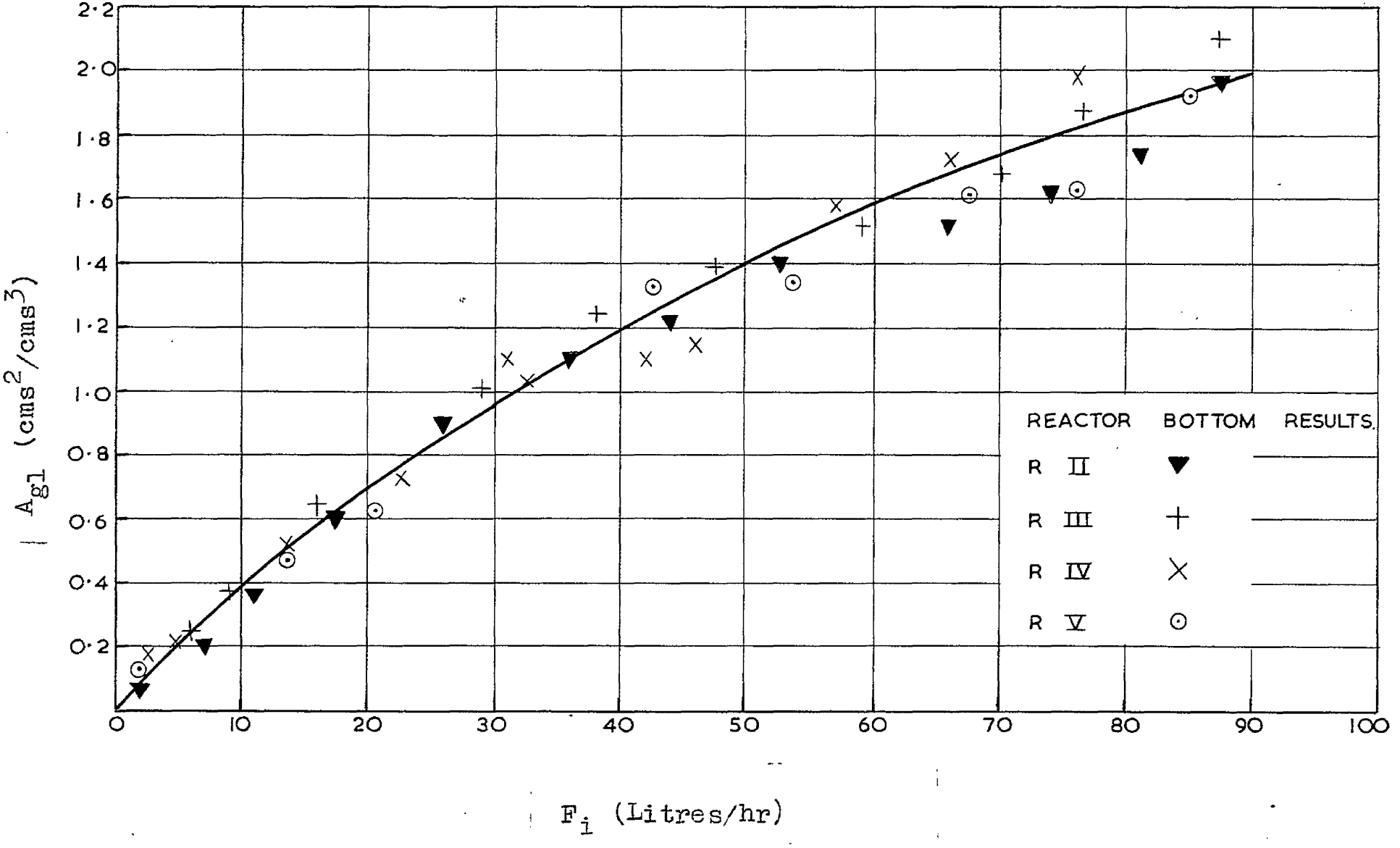
2·2
2·0
1·8
1·6
1·4
1·2
1·0
0·8
0·6
0·4
0·2
0
10
20
30
40
50
60
70
80
90
100
A_{gl} (cms^2/cms^3)
F_i (Litres/hr)
REACTOR BOTTOM RESULTS.
R II
R III
R IV
R V

FIG. A2.2.

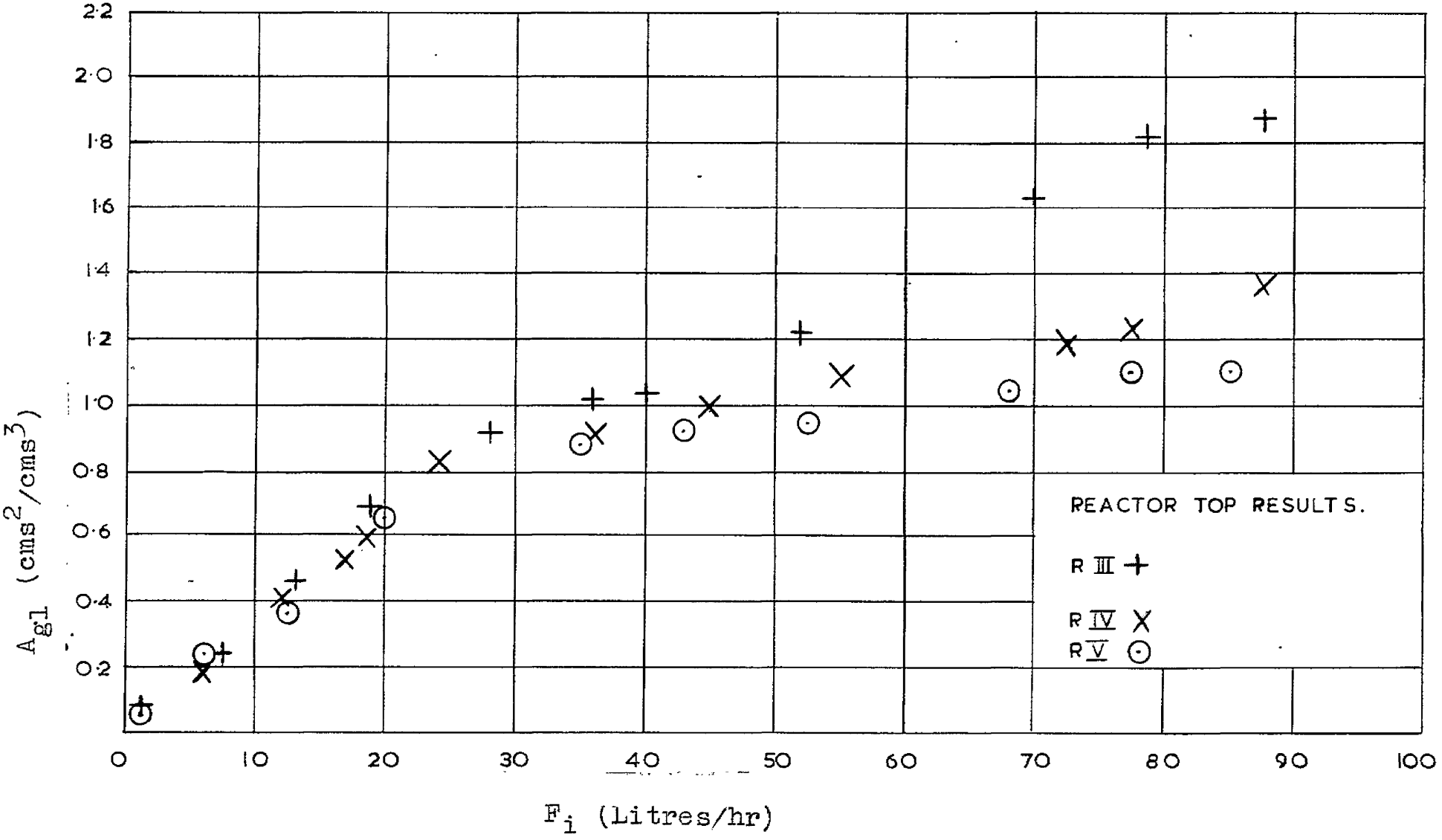
2·2
2·0
1·8
1·6
1·4
1·2
1·0
0·8
0·6
0·4
0·2
0
10
20
30
40
50
60
70
80
90
100
A_{gl} (cms^2/cms^3)
F_i (Litres/hr)
REACTOR TOP RESULTS.
R III
R IV
R V

FIG. A.2.3.

Fig. A 2. 4.

1. Bottom
Low Flow Rate.

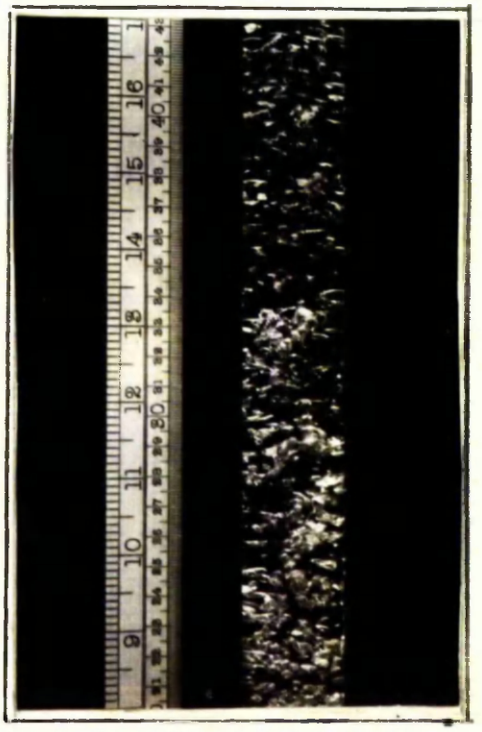

2. Bottom
Medium Flow Rate.

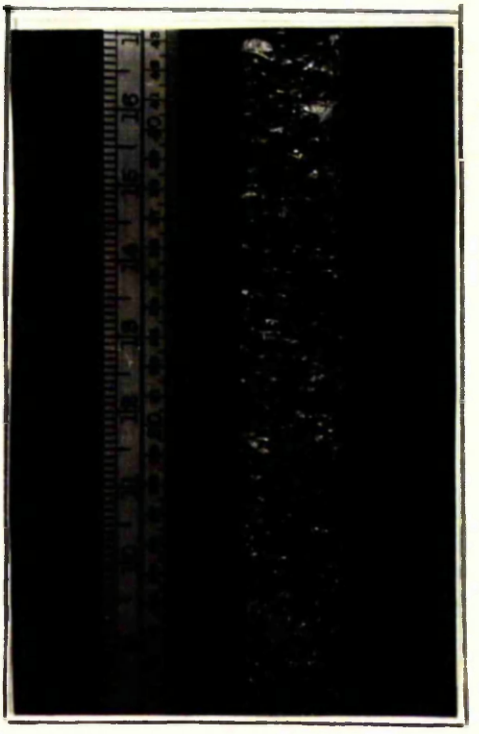

3. Bottom
High Flow Rate.

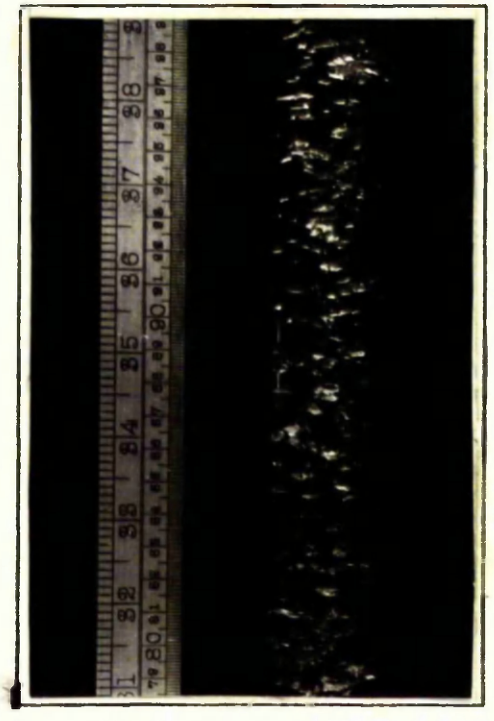

4. Top
Low Flow Rate.

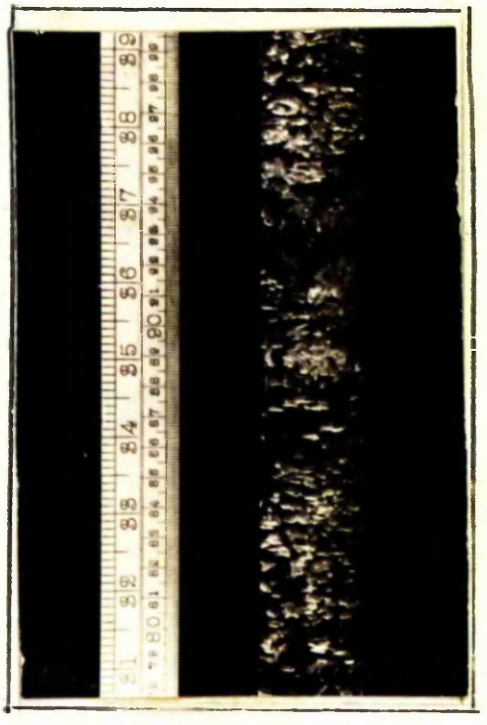

5. Top
Medium Flow Rate.

6. Top
High Flow Rate.

surface area/unit volume data used was taken from results obtained at reactor bases. It is felt that the consequences of these assumptions may be seen in the variations of K_{gb} in 3. A more complete investigation of bubble surface areas might lead to an explanation of these variations.

Fig. A 2. 5 shows results obtained with reactor IV A. As might be expected values of A_{gl} are less than those obtained with the narrower reactors. Only one measuring position was possible with this reactor.

Fig. A 2. 6 shows results obtained at the base of reactors V and II with various inlet gas compositions. The values of A_{gl} do not seem affected by gas compositions and this plot may be shown to be superimposable on A 2. 2.

Fig. A 2. 7 shows results obtained at the base of reactors V and II with water and decalin in the reactors. Once again A_{gl} values seem unaffected by the change in conditions. This is surprising as one might have expected the different physical properties of the liquids to have some effect.

An expression for a mean value of A_{gl} between reactor bottom and top is derived thus:-

Gas flow in = F_I litres/hr.
Gas flow out = F_O litres/hr.

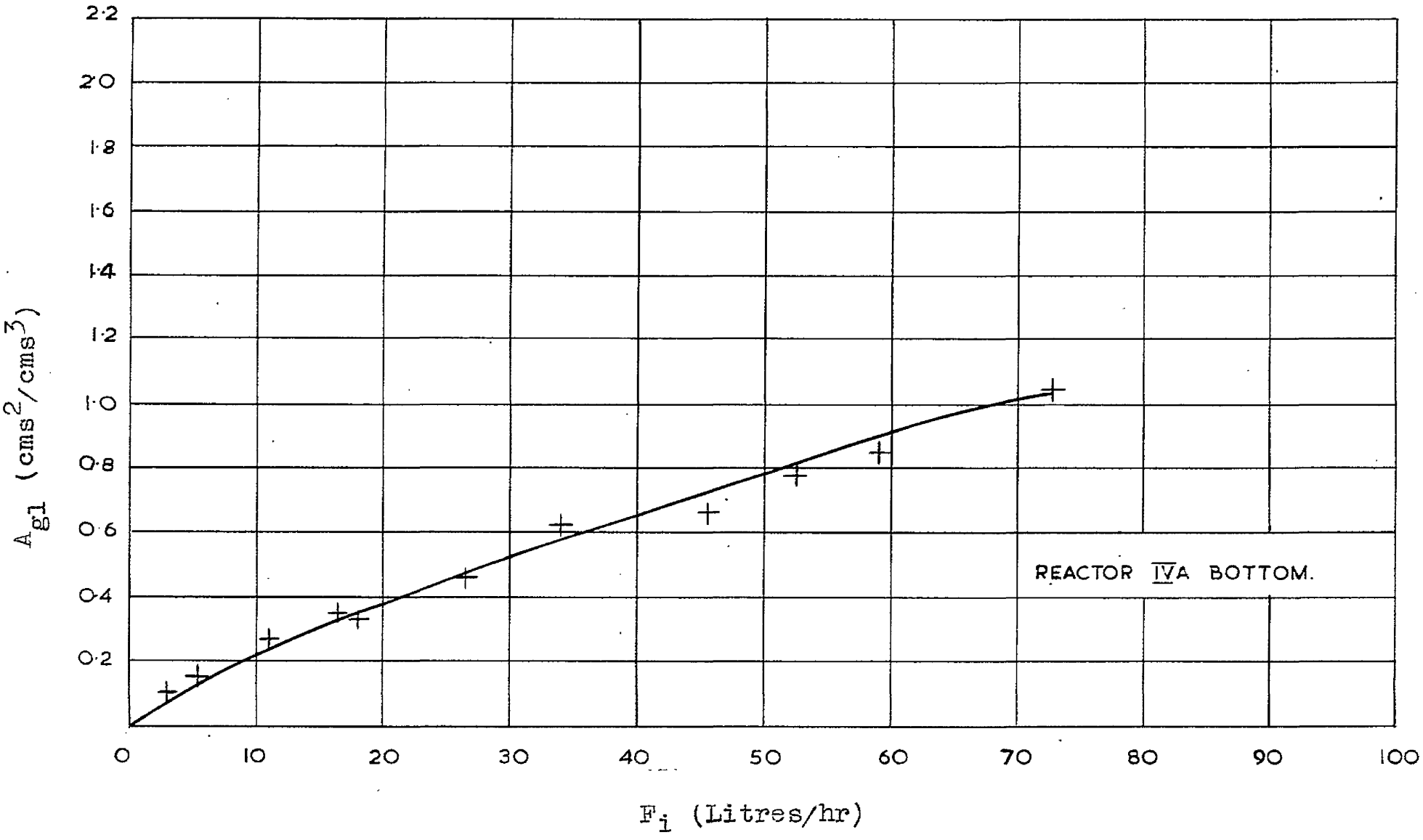
2·2
2·0
1·8
1·6
1·4
1·2
1·0
0·8
0·6
0·4
0·2
0
10
20
30
40
50
60
70
80
90
100
A_{gl} (cms^2/cms^3)
F_i (Litres/hr)
REACTOR IVA BOTTOM.

FIG.A.2.5.

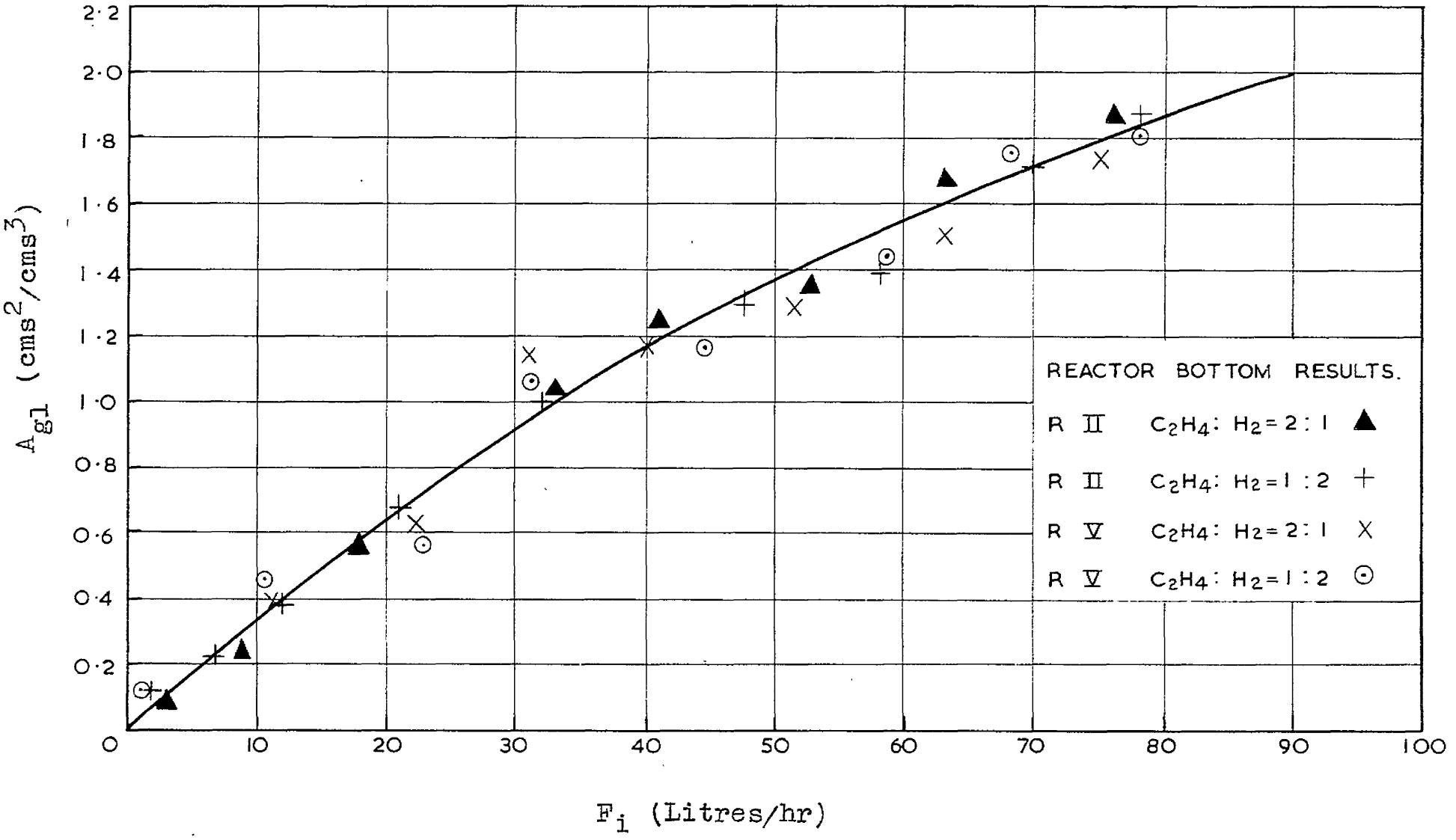
2·2
2·0
1·8
1·6
1·4
1·2
1·0
0·8
0·6
0·4
0·2
0
10
20
30
40
50
60
70
80
90
100
A_{gl} (cms^2/cms^3)
F_i (Litres/hr)
REACTOR BOTTOM RESULTS.
R II C_2H_4: H_2 = 2 : 1
R II C_2H_4: H_2 = 1 : 2
R V C_2H_4: H_2 = 2 : 1
R V C_2H_4: H_2 = 1 : 2

FIG. A. 2.6.

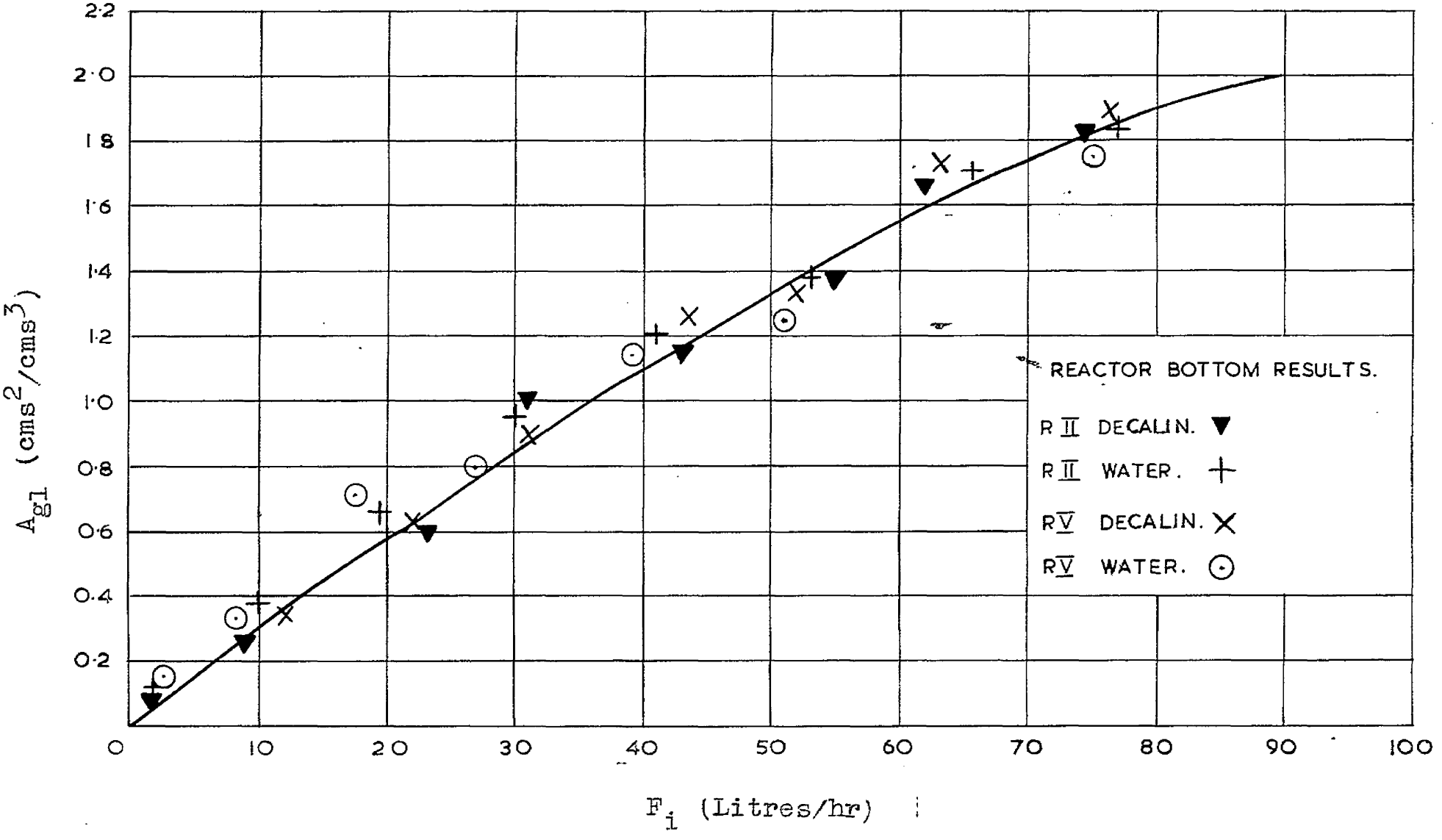
2·2
2·0
1·8
1·6
1·4
1·2
1·0
0·8
0·6
0·4
0·2
0
10
20
30
40
50
60
70
80
90
100
A_{gl} (cms^2/cms^3)
F_i (Litres/hr)
REACTOR BOTTOM RESULTS.
R II DECALIN.
R II WATER.
R V DECALIN.
R V WATER.

FIG. A.2.7

For the reaction $A + B \longrightarrow C$, it may be shown by a simple mass balance that

$$\frac{F_o}{F_i} = (1 - Y_{ai} x)$$

where Y_{ai} = mole fraction of component A at inlet

x = conversion of component A.

Suppose F_i is divided into n bubbles at inlet.

The volume of each bubble, $V_i = \frac{F_i}{n}$

Also $V_i = \frac{4}{3} \pi r_i^3 . 10^{-3}$ [r_i = bubble radius at inlet (cms.)]

$$r_i = \sqrt[+3]{\left(\frac{3 V_i}{4 \pi}\right)} . 10$$

Hence, area of bubble $A_i = 4 \pi \left(\frac{3 V_i}{4 \pi}\right)^{2/3} . 10^2$

Similarly at reactor outlet, bubble surface area

$$A_o = 4 \pi \left(\frac{3 V_o}{4 \pi}\right)^{2/3} . 10^2$$

Since no. of bubbles entering reactor = no. of bubbles leaving

$$\frac{A_{gl\,o}}{A_{gli}} = \frac{A_o}{A_i} = \left(\frac{V_o}{V_i}\right)^{2/3} = \left(\frac{F_o}{F_i}\right)^{2/3}$$

Now $\frac{F_o}{F_i} = (1 - Y_{ai} x)$

Hence $A_{glo} = A_{gli} (1 - Y_{ai} x)^{2/3}$

Hence A_{glo} may be computed for any value of A_{gli} when inlet composition and conversion are known. If the mean A_{gl} value is assumed to be the arithmetic mean

of A_{gli} and A_{glo}, correction factors may be calculated. Multiplication of A_{gli} by these gives the value of A_{glm}.

A 2. 8 and A 2. 9 are graphs from which $\frac{A_{glo}}{A_{gli}}$ and correction factors may be obtained at any conversion. Calculated values are also tabulated. $(C = x.10^2)$

$C_2H_4 : H_2 = 1:1$

C	$\frac{A_{glo}}{A_{gli}}$	Correction Factor
0	1.00	1.00
10	0.965	0.983
20	0.930	0.965
30	0.896	0.948
40	0.860	0.930
50	0.825	0.913
60	0.790	0.895
70	0.750	0.875
80	0.710	0.855
90	0.680	0.840
100	0.630	0.815

$C_2H_4 : H_2 = 1:2$
$C_2H_4 : H_2 = 2:1$

C_1	C_2	$\frac{A_{glo}}{A_{gli}}$	Correction Factor
0	0	1.00	1.00
10	20	0.955	0.978
20	40	0.908	0.954
30	60	0.860	0.930
40	80	0.815	0.908
50	100	0.762	0.881

A_{glm} may be estimated thus:-

Run B 5 F_i=33·6 litres/hr., C = 67.6 %. x = 0.676

From A 2. 2 A_{gli} = 1.06 cms^2/cms^3

From A 2. 8 correction factor = 0.875

A_{glm} = 0.925

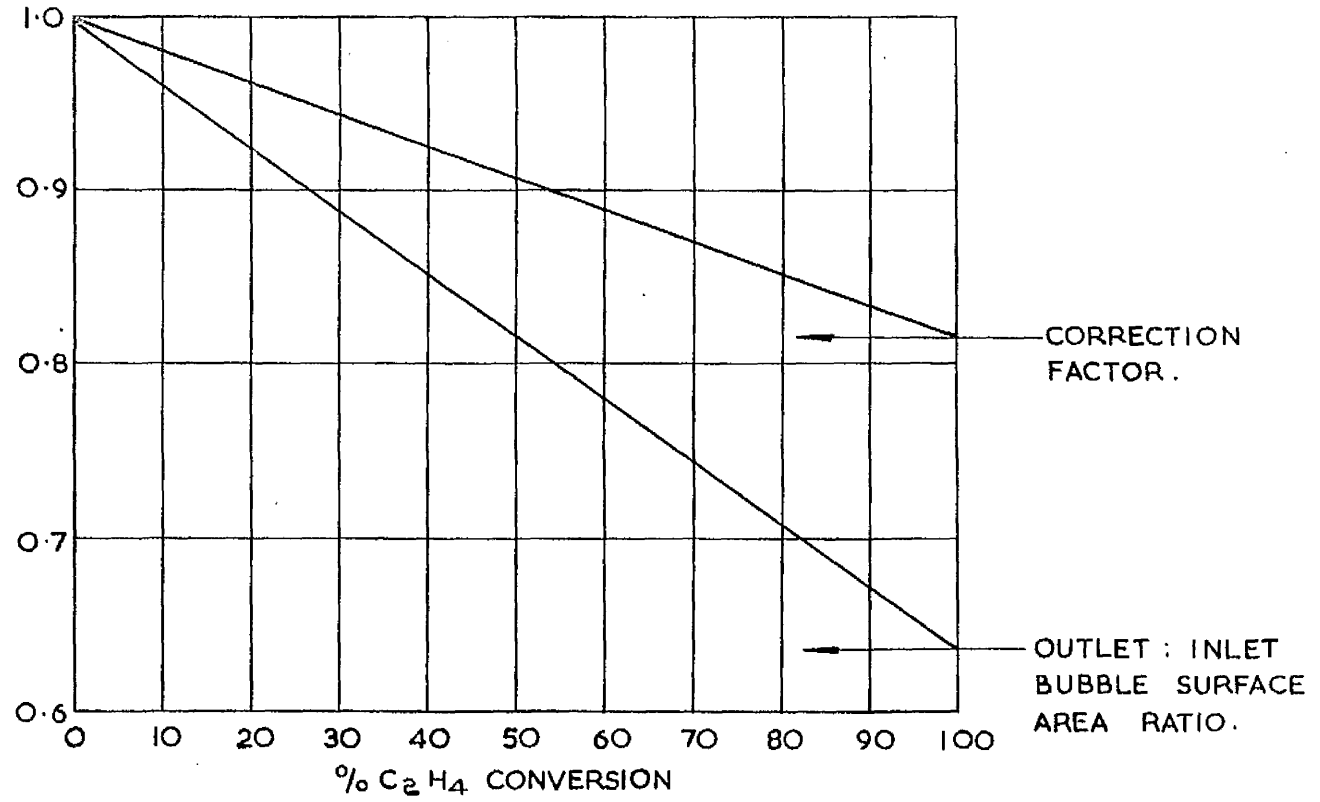

FIG. A. 2.8

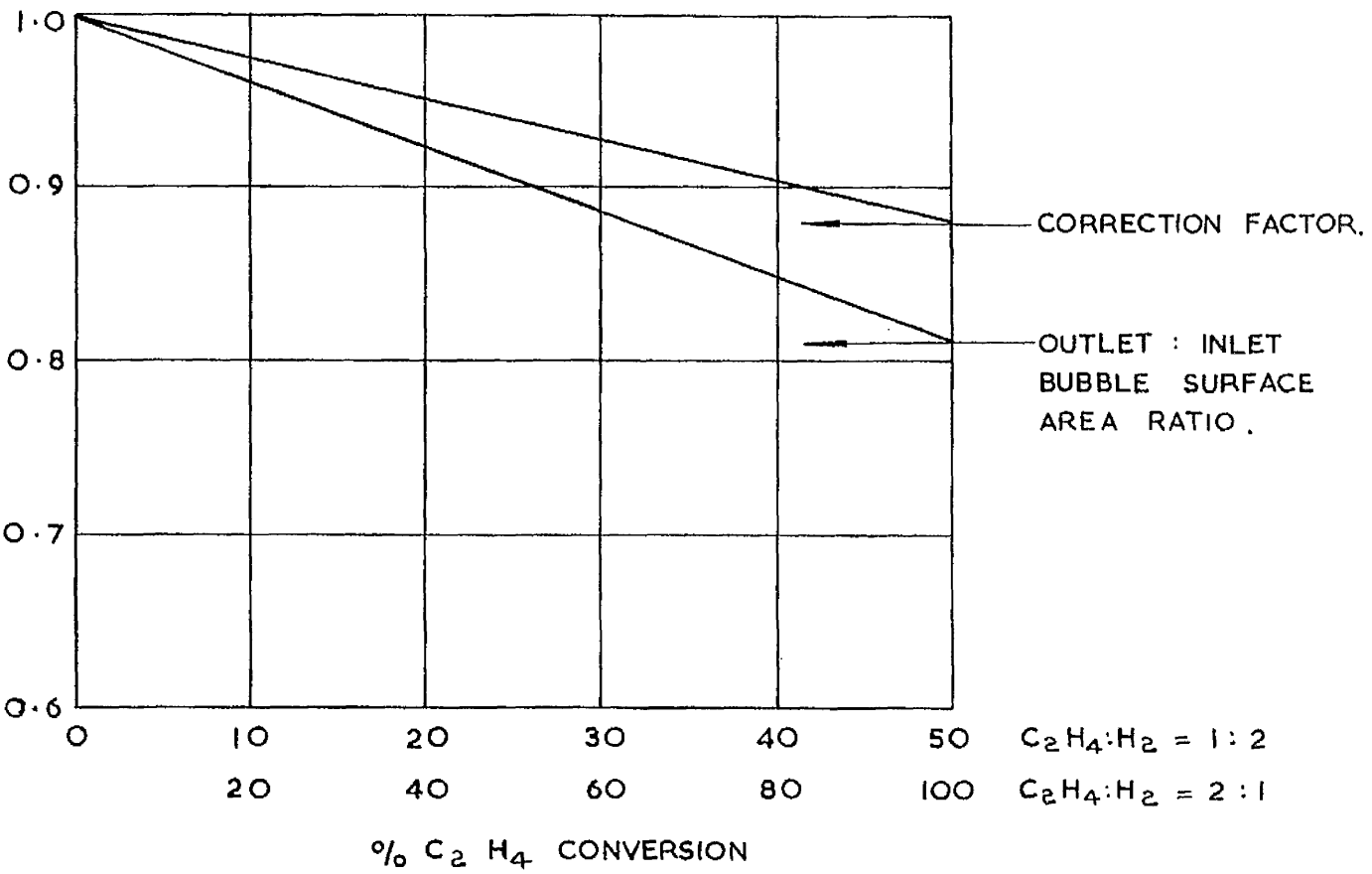

FIG. A. 2.9

APPENDIX 3.

The average catalyst particle size was obtained by a sedimentation method (60). The apparatus was devised by Deans (61).

The apparatus consists of a long vertical tube, 2 cm. I.D. and 115 cm. long, surrounded by a water jacket. Near the top of the tube is a glass stop-:cock equal in bore to the tube. The funnel at the top of the narrow bore deposition tube fits into the base of the main column and is held in position by a rubber bung. At the bottom of the narrow bore tube is a capillary stopcock. A centimetre scale is attached to the tube. The arrangement is shown in F. A 3. 1.

The apparatus is operated thus:-
The deposition tube is filled with mercury to a zero mark and then fitted into the main column. The settling medium, xylene, is then poured into the main tube to a level above the large stopcock. Water is then passed through the water jacket and the apparatus left for half an hour in order to minimise thermal eddy currents. The large stopcock is shut and a sample of catalyst introduced into the top section. The cock is then opened and a stop-:clock simultaneously started. The particles descend through the stagnant liquid and build up in

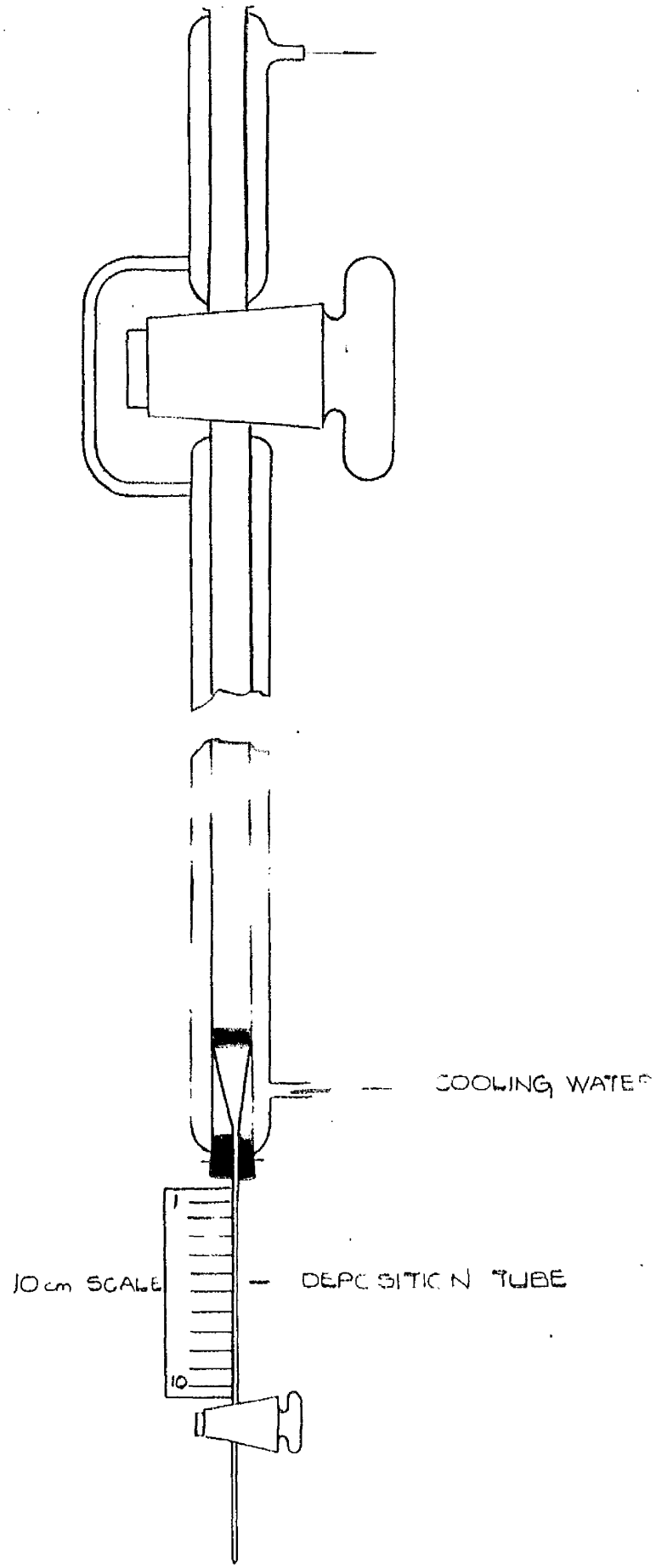

FIG. A.3.1. SINGLE ANALYSIS APPARATUS.

the deposition tube. As the particles build up the mercury level is dropped so that the top of the particle bed remains more or less constant at the zero mark on the scale. This results in a constant deposition length. The increases in particle bed length with time are noted.

The basis for particle size analysis by sedimentation is Stoke's Law. For a particle settling at constant velocity in a liquid

Total viscous force = $3\pi\eta D_p u$

Total gravitational force = $\frac{1}{6}\pi D_p^3(\rho_1 - \rho_2)g$

At constant velocity

$$u = \frac{D_p^2 . g . (\rho_1 - \rho_2)}{18\eta}$$

u = velocity cm/sec.

g = 981 cm/sec.^{2}

D_p = particle diameter cm.

ρ_1 = density of settling material gm./cc.

ρ_2 = density of liquid gm./cc.

η = viscosity of settling medium poises.

θ = settling time mins.

In this case $U = \frac{\text{length of deposition tube (cm.)}}{\theta \times 60}$

$$= \frac{115}{\theta \times 60} \text{ cm./sec.}$$

Thus $\frac{115}{\theta \times 60} = \frac{D_p^2 \times g \times (\rho_1 - \rho_2)}{18\eta}$

For nickel ρ_1 = 8.9 gms./cc.

xylene ρ_2 = 0.867 gms./cc. (25°C)

η = 0.0065 poise (25°C)

Hence $D_p = \frac{52.5}{\sqrt{\theta}}$

From this equation the particle diameter for every time reading in the run is calculated. A graph of percentage height against particle diameter may then be drawn. From this graph, the percentage of particles in any size range may be found and this enables a distribution graph to be drawn. The area under this latter graph is then bisected by a vertical line, the point at which this line meets the x - axis represents the mean particle diameter.

This procedure was repeated twice for each batch of catalyst. The results are shown in tables A 3. 1 - 4, and specimen graphs in Figs. A 3. 2 and A 3. 3.

CATALYST A.

TABLE A 3. 1.

Ht. cms.	θ	$\sqrt{\theta}$	% Ht.	D_p microns
0.00	0.00	-	-	-
0.00	0.50	-	-	-
0.30	1.00	1.00	5.9	52.5
0.70	1.50	1.225	13.7	42.8
0.80	2.00	1.415	15.7	37.1
1.80	2.67	1.63	35.3	32.2
3.70	4.00	2.00	72.9	26.3
3.90	4.50	2.12	76.5	24.8
4.20	6.00	2.45	82.5	21.4
4.30	7.00	2.64	84.5	19.9
4.40	8.00	2.83	86.2	18.55
4.50	9.00	3.00	88.4	17.5
4.55	10.00	3.16	89.3	16.6
4.70	14.00	3.74	92.2	14.05
4.80	18.00	4.12	94.3	12.75
5.0	26.00	5.10	98.0	10.0
5.1	40.00	5.47	100	9.60

TABLE A 3. 2.

Ht. cms.	θ	$\sqrt{\theta}$	% Ht.	D_p microns
0.00	0.00	-	-	-
0.00	0.50	-	-	-
0.40	1.00	1.00	9.10	52.5
0.80	2.00	1.415	18.2	37.1
1.00	2.33	1.53	22.8	34.3
1.30	3.00	1.73	29.6	30.4
2.20	3.50	1.87	50.0	28.1
3.00	4.33	2.08	68.1	25.2
3.50	5.00	2.24	79.5	23.4
3.70	6.00	2.45	84.1	21.4
3.80	7.00	2.65	86.5	19.8
3.90	8.00	2.83	88.6	18.55
4.00	10.00	3.16	91.0	16.6
4.20	15.00	3.87	95.5	13.6
4.30	20.00	4.47	97.9	11.75
4.35	25.00	5.00	99.0	10.5
4.40	30.00	5.48	100	9.60

CATALYST B.

TABLE A 3. 3.

Ht. cms.	θ	$\sqrt{\theta}$	% Ht.	D_p microns
0.00	0.00	-	-	-
0.00	0.50	-	-	-
0.05	1.00	1.00	1.33	52.25
0.25	2.00	1.415	6.68	37.1
0.40	2.50	1.58	10.7	33.2
0.70	3.00	1.73	18.7	30.4
1.00	3.50	1.87	26.7	28.1
1.50	4.00	2.0	40.0	26.2
1.90	4.50	2.12	50.6	24.8
2.60	5.00	2.24	69.4	23.4
2.90	6.00	2.45	77.4	21.4
3.00	7.00	2.64	80.0	19.9
3.10	8.00	2.82	82.6	18.6
3.20	10.00	3.16	85.4	16.6
3.30	12.00	3.46	88.0	15.2
3.40	15.00	3.87	90.6	13.53
3.55	20.00	4.47	94.8	11.75
3.70	30.00	5.48	98.8	9.57
3.75	40.00	6.32	100	8.3

TABLE A 3. 4.

Ht. cms.	θ	$\sqrt{\theta}$	% Ht.	D_p microns
0.00	0.00	-	-	-
0.00	0.50	-	-	-
0.20	1.00	1.00	4.2	52.25
0.40	2.50	1.58	8.42	33.2
0.50	3.00	1.73	10.5	30.4
1.00	4.00	2.00	21.0	26.2
1.30	4.50	2.12	27.4	24.8
1.70	5.00	2.24	35.8	23.4
2.90	6.00	2.45	61.1	21.4
3.80	7.00	2.65	80.0	19.8
4.00	8.00	2.83	84.2	18.55
4.20	9.00	3.00	88.5	17.5
6.30	10.00	3.16	90.6	16.6
4.40	15.00	3.87	92.6	13.55
4.50	20.00	4.47	94.9	11.75
4.60	25.00	5.00	97.1	10.5
4.75	35.00	5.91	100	8.85

For catalyst A in run A 3. 1 D_p = 27.6 μ

" " A 3. 2 D_p = 27.2 μ

Hence D_{pM} = 27.4 μ

For catalyst B in run A 3. 3 D_p = 25.1 μ

" " A 3. 4 D_p = 24.7 μ

Hence D_{pM} = 24.9 μ

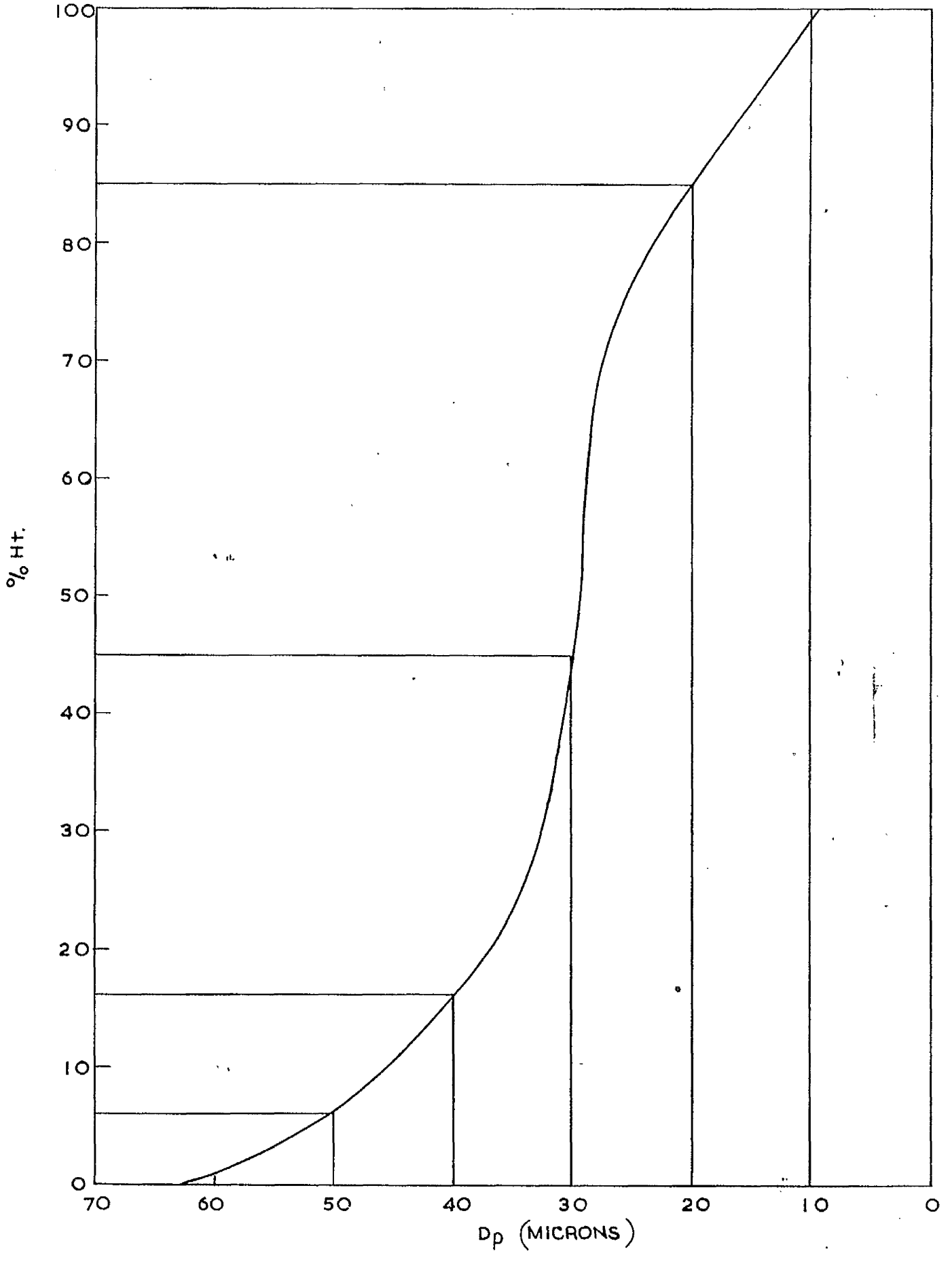

FIG. A. 3.2

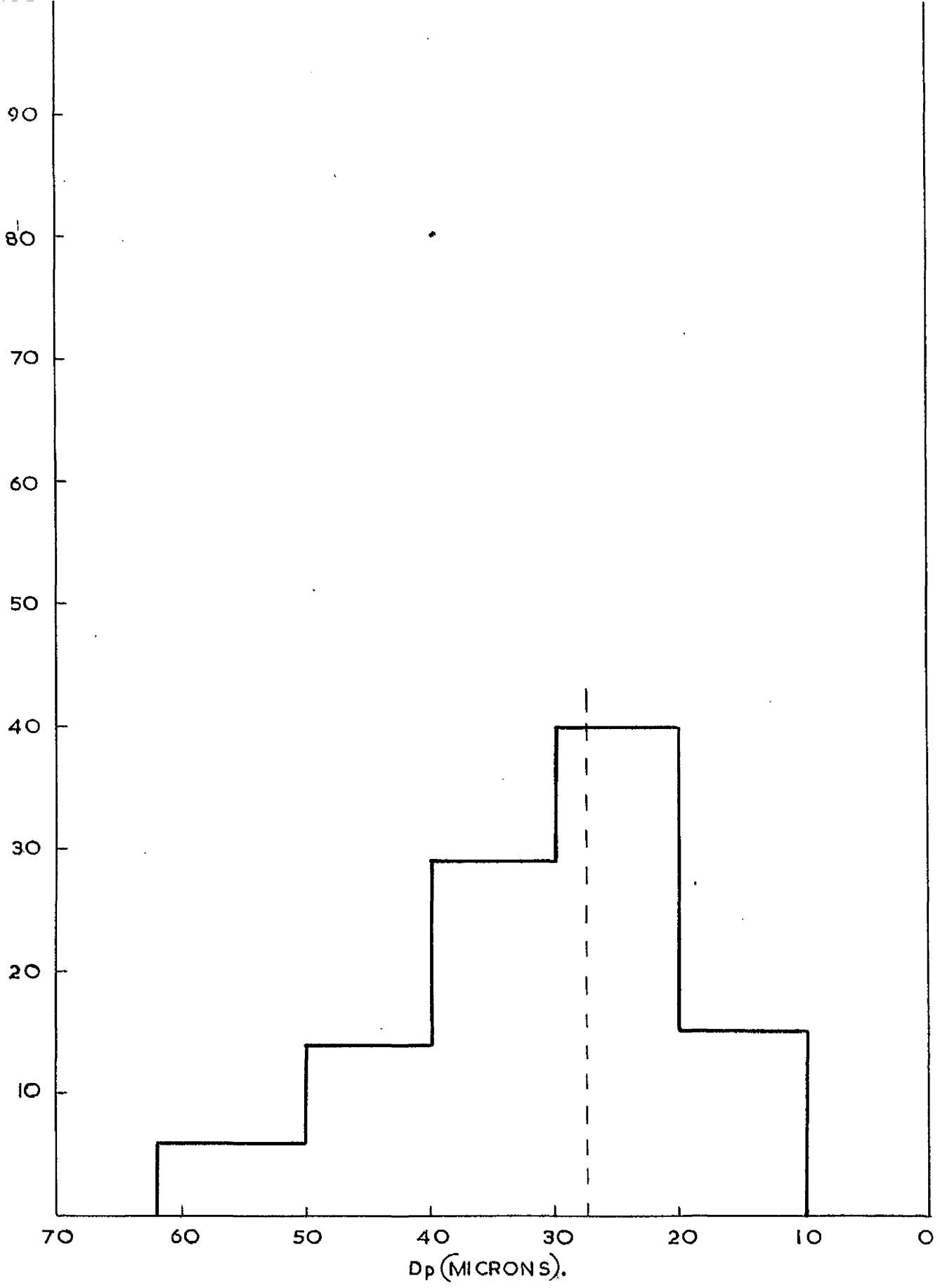

FIG. A. 3.3.

If each catalyst particle is considered to be a sphere, the volume of the average sphere is given by

$$\frac{4}{3}\ \pi\ \left(\frac{27.4}{2 \times 10^4}\right)^3 \quad cm^3$$

in the case of catalyst A.

The density of nickel is 8.9 gms./cc.

Hence the no. of spheres/gm. is given by

$$\frac{1}{8.9 \times \frac{4}{3} \times \pi \times \left(\frac{27.4}{2 \times 10^4}\right)^3}$$

Surface area of the average sphere = $4\pi \left(\frac{27.4}{2 \times 10^4}\right)^2$ cm^2.

Surface area/gm. of catalyst =

$$4\pi \left(\frac{27.4}{2 \times 10^4}\right)^2 \times \frac{1}{8.9 \times \frac{4}{3} \times \pi \times \left(\frac{27.4}{2 \times 10^4}\right)^3}$$

$$= 247\ cm^2/gm.$$

For catalyst B, surface area/gm. of catalyst = 271 cm^2/gm.

When the catalyst concentration is 2.5 gms./100 cc. of reactor this results in a liquid solid interfacial area/cm^3, A_{ls}, of 6.17 cm^2/cc for A

and 6.76 cm^2/cc for B.

It must be pointed out here that this surface area is probably considerably less than the actual one. Each particle is assumed to be a sphere whereas it is, from microscopic examination, a spongy irregular lump.

Such particles have much higher surface areas. The solid-liquid interfacial area is, at this catalyst concentration, always in excess of the gas liquid interfacial area.

BIBLIOGRAPHY.

1. Fischer, F., Brenstoff Chem. 12 286 (1931).

2. British Patent No. 294,737.

3. Roelen, O., B.I.O.S. Final Report 447.

4. Kölbel, H., B.I.O.S. Final Report 1712.

5. F.I.A.T. Final Report 1,267.

6. Storch, H. H., Golumbic N., and Anderson, R. B., "The Fischer Tropsch and Related Synthesis" Wiley (1951).

7. Kölbel, H., and Hammer, H., Chemical and Process Eng. 42 105 (1961).

8. Hall, C. C., Gall, D., and Smith, S. L. J. Inst. Pet. 38 845 (1952).

9. Macrae, D., Ph. D. Thesis, Edinburgh, 1953.

10. Calderbank, P. H., et al, Inst. of Chem. Engrs., "Catalysis in Practice" (1963). Paper No. 598.

11. Schlesinger, M. D., Crowell, J. H. Leva, M., and Storch, H. H., Ind. and Eng. Chem. 43 1474 (1951).

12. Newton, R. N., and Schimp, M. G., Trans. A. I. Chem. E. 41 1208 (1945).

13. Leva, M., "Fluidisation" p.181 McGraw Hill (1959).

14. Van Heerden, C., Nobel, A. P. P. and Van Krevelen, D. W., Ind. Eng. Chem. 45 1237 (1953).

15. Van Heerden, C., Chem. Eng. Sci. 51 1951-52.

16. Scharmann, W. G., U.S. Pat. 2,463,912, 1949.

17. Warmsley and Johanson, Chem. Eng. Prog. 50 352 (1954).

18. Hemminger, H., U.S. Pat. 2,464,505, 1949.

19. Kölbel, H. et al. Chem. Ing. Techn. 30 400 (1958).

20. Kölbel, H. et al. Chem. Ing. Techn. 30 727 (1958).

21. " " Chem. Ing. Techn. 32 84 (1960).

22. Gunness, R. C., Chem. Eng. Prog. 49 113 (1953).

23. Keith, F. C., Oil and Gas. J. 45 102 (1946).

24. Slesser, C. G. M., Ph. D. Thesis, Edinburgh, 1949.

25. Kölbel, H. et al. 4th World Petroleum Congress, Paper No. 9.

26. Whitman, W. G., Chem. and Met. Eng. 29 147 (1923).

27. Higbie, R., Trans. A. I. Chem. E., 31 365 (1935).

28. Danckwerts, P. V. et al. Chem. Eng. Sci. 18 63 (1963).

29. Van der Vusse, J. G., Chem. Eng. Sci. 16 21 (1961).

30. Smith, J. M., "Chemical Engineering Kinetics" p. 243. McGraw Hill 1956.

31. Emmett, P., "Catalysis" Vol. III. Reinhold 1955.

32. Lampichler, F. G., Ind. Eng. Chem. 35 522 (1943).

33. Hart, D. M., Ind. Eng. Chem. 35 522 (1945).

34. Narsimhan, G., and Doraiswamy, L. K., British Chem. Eng. 5 845 (1960).

35. Rideal, E. K., J. Chem. Soc. 121 389 (1922).

36. Pease, R. N., Am. Chem. Soc. Trans. 54 1877 (1932).

37. Treadwell, W. D., Helv. Chem. Acta., 2 601 (1934).

38. Lamb, L., and Thomson, R., B. Sc., Thesis, Glasgow 1960.

39. Berkmann, S., Morrell, J. C., and Egloff, G., "Catalysis" Reinhold (1940).

40. Pauls, A. C., A. I. Chem. E. J. 5 453 (1959).

41. Janek, J., Collection of Czeck. Chem. Comm., 19 684,700,917 (1954).

42. Raney, Ind. Eng. Chem. 32 1199 (1940).

43. Covert, L. W., and Adkins, H., J. A. Chem. Soc. 55 4116 (1933).

44. Seidell, A., "Solubilities of Inorganic Compounds" Van Norstrand.

45. Seidell, A., "Solubilities of Organic Compounds" Van Norstrand.

46. Seymour, C., and Kapp, G., Chemical Engineering 70 105 (1963).

47. Calderbank, P. H., and Moo Young, M. B. Chem. Eng. Sci. 16 39 (1961).

48. Wilke and Chang. A. I. Chem. E. J. 1 264 (1955).

49. "International Critical Tables". McGraw Hill (1933).

50. Perry, J. H., "Chemical Engineers' Handbook" McGraw Hill (1950).

51. Wynkoop, R., and Wilhelm, R. H., Chem. Eng. Prog. 46 300 (1950).

52. Barford, J. A. Chem. Soc. 67 331 (1945).

53. Unpublished Information, R.C.S.T. Glasgow (1962).

54. Smith, J. M., "Chemical Engineering Kinetics", Chap. 2. McGraw Hill 1956.

55. McAdams, W. H., "Heat Transmission". McGraw Hill (1942).

56. Moore, W. J., "Physical Chemistry". Longmans (1957).

57. "Selected Values of Properties of Hydrocarbons". Nat. Bureau of Standards, C461 (1947).

58. Hougen, O. A., and Watson, K. M., "Chemical Process Principles". Wiley (1947).

59. Calderbank, P. H., Trans. I. Chem. E. 36 443 (1958).

60. Werner, Trans. Far. Soc. 21 381 (1925).

61. Deans, B. Sc., Thesis. R.C.S.T. Glasgow (1958).

62. Chilton T.H. and Colburn A.P. Ind. Eng. Chem. 27 (1933) 255